Etablierung und Analyse patientenindividueller Glioblastoma multiforme Modelle *in vitro* und *in vivo*

Kumulative Dissertation

zur

Erlangung des akademischen Grades

doctor rerum naturalium (Dr. rer. nat.)

der Mathematisch-Naturwissenschaftlichen Fakultät

der Universität Rostock

vorgelegt von

Doreen William, geb. am 12.02.1989 in Dresden

aus Dresden

Rostock, 05.03.2018

urn:nbn:de:gbv:28-diss2018-0121-8

1.Gutachter: Prof. Dr. med. Carl Friedrich Classen

Universitäts-Kinder- und Jugendklinik Rostock

Universitätsmedizin Rostock

2.Gutachter: Prof. Dr. rer. nat. Reinhard Schröder

Institut für Biowissenschaften, Abteilung Genetik

Universität Rostock

Tag der öffentlichen Verteidigung: 09.07.2018

Inhalt

Abkürzungsverzeichnis

Chr. – Chromosom
CNA – copy number alteration
CSC – cancer stem cells
Dox – Doxyzyklin
FFPE – Formalin-fixiert Paraffin-eingebettet
FKS – Fötales Kälberserum
FUT – Fukosyltransferase
GBM – Glioblastoma multiforme
HE – Hämatoxylin Eosin
MMP – Matrixmetalloproteinase
PDX – Patient derived Xenograft
RA – Retinoic Acid
RTK – Rezeptor-Tyrosin-Kinase
TKI – Tyrosin-Kinase-Inhibitor
TMZ – Temozolomid
WHO – World Health Organisation

1. Zusammenfassung

Das Glioblastoma multiforme (GBM) ist der am häufigsten auftretende primäre Hirntumor im Erwachsenenalter [1,2]. Das durchschnittliche Alter bei der Diagnosestellung von Glioblastomen liegt bei etwa 64 Jahren [3]. Die Inzidenz in Europa liegt bei ca. 3,5 Neuerkrankungen pro 100.000 Menschen jährlich, wobei Männer etwas häufiger betroffen sind als Frauen (Verhältnis 1,34:1) [3].

Glioblastome gehören zur Gruppe der Gliome und werden in der Klassifikation der Weltgesundheitsorganisation (World Health Organisation, WHO) aufgrund ihrer hohen Malignität, ihrer Histologie und Morphologie dem höchsten Grad 4 zugeordnet [4,5].

Allgemein sind Glioblastome histologisch durch eine hohe Zelldichte, Zell- und Kernpleomorphie, einen hohen Vaskularisierungsgrad und charakteristische Nekrosen gekennzeichnet [6,7].

Molekularpathologisch präsentieren sich Glioblastome jedoch deutlich heterogener und lassen sich daher anhand verschiedener genetischer Aberrationen in folgende vier Subtypen unterteilen: proneural (Amplifikation von 4q12 (PDGFRA), 10q23 Deletion (PTEN), Mutationen in p53, IDH1 und PIK3CA/PIK3R1), neural (Amplifikation von Chr. 7 und Verlust von Chr. 10), klassisch (Amplifikation von Chr. 7, Verlust von Chr. 10, Deletion von 9p21.3 (CDKN2A/B) und mesenchymal (Deletion von 17q11.2 (NF1), Mutationen in PTEN) [8,9].

Trotz multimodaler Behandlung, bestehend aus chirurgischer Resektion, Radiotherapie und Chemotherapie, beträgt die mittlere Überlebensdauer lediglich 12-15 Monate [10].

Angesichts dieser desaströsen Prognose ist die Entwicklung neuer Therapieansätze dringend notwendig. Dies wird jedoch durch die für Glioblastome charakteristische hohe inter- und intratumorale Heterogenität verkompliziert [11]. Diese ist, neben genetischen Merkmalen, durch eine Vielzahl von Einflussfaktoren begründet.

So spielen physische Gegebenheiten wie die anatomische Struktur an der Lokalisation des Tumors und die Entfernung zu Blutgefäßen eine Rolle, da sie die Versorgung mit Sauerstoff und Nährstoffen beeinflussen [12-14].

Auch Zell-Zell-Interaktionen zwischen Tumorzellen, inflammatorischen Zellen, Stromazellen und Endothelzellen sowie die mögliche Kooperation zwischen verschiedenen Tumorzell-Subklonen tragen zur Entstehung und Erhaltung der intratumoralen Heterogenität bei [14-17].

Obwohl eine molekularpathologische Subklassifizierung von Glioblastomen ein detaillierteres Verständnis über deren unterschiedliche Pathomechanismen ermöglicht als eine histologische Klassifikation allein, bleibt diese jedoch bislang weitgehend ohne klinische Konsequenz [9].

Darüber hinaus haben Studien belegt, dass die diagnostizierten molekularen Subklassen nicht unbedingt stabil sind und sich durch chirurgische Resektion sowie Radiochemotherapie durchaus verändern können [14,18,19]. Auch wurden durch eine Analyse von Genexpressionsmustern auf Einzelzellebene mehrere molekulare Subgruppen innerhalb des gleichen Glioblastoms identifiziert [20]. So ist es möglich, dass Tumorgewebe, dass nicht resektiert werden konnte, einer anderen molekularen Subklasse zugeordnet werden kann, als das erfolgreich resektierte Gewebe [14,18-20].

Weiterhin gibt es Evidenz dafür, dass Glioblastome – und andere Tumorentitäten – aus phänotypisch und funktional verschiedenen Zellpopulationen bestehen, die zudem von der Mikroumgebung des Tumors beeinflusst werden [14,21,22]. So wurde bei Glioblastomen eine Subpopulation von Zellen identifiziert, die Ähnlichkeit mit neuronalen Stammzellen zeigen [23].

Diese wurden entsprechend als Tumorstammzellen („Cancer stem(-like) cells“, CSCs) bezeichnet. Sie weisen klassische Stammzelleigenschaften wie die Fähigkeit zur Selbsterneuerung auf und sind ebenfalls eher undifferenziert [23-25].

Zudem gelten CSCs als resistenter gegenüber Radio- und Chemotherapie und zeigen ein vergleichsweise höheres Tumorigenitätspotential [26,27]. Dies lässt vermuten, dass GBM-CSCs eine mögliche Ursache für das Auftreten von Lokalrezidiven sind, die bei Glioblastomen äußerst häufig vorkommen [27].

Es wurde anfangs noch angenommen, dass in einem Glioblastom ein gewisser CSC-Pool vorhanden ist, aus dem durch Differenzierung proliferativere Zelltypen entstehen, welche letztlich die Hauptmasse des Tumors bilden [23]. Jedoch zeigten spätere Studien, dass

auch differenzierte Glioblastomzellen CSC-Eigenschaften zurückgewinnen können, wobei die genauen Ursachen und Mechanismen dafür noch unbekannt sind [12,27].
Dies unterstreicht den hohen Grad an Heterogenität bei Glioblastomen, der zu ihrer schlechten Therapierbarkeit maßgeblich beiträgt [11]. Dennoch kann die Identifikation tumorspezifischer Merkmale eine wertvolle Grundlage für die Entwicklung von Therapiestrategien darstellen, die auf die molekularen Gegebenheiten eines individuellen Tumors zugeschnitten sind [28].
Dadurch könnte ein besserer Behandlungserfolg bei - im Vergleich zur klassischen Chemotherapie - geringeren Nebenwirkungen erreicht werden.
So gab es beispielsweise mehrere klinische Studien zur Behandlung von Glioblastomen mit verschiedenen Tyrosinkinase-Inhibitoren, da Rezeptor-Tyrosin-Kinasen (RTK) in vielen GBM-Fällen dereguliert sind [29-31]. Allerdings blieb ein durchschlagender Behandlungserfolg bisher aus [29-31].
Daraus wird ersichtlich, dass neben der Identifikation genetischer Aberrationen innerhalb individueller Glioblastome ein besseres Verständnis über mögliche Resistenzmechanismen notwendig ist. Um dieses Ziel zu erreichen, sind patientenindividuelle Modelle – *in vitro* und *in vivo* – unerlässlich [32,33].
Die Etablierung solcher Modelle ausgehend von Tumorgewebe bietet den Vorteil, dass sich durch möglichst geringes Passagieren von Tumorzelllinien oder Xenografts genetische sowie epigenetische Alterationen eher vermeiden lassen [34. Auf diese Weise können die Eigenschaften des Originaltumors besser beibehalten werden [34].
Jedoch unterliegt die genetische Stabilität von patientenindividuellen GBM-Modellen gewissen Einschränkungen. Während beispielsweise Punktmutationen oder Deletionen in Modellen – *in vitro* und *in vivo* – eher stabil erhalten bleiben, können sich Merkmale wie die Amplifikation von Onkogenen teilweise stark verändern [35-38].
Eine bei Glioblastomen häufig vorkommende Genamplifikation betrifft den epidermal growth factor receptor (EGFR), die in ca. 40% der Fälle auftritt [39,40].
EGFR gehört zur Superfamilie der Rezeptor-Tyrosin-Kinasen und ist als solche ein wichtiger Regulator von Zellproliferation und Zellüberleben [41]. Die Dysregulation von

EGFR spielt eine wichtige Rolle bei der Entstehung und Progression von Glioblastomen [40,42].

Dabei sind mehrere von EGFR aktivierte Signalwege bedeutsam. Über den Ras/Raf/MAPK Signalweg werden vornehmlich Zellmigration und –proliferation induziert, wohingegen die Aktivierung des PI3K/Akt/mTOR Signalwegs zu Zellwachstum und Apoptose-Resistenz beiträgt [43,44].

Weiterhin führt verstärkte EGFR-Aktivität zu einer Aktivierung von STAT Proteinen – insbesondere STAT3 und STAT5 – was die Onkogenese und Tumorprogression fördert [45].

Neben der Amplifikation von EGFR können auch Mutationen des Rezeptors auftreten [40]. Dabei ist die häufigste Mutation eine in-frame Deletion der Exons 2-7 (EGFRvIII; [14]). Diese Deletion betrifft die extrazelluläre Domäne von EGFR, wodurch der Rezeptor außerstande ist, Liganden zu binden, jedoch stattdessen konstitutiv aktiv ist und die Onkogenese fördert [46,47].

Aufgrund der Häufigkeit von EGFR-Aberrationen und deren zentraler Stellung bei der Onkogenese und Progression von Glioblastomen eignen sich EGFR sowie Effektoren von EGFR-aktivierten Signalwegen für zielgerichtete Therapie-Ansätze [48].

Dementsprechend wurde eine Vielzahl von EGFR-Inhibitoren entwickelt und in klinischen Studien getestet [49].

Darunter waren Tyrosin-Kinase-Inhibitoren (TKIs) wie Erlotinib, Gefitinib oder Vandetanib und therapeutische Antikörper wie Cetuximab [49]. Die Ergebnisse waren bislang jedoch insgesamt nicht zufriedenstellend, da keines dieser Medikamente eine signifikante Verbesserung der Gesamtüberlebensdauer hervorrufen konnte [29-31].

Zur Ursache des Therapieversagens gibt es einige Hypothesen. Es ist denkbar, dass die Substanzen nicht in ausreichendem Umfang die Blut-Hirn-Schranke passieren können und so eine unzureichende Inhibition von EGFR verursachen [50]. Weiterhin erscheint plausibel, dass Glioblastome nach Inhibition von EGFR auf alternative Signalwege und RTKs ausweichen [50-53].

Die Verteilung von EGFR-amplifizierten Tumorzellen ist innerhalb eines Tumors ungleichmäßig, sodass durch EGFR-Inhibition womöglich nicht alle Tumorzellen eliminiert werden können, da jene ohne EGFR-Amplifikation überleben [51].
Zudem liegt die EGFR-Amplifikation meist auf extrachromosomalem DNA-Material, welches während der Zellteilung ungleichmäßig auf die Tochterzellen verteilt werden kann [38,54].
Dieser Umstand ermöglicht es Tumorzellen flexibel auf äußere Einflüsse, wie beispielsweise EGFR-Inhibition durch Therapeutika, zu reagieren und fördert somit die genetische Heterogenität des Tumors [38,54].
Gleichsam wird dadurch eine relativ realitätsgetreue Nachbildung der extrachromosomalen EGFR-Amplifikation in GBM-Modellen erschwert. Letztere sind jedoch notwendig, um die genauen Mechanismen der Resistenzentwicklung gegen zielgerichtete Therapien besser zu verstehen und im Optimalfall künftig vorhersagen zu können. Der erste notwendige Schritt ist dabei die Verfügbarkeit von geeigneten *in vitro* Zellkulturmodellen.
Jedoch beobachtet man einen kompletten Verlust von extrachromosomaler EGFR-Amplifikation in konventionellen GBM-Zellkulturen mit Serum-supplementiertem (FKS; fötales Kälberserum) Medium [55,56]. Somit ist das gängigste Zellkulturmodell für die gezielte Analyse von EGFR-amplifikationspezifischen Auswirkungen bei Glioblastomzellen nicht geeignet.
Doch nicht nur aus diesem Grund treten andere Formen der Zellkultur weiter in den Vordergrund. So ist mittlerweile Konsens, dass dreidimensionale Zellkulturmodelle, in denen GBM-Tumorzellen als multizelluläre Sphäroide in Suspension wachsen, Morphologie und Zell-Zell-Interaktionen eines Tumors besser nachbilden, als adhärent wachsende Zellkulturen [57-59].
Dazu wurden GBM-Zellen in serumfreiem Medium supplementiert mit B-27, FGF und EGF kultiviert (im Folgenden als „SC-Medium“ bezeichnet) [55,56,60]. Unter diesen Bedingungen wurde auch häufig eine spontane Sphäroidbildung von GBM-Zellen beobachtet [55,56,60].

Eine detaillierte Untersuchung der Genexpressionsprofile von 71 GBM-Sphäroidkulturen etabliert aus GBM Gewebematerial von 68 Patienten zeigte, dass wichtige Aspekte der GBM-Biologie in dreidimensionalen Sphäroidmodellen erhalten bleiben [61]. Die molekulare Subklassifizierung des ursprünglichen Glioblastoms (klassisch, mesenchymal, proneural oder neural) war in vielen Fällen auch im entsprechenden Sphäroidmodell nachweisbar [61].

Außerdem konnten neben eigenen Studien auch weitere Studien zeigen, dass die Kultivierung von GBM-Zellen ausgehend von Tumorgewebe mit EGFR-Amplifikation in serumfreien Medien und definierter Wachstumsfaktor-Konzentration zur Erhaltung der EGFR-Amplifikation *in vitro* führt [55,56,60,62]. Dabei scheint die Erhaltung der EGFR Amplifikation *in vitro* abhängig von der verfügbaren EGF-Konzentration zu sein.

Wir konnten zeigen, dass aus Tumorgewebe etablierte GBM-Zelllinien unter Konditionen mit geringen EGF-Konzentrationen ihre EGFR Amplifikation beibehalten [55]. Ähnliches konnten auch weitere Studien belegen [56,60,62]. Stockhausen *et al*. demonstrierten, dass die EGFR Amplifikation in Zellkulturen erhalten blieb, die in SC-Medium mit 10 ng/ml FGF und 10 ng/ml EGF kultiviert wurden [56]. Weiterhin zeigten Schulte *et al*., dass die EGFR Kopiezahl von frisch aus Gewebe etablierten GBM-Zelllinien in SC Medium mit hohen EGF Konzentrationen von 20 ng/ml abnimmt [60]. Bei niedrigen EGF Konzentrationen von 0 ng/ml und 5 ng/ml wiesen die Zelllinien noch eine EGFR Amplifikation auf [60].

Während in der Studie von Stockhausen *et al*. unter Zugabe von 10 ng/ml EGF die Amplifikation von EGFR erhalten blieb, zeigte sich in der Studie von Schulte *et al*. ein Verlust der EGFR Amplifikation in einer der getesteten Zelllinien unter diesen Bedingungen [56,60].

Eigene Daten zeigten ähnliche Ergebnisse unter *in vitro* Bedingungen mit 10 ng/ml EGF [55]. Ausgehend von patientenindividuellen GBM Xenografts (GBM-PDX; patient derived xenograft), die eine Amplifikation des EGFR Gens aufwiesen, wurden Zelllinien in SC-Medium mit unterschiedlichen EGF Konzentrationen etabliert [55]. Ein besonderes Augenmerk lag dabei auf der Analyse von *in vitro* Konditionen mit geringen EGF Konzentrationen von 0 ng/ml bis 2,5 ng/ml in 0,5 ng/ml Intervallen [55].

Aufgrund vorangegangener Studien anderer Arbeitsgruppen, die einen Zusammenhang zwischen EGF-Konzentration und EGFR-Amplifikation *in vitro* zeigten, war es naheliegend, zu untersuchen ob sich die EGFR-Amplifikation *in vitro* durch die Steuerung der Ligandenzufuhr gezielt modulieren lässt [56,60]. Wir konnten anhand von zwei GBM-PDX Zelllinien mit EGFR-Amplifikation im Ursprungs-Gewebe bestätigen, dass die Amplifikation des EGFR Gens mit 0 ng/ml bis 2,5 ng/ml EGF über mindestens 10 Passagen *in vitro* erhalten bleibt [55].

Dabei konnte kein Unterschied in der Ausprägung der EGFR-Amplifikation zwischen allen Konditionen von 0 ng/ml EGF bis 2,5 ng/ml EGF festgestellt werden [55]. Zudem konnten wir ebenfalls den bereits nach wenigen *in vitro* Passagen eintretenden Verlust der EGFR-Amplifikation unter Zugabe von 30 ng/ml EGF beobachten [55].

Im Fall von xHROG33 konnte auch eine Zelllinie unter Standardbedingungen (10% FKS-Supplementierung) etabliert werden. Diese zeigte ebenfalls einen rapiden Verlust der EGFR-Amplifikation nach nur wenigen Passagen *in vitro* [55].

Eine mögliche Ursache dafür könnte das durch FKS-Supplementierung verursachte Überangebot an Wachstumsfaktoren sein. Durch die ausreichende Versorgung mit in FKS enthaltenen Wachstumsfaktoren entfällt möglichweise ein selektiver Druck für die Erhaltung zusätzlicher EGFR-Genkopien sowie die damit einhergehende Rezeptor-Produktion. Auch die Zugabe einer hohen EGF-Menge (30 ng/ml [55], bzw. 20 ng/ml [60]) verursacht einen EGFR-Amplifikationsverlust nach wenigen Passagen *in vitro*.

Es ist denkbar, dass Zellen ohne EGFR-Amplifikation unter diesen Bedingungen positiv selektiert werden [36,63]. Jedoch sollte in diesem Fall ein durch Liganden-Überschuss verursachter Verlust der EGFR-Amplifikation *in vitro* stabil sein. Eigene Daten zeigten jedoch, dass der in zwei GBM-PDX Zelllinien (xHROG33 und xHROG59), durch EGF-Überschuss verursachte Verlust der EGFR-Amplifikation durch EGF-Entzug reversibel ist [55].

Beide Zelllinien zeigten nach Umstellung von 30 ng/ml EGF auf 0 ng/ml EGF innerhalb weniger Passagen einen Wiederanstieg der EGFR-Amplifikation [55]. Auch die mit dem EGFR-Amplifikationsverlust einhergehende verringerte EGFR Proteinexpression stieg nach EGF-Entzug wieder an [55]. Diese Daten sind vergleichbar mit denen aus der Studie

von Mazzoleni *et al*. in der nach Reduktion der EGF-Menge von 20 ng/ml EGF auf 5 ng/ml EGF ein Wiederanstieg der EGFR-Expression beobachtet wurde [62].

Interessanterweise führte der Entzug von EGF *in vitro* in Zelllinien, die zuvor mit hohen EGF-Konzentrationen kultiviert wurden zum Proliferationsstop und im Folgenden zum Absterben der Zellen in anderen Studien [60,64].

Das lässt vermuten, dass mehrere Mechanismen bei der Aufrechterhaltung bzw. Wiederherstellung der EGFR-Amplifikation *in vitro* zum Tragen kommen. Neben der Selektion von Zellen ohne EGFR-Amplifikation durch äußere Einflüsse wie Ligandenüberschuss konnte auch gezeigt werden, dass eine Adaption stattfinden und die EGFR-Amplifikation den Umständen flexibel angepasst werden kann [38,55].

Ein ähnlicher Effekt der Wiederherstellung einer extrachromosomalen EGFR-Amplifikation wurde in einer Studie mit dem EGFR-Inhibitor Erlotinib beobachtet [54]. Nathanson *et al*. beobachteten einen Verlust der extrachromosomalen EGFR-Amplifikation, wenn GBM-Zellen *in vitro* mit Erlotinib behandelt wurden [54]. Nach Entfernung des Inhibitors war die extrachromosomale Amplifikation von EGFR wieder nachweisbar [54].

Obwohl der jeweilige Auslöser für den Verlust der extrachromosomalen EGFR-Amplifikation verschieden ist – EGFR-Inhibition durch Erlotinib [54] oder EGF-Überschuss [55,62] – könnte der Mechanismus von Verlust und Wiederherstellung der Genamplifikation möglichweise ähnlich sein. So konnte in der Studie von Nathanson *et al*. die Bildung eines sogenannten Marker-Chromosoms unter Erlotinib-Behandlung nachgewiesen werden. Dieses bestand aus Genkopien von EGFR und könnte daher als „EGFR-Reservoir“ dienen und so den Zellen nach der Entfernung des Inhibitors die Wiederherstellung der extrachromosomalen EGFR-Amplifikation ermöglichen [54].

Jedoch bleibt unklar, unter welchen Bedingungen eine Wiederherstellung der zurückgegangenen EGFR-Amplifikation erfolgen kann oder wann die Zellen, wie in anderen Studien beobachtet wurde, durch Entzug von EGF absterben [60,64]. Dabei kommen neben Selektionsprozessen und möglicher Adaption der Zellen in Abhängigkeit von ihrer Mikroumgebung zellintrinsische Merkmale, wie beispielsweise der Grad der Differenzierung infrage.

In der Tat legen Studien einen Zusammenhang zwischen EGFR-Amplifikation bzw. EGFRvIII-Amplifikation, die in vielen Fällen mit der Wildtyp-Rezeptor-Amplifikation einhergeht, und CSCs nahe [62,64,65]. So konnte gezeigt werden, dass EGFRvIII präferentiell in CD133-positiven (CD133+) Zellen exprimiert wird [65].

CD133 ist zwar der prominenteste Marker zur Identifikation von GBM-CSCs, jedoch ist dessen Aussagekraft zunehmend umstritten [66-68]. Doch auch auf funktionaler Ebene konnte die Studie von Emlet *et al*. nachweisen, dass EGFRvIII+/CD133+ Zellen im Vergleich zu EGFRvIII+/CD133- und EGFRvIII-/CD133- Zellen das höchste Tumorigenitätspotential *in vitro* aufwiesen [65]. Diese Studie berücksichtigte jedoch nicht die Amplifikation des Wildtyp Rezeptors.

Jedoch belegen weitere Studien, dass GBM-Zelllinien die in serumfreiem Medium als multizelluläre Sphäroide kultiviert wurden und eine EGFR/EGFRvIII-Amplifikation aufweisen, tumorigener sind als differenzierte GBM-Zellen bzw. GBM-Zellen ohne EGFR/EGFRvIII-Amplifikation [60,62,69]. Zudem führte die Zugabe von FKS zum Verlust der EGFR/EGFRvIII-Amplifikation *in vitro* sowie zu einer morphologischen Veränderung der GBM-Zelllinien [65,69].

GBM-Zelllinien, die unter serumfreien Bedingungen als multizelluläre Sphäroide dreidimensional in Suspension wuchsen, wiesen nach Zugabe von FKS ein adhärentes Zellwachstum auf [69]. Zudem stieg die Expression von GFAP (glial fibrillary acidic protein) nach FKS-Zugabe an, was auf einen höheren Differenzierungsgrad der Zellen hindeutet [69].

Ähnliche Effekte wurden in dieser Studie auch durch Zugabe von Retinoidsäure (retinoic acid; RA) erzielt [69]. RA induziert die Zelldifferenzierung, wodurch CSCs ihr malignes Tumorigenitätspotential verlieren [70,71].

Diese Strategie könnte therapeutisch an Bedeutung gewinnen, insbesondere da bei mehreren Tumorentitäten von der Existenz von CSCs ausgegangen werden muss [11-13,21-23].

Obgleich die Zugabe von RA in geringerem Maße zur Erhöhung der Expression von GFAP führte, als die Zugabe von FKS, senkten beide Substanzen in ähnlicher Weise die Expression von EGFR und EGFRvIII [69]. Zudem führte die Behandlung von GBM-CSCs

mit einem Tyrosinkinase-Inhibitor (AG1478), der die Phosphorylierung und somit Aktivierung von EGFR unterbindet, zu einer gesteigerten Expression von GFAP in diesen Zellen [69].

So gibt es zunehmend Hinweise dafür, dass eine erhöhte Expression von EGFR bzw. EGFRvIII bei Glioblastomen mit einem CSC-Phänotyp assoziiert ist [60,62,64,65,69]. Das könnte eine mögliche Ursache dafür sein, dass der Entzug von EGF *in vitro* nicht in allen Fällen zu einer Wiederherstellung der EGFR-Amplifikation führt.

Es wäre denkbar, dass der Verlust der extrachromosomalen EGFR-Amplifikation und die damit einhergehende geringere EGFR Expression nach Zugabe von hohen Mengen EGF *in vitro* eine Zelldifferenzierung initiiert. Diesem Gedanken folgend könnte die Dauer der Kultivierung von ursprünglich EGFR-amplifizierten GBM-Zellen mit hohen EGF-Konzentrationen im Medium bedeutend für eine spätere Wiederherstellbarkeit der EGFR-Amplifikation durch EGF-Entzug sein.

Möglicherweise kann *in vitro* ein „point of no return“ erreicht werden, ab dem eine induzierte Zelldifferenzierung unter den untersuchten Bedingungen (SC-Medium und EGF-Entzug) nicht mehr rückgängig gemacht werden kann. Weiterhin erscheint es möglich, dass die Ursache für die unterschiedlichen Effekte von EGF-Entzug nach Kultivierung mit hohen EGF-Konzentrationen auch in der für Glioblastome typischen Heterogenität begründet liegen kann.

Das sind jedoch rein spekulative Annahmen, die experimentell zukünftig weiter untersucht werden müssen.

Die Form der dreidimensionalen Sphäroidkultur von Tumor-Zelllinien unter serumfreien Bedingungen erlaubt jedoch allgemein eine realitätsnähere *in vitro* Analyse, insbesondere von CSCs [57-59].

Das trifft nicht nur auf Glioblastom-Zellen zu, sondern auch auf *in vitro* Modelle anderer Tumorentitäten [72]. Dementsprechend wäre es auch denkbar, dass CSCs verschiedener Tumorentitäten möglicherweise eine gemeinsame Schwachstelle besitzen, die man therapeutisch nutzbar machen könnte.

Eine Analyse des Proteoms von CSCs verschiedener Tumorentitäten zeigte, dass CSCs eine deutlich höhere Expression von Proteinen, die mit Mitochondrien assoziiert sind,

aufweisen als adhärente *in vitro* Modelle der entsprechenden Tumoren [73]. Dies stünde auch im Einklang mit der Hypothese, dass CSCs einen anabolen Stoffwechsel aufweisen und daher vermehrt auf Mitochondrien angewiesen sind [73].

Diese erhöhte Abhängigkeit von Mitochondrien könnte jedoch auch einen Ansatzpunkt für die gezielte Inhibierung von CSCs darstellen [74]. So konnte gezeigt werden, dass einige Antibiotika effektiv CSCs inhibieren können [74].

Toxizität gegen Mitochondrien ist eine bekannte Nebenwirkung einiger Antibiotika-Klassen, wie beispielsweise der Tetrazykline oder der Erythromyzine [74]. Diese binden selektiv an die kleine Untereinheit (Tetrazykline) oder die große Untereinheit (Erythromyzine) mitochondrieller Ribosomen und inhibieren somit die Proteinsynthese [74].

Weiterhin hätte eine (Chemo-)Therapie-Ergänzung durch Antibiotika den Vorteil, dass es sich bei Letzteren um bereits bekannte und zugelassene Medikamente handelt. Somit wären die Hürden für die Übertragbarkeit dieses Konzeptes in klinische Studien vergleichsweise gering.

Bei Glioblastomen wäre ein weiterer interessanter Aspekt einer möglichen Ergänzung der Chemotherapie mit Temozolomid (TMZ) durch Zugabe von Antibiotika die Eindämmung von TMZ-induzierten Effekten auf CSCs. Eine Studie hat belegt, dass klinisch relevante Dosen von TMZ zu einer Konversion von differenzierten GBM-Zellen in einen CSC-Phänotyp *in vitro* führen können [27].

Als klinisch relevante Dosis wurden dabei Konzentrationen definiert, die im Serum (50µM TMZ) oder im Liquor (5µM TMZ) von Patienten gemessen werden konnten [75-78]. Dabei zeigte sich bei primären, von frischem GBM Gewebe etablierten Zelllinien und auch bei bereits länger etablierten Zelllinien (z.B. U251) ein Anstieg der CSC Population nach TMZ Behandlung *in vitro* und *in vivo* [27]. Zudem wurde gezeigt, dass es sich primär um eine phänotypische Umwandlung von differenzierten non-CSCs in CSCs handelt und nicht um eine durch TMZ verursachte Selektion bzw. Anreicherung von CSCs [27].

Diese konvertierten CSCs zeigten eine gesteigerte Expression von mit Pluripotenz assoziierten Markern wie CD133, SOX2, Oct4 und Nestin [27]. Nach Implantation dieser

Zellen in Nacktmäuse bildeten sich mit größerer Effizienz als bei implantierten non-CSCs Tumoren mit einem invasiven Phänotyp [27].

Demnach scheint ein Tumor nicht ausschließlich einer hierarchischen Zellordnung zu unterliegen, bei der – der Tumorstammzellhypothese [23] folgend – eine CSC-Subpopulation innerhalb des Tumors vorhanden ist, aus der ausdifferenzierte Tumorzellen hervorgehen, welche dann die Hauptmasse des Tumors bilden [22-26]. Es besteht auch die Möglichkeit der De-Differenzierung von Tumorzellen, wobei die Mechanismen noch nicht vollständig geklärt sind [12,21,22].

Diese De-Differenzierung kann im Fall von Glioblastomen durch Exposition mit TMZ hervorgerufen werden [27]. Dies könnte ein weiterer Resistenzmechanismus von GBM-Zellen gegen TMZ sein [27]. Eine durch TMZ hervorgerufene De-Differenzierung von undifferenzierten GBM-Zellen könnte so auch die Entstehung von Rezidiven begünstigen [27]. Dieser Effekt könnte durch eine Therapie-Ergänzung mit Substanzen wie Doxyzyklin (Dox), die CSC-inhibierend wirken, möglicherweise eingedämmt oder gar unterbunden werden [74,79].

Diese Hypothese wurde anhand von 4 primären patientenindividuellen GBM-Zelllinien *in vitro* untersucht [79]. Dabei wurden Parameter wie Zellviabilität, Tumorigenität sowie die Expression verschiedener GBM-CSC Marker und die Menge der Mitochondrien in den Zelllinien unter Behandlung mit TMZ, Dox und einer Kombination aus beiden Medikamenten analysiert [79].

Bei Zutreffen der Hypothese einer TMZ-induzierten De-Differenzierung, müsste die Behandlung mit TMZ eine tumorigenitätssteigernde Wirkung haben, welche sich durch Zugabe von Dox eindämmen lassen sollte [79]. Weiterhin wäre eine gesteigerte Expression von GBM-CSC-Markern wie CD15 und Nestin sowie ein erhöhter Mitochondriengehalt unter TMZ-Gabe, nicht jedoch unter Zugabe von Dox, zu erwarten [79].

Die dahingehende Analyse von vier verschiedenen patientenindividuellen GBM-Zelllinien zeigte jedoch, dass mehrere Mechanismen der Therapieresistenz infrage kommen [79]. Tatsächlich zeigte nur eine der vier Zelllinien alle erwarteten Merkmale [79].

Obgleich alle vier untersuchten Zelllinien bei der applizierten Dosis von 50µM TMZ keinen Unterschied in der Zellviabilität im Vergleich zu unbehandelten Kontrollzellen zeigten, stieg die *in vitro* Tumorigenität jedoch in drei von vier Zelllinien an [79].

Bei zwei Zelllinien konnte durch Zugabe von 50µM Dox eine signifikante Reduktion der TMZ-induzierten erhöhten Tumorigenität *in vitro* erreicht werden; bei einer dritten Zelllinie zeigte sich zumindest ein Trend (p=0,066) zur Reduktion der Tumorigenität [79]. Das ist zumindest auf funktionaler Ebene ein möglicher Hinweis für eine TMZ-induzierte De-Differenzierung von GBM-Zellen in drei untersuchten Zelllinien [79]. Jedoch zeigte sich bei zwei dieser Zelllinien keine Steigerung der Nestin-Expression oder des Mitochondriengehalts unter TMZ-Gabe, was auf weitere mögliche TMZ-Resistenz-Mechanismen hindeutet [79].

So wäre es denkbar, dass die Behandlung mit Dox *in vitro* zu proteotoxischem Stress in den Mitochondrien führt und so deren Funktionalität einschränkt ohne dabei die Mitochondrien-Biomasse zu verringern [80]. Dox selbst hatte einen moderaten zytotoxischen Effekt auf alle vier getesteten, primären GBM Zelllinien [79]. Ähnliches wurde in anderen Studien auch bei etablierten GBM-Zellinien (U87 und U251HF) beobachtet [81]. Eine weitere Funktion von Dox ist die unspezifische Inhibition von Matrix-Metalloproteinasen (MMPs) [81]. Dieser Effekt könnte mitverantwortlich für eine reduzierte *in vitro* Tumorigenität nach Dox-Gabe sein [79].

Interessanterweise führte die Behandlung von GBM-Zelllinien mit Dox zu einer erhöhten Expression von MMP2 in einer untersuchten Zelllinie, wohingegen bei einer weiteren Zelllinie unter gleichen Bedingungen eine verringerte MMP2 Expression beobachtet wurde [81].

Dadurch wird deutlich, dass die Wirkung von Dox auf GBM-Zellen auch maßgeblich vom genetischen Hintergrund einer individuellen Zelllinie abhängig ist [79,81].

In einer eigenen Studie zeigte eine der vier untersuchten GBM-Zelllinien keine Reaktion hinsichtlich *in vitro* Tumorigenität oder CSC-Marker Expression nach Behandlung mit TMZ, Dox oder einer Kombination aus beiden Medikamenten [79].

Jedoch zeigte sich bei dieser sonst unresponsiven Zelllinie eine deutliche Reduktion des Mitochondrien-Gehalts der Zellen unter Behandlung mit TMZ, Dox oder der Kombinationstherapie [79].

Dies erlaubt Spekulationen über weitere Mechanismen von Tumorzellen, die bei einer Häufung dysfunktionaler Mitochondrien in den Zellen zum Tragen kommen können.

So wäre denkbar, dass die effektive Reduktion dysfunktionaler Mitochondrien für Tumorzellen geeignet ist, einen durch diese dysfunktionalen Mitochondrien verursachten Phänotyp zu kompensieren [82]. Ähnliches konnte bei einer Studie an mit Parkinson-assoziierten Genen gezeigt werden [82].

In dieser Studie wurde die Mitochondrien-Dysfunktionalität durch den Verlust von Mortalin induziert, der häufig in den Gehirnzellen von Parkinson Patienten auftritt [82]. Mortalin ist essenziell für effektiven Import und korrekte Faltung von mitochondriellen Matrix-Proteinen sowie für den Abbau von fehlerhaften Mitochondrien-Proteinen [83,84].

Als solches hat Mortalin eine zentrale Stellung bei der Stress-Antwort von Mitochondrien und programmiertem Zelltod [85,86].

Der durch Mortalin-Verlust ausgelöste Phänotyp konnte durch Parkin und PINK1 vermittelten, erhöhten lysosomalen Abbau von defekten Mitochondrien kompensiert werden, wodurch weitere Zellschäden verhindert wurden – ein intakter Autophagie-Apparat vorausgesetzt [82].

Parkin und PINK1 sind wichtige Regulatoren in der zellulären Qualitätskontrolle von Mitochondrien [82]. Mutationen in diesen Genen sind ebenfalls mit Neurodegeneration und Parkinson [87,88].

Es wäre denkbar, dass auch bei Glioblastomen über einen ähnlichen Mechanismus vermittelter Abbau dysfunktionaler Mitochondrien zu einer Kompensation des so induzierten Phänotyps führen kann. Das könnte eine weitere mögliche Erklärung für die beobachtete Reduktion der Mitochondrien-Biomasse nach Dox-Behandlung sein [79].

Obwohl sich alle vier Zelllinien in unserer Studie insgesamt unter TMZ-Behandlung recht unterschiedlich verhielten, zeigten jene drei Zelllinien, bei denen TMZ zu einer erhöhten Tumorigenität *in vitro* führte, auch eine erhöhte Expression des CSC-Markers CD15 [79].

Die immunhistochemische Analyse der Expression von CD15 und Nestin an formalin-fixiertem, paraffin-eingebettetem (FFPE) GBM-Gewebe von zwei verschiedenen GBM-Fällen zeigte ähnliche Resultate [79].

Diese Fälle stammen aus dem Archiv des Instituts für Pathologie der Universitätsmedizin Rostock und repräsentieren GBM-Gewebe-Material von zwei Patienten, bei denen jeweils sowohl das neu auftretende GBM als auch das rezidivierende GBM in Rostock operiert wurde.

Von beiden Fällen wurden Gewebe der jeweiligen Glioblastome vor Beginn der Chemotherapie mit TMZ sowie das Gewebe des entsprechenden Rezidivs post Chemotherapie analysiert [79].

Trotz recht heterogener Distribution der Signale wurde ersichtlich, dass CD15 in beiden Fällen im Rezidiv höher exprimiert wurde als im entsprechenden GBM vor Chemotherapie mit TMZ [79]. Die Expression von Nestin war in beiden klinischen Fällen zwischen pre und post Chemotherapie Tumor nicht verändert [79]. Dementsprechend wäre es denkbar, dass die erhöhte CD15 Expression nach Behandlung mit TMZ *in vitro* und in zwei GBM Rezidiven *in vivo* eher der intrinsischen Funktion von CD15 geschuldet ist und weniger der Rolle von CD15 als GBM-CSC Marker [79].

CD15 gehört zur Familie der Fucosyltransferasen (FUTs), welche für den Aufbau von fucosylierten Kohlenhydratstrukturen bedeutsam sind [89]. Interessanterweise ist bislang wenig über die genauen Auswirkungen von erhöhter CD15 Expression bei Glioblastomen bekannt.

In der epidermoiden Karzinom-Zelllinie A431 wurde CD15 mit gesteigerter Proliferation und Zellzyklus-Progression in Assoziation mit PI3K/Akt und MAPK in Verbindung gebracht [90]. Weiterhin wurden neben CD15 auch weitere Mitglieder der FUT-Familie mit durch PI3K/Akt vermittelte Therapie-Resistenz in Leberkarzinom-Zellen *in vitro* in Verbindung gebracht [91]. Dabei waren erhöhte FUT4 (CD15), FUT6 und FUT8 Level verantwortlich für die Resistenz gegen Chemotherapeutika wie 5-Fluoruracil von Leberkarzinom-Zellen *in vitro* und *in vivo* [91].

Zudem ließ sich durch Modulation von FUT4, FUT6 und FUT8 in diesen Zellen die Aktivität der PI3K/Akt Signalkaskade sowie die Expression von MRP1 (Multi drug resistance related protein 1) direkt regulieren [91].

Die PI3K/Akt Signalkaskade ist in Glioblastomen häufig dereguliert und könnte in Zusammenhang mit Fucosyltransferasen wie CD15 ebenfalls zu gesteigerter Therapie-Resistenz beitragen [40,92].

Darüber hinaus gibt es Hinweise für die erhöhte Expression von fucosylierten Glykanen in anderen Tumorentitäten, unter anderem bei Mamma-Karzinomen, bei Lungen-Karzinomen und bei kolorektalen Karzinomen [93-96]. Gesteigerte CD15 Expression hat durch die Verringerung der Wirksamkeit von EGFR- oder VEGF-Inhibitoren klinische Relevanz in metastasierenden kolorektalen Karzinomen [97].

Somit ist es naheliegend, den Einfluss von CD15 auf die Entwicklung von Resistenzen gegen Therapeutika sowie die genauen Mechanismen auch bei Glioblastomen zu untersuchen.

Die bei Glioblastomen häufig vorkommende Deregulation der PI3K/Akt/mTOR Signalkaskade wird häufig durch genetische Aberrationen des EGFR Gens verursacht [14,44,92]. Daher ist EGFR auch bei GBM ein möglicher Ansatzpunkt für therapeutische Interventionen [28,40,41]. Sowohl für eine Beeinflussung der PI3K/Akt Signalkaskade als auch für die Wirksamkeits-Verringerung von EGFR-Inhibitoren wurde ein Zusammenhang mit CD15 für andere Tumorentitäten beschrieben [93-97].

Jedoch zeigt eine Datenbank-Analyse zu Alterationen in CD15 von 585 GBM-Fällen lediglich 1,5% der Fälle eine Alteration von CD15 [98,99]. Analysiert wurden dabei die mRNA-Expression, Anzahl der Genkopien und auftretende Mutationen [98,99]. Im Vergleich dazu zeigte eine Analyse von EGFR in der gleichen Kohorte Alterationen von EGFR in 46% der Fälle.

Die große Mehrzahl des in diesen Studien analysierten GBM-Gewebes stammt von Patienten, die vor der Resektion des Tumors noch keine Chemotherapie oder Bestrahlung erhalten haben [92].

Das unterstützt die Hypothese, dass eine Steigerung der CD15 Expression möglicherweise als Reaktion auf eine therapeutische Intervention wie beispielsweise eine

Chemotherapie mit TMZ erfolgt und so zur Resistenz gegen die Therapie beitragen könnte. Das wäre ein weiterer, bislang bei Glioblastomen nicht näher untersuchter, Resistenzmechanismus gegen das Standardtherapeutikum TMZ [79]. Zahlreiche Studien mit GBM-Zelllinien *in vitro* verdeutlichten, dass es mehrere sich gegebenenfalls auch ergänzende Resistenzmechanismen gegen TMZ gibt [22,27,79,97]. Zudem wurde ebenso deutlich, dass diese maßgeblich auch vom genetischen Hintergrund eines individuellen Tumors bzw. einer individuellen Zelllinie abhängig sind [79-81]. Das unterstreicht die Notwendigkeit für patienten- bzw. tumorindividuelle Modelle nicht nur in der Zellkultur, sondern auch in entsprechenden präklinischen Tiermodellen. Um *in vitro* identifizierte Zielstrukturen für Therapeutika auf ihren klinischen Nutzen zu überprüfen, sind adäquate Tiermodelle unumgänglich [100].

Eine mittlerweile gängige Methode ist die Etablierung von patientenindividuellen Xenografts, sogenannten PDX (patient-derived xenograft) Modellen [101,102]. Dabei werden Tumorzellen oder Tumorgewebe in immunsupprimierte Versuchstiere – meist Mäuse – injiziert und wachsen zu einem Xenografttumor heran [101-103].

Dabei wird zwischen orthotopen und heterotopen Xenografts unterschieden. Bei orthotopen GBM Modellen werden Tumorzellen bzw. Gewebe direkt an einer definierten Stelle stereotaktisch in das Gehirn des Versuchstiers injiziert [103]. Das bietet den Vorteil einer anatomisch und physiologisch realistischeren Umgebung für das Xenograft, als die subkutane Implantation von GBM-Gewebe in die Flanke des Versuchstiers (heterotopes Xenograft) [100,103].

Trotz der physiologisch abweichenden Umgebung der heterotopen, subkutanen GBM Xenografts bieten diese dennoch zahlreiche Vorteile. So bleiben, wie auch bei den orthotopen Modellen, die intratumorale Heterogenität und genomische Aberrationen weitgehend erhalten [100,103]. Ein großer Vorteil von heterotopen GBM-PDX gegenüber der orthotopen Modelle ist die Generierung von größeren Mengen Gewebe für weiterführende molekularbiologische und funktionale Analysen ermöglichen [106,107].

Ein weiterer wichtiger Aspekt ist die vergleichsweise einfachere technische Umsetzung, wodurch die Etablierung heterotoper Modelle weit verbreitet ist [106,107]. Dennoch ist die

Zusammenarbeit mehrerer Abteilungen auch bei der Etablierung von heterotopen GBM PDX ausschlaggebend [106,107].

Logistische Prozesse, sowie die Bereitstellung und Einhaltung standardisierter Protokolle müssen meist abteilungsübergreifend zwischen Chirurgie, Forschungslaboren und Versuchstieranlagen gewährleistet werden [106,107]. Ein Problem bei der Etablierung von subkutanen GBM-PDX ist jedoch die geringe Erfolgsquote von etwa 20-25% [108]. Dabei spielen verschiedene Faktoren eine Rolle.

Darunter sind schwer zu beeinflussende Faktoren, wie die Qualität des Tumorgewebes für die Implantation [106,107,109]. So ist beispielsweise der Anteil an vitalen Tumorzellen in einem Gewebestück makroskopisch nicht ohne weiteres feststellbar, kann aber einen Einfluss auf die erfolgreiche Etablierung eines PDX Models haben.

Beeinflussbare Faktoren sind hingegen beispielsweise die Wahl des Mausstamms für die PDX-Etablierung, sowie die Optimierung der Arbeitsabläufe. Studien über die Etablierung von PDX anderer Tumorentitäten zeigten, dass sich auch vital eingefrorenes Tumorgewebe für die Etablierung subkutaner PDX Modelle eignet [107].

Ein direkter Vergleich der Implantation von frischem GBM-Gewebe und vital eingefrorenem GBM-Gewebe zeigte keine Unterschiede bei der Erfolgsrate [106]. Durch die Möglichkeit GBM-Gewebe vital einzufrieren und über einen längeren Zeitraum lagern zu können bevor es für die PDX-Etablierung verwendet wird, fallen viele logistische Hürden bei diesem Prozess weg [106]. Das führt wiederum zu einer besseren Standardisierung aller essentiellen Arbeitsschritte, wie beispielsweise die Transportkonditionen und Transportzeit des Gewebes sowie die Verfügbarkeit geeigneter Mäuse für die Transplantation [106,107].

Interessanterweise haben wir in keinem der getesteten GBM-Fälle die erfolgreiche Etablierung eines PDX ausgehend von frischem und vital eingefrorenem Gewebe des gleichen Falles beobachten können [106].

Das könnte auf mögliche Einflüsse der Gewebequalität selbst hindeuten, unabhängig davon ob es eingefroren wurde oder frisch implantiert wurde [106]. Es ist auch denkbar, dass individuelle mausspezifische Faktoren eine Rolle bei der erfolgreichen PDX-Etablierung spielen könnten, die jedoch bislang unbekannt sind [109].

Auch die Wahl des Mausstamms kann bei der PDX-Generierung eine Rolle spielen. Zwei gängige Mausstämme zur Generierung von PDX Modellen sind NOD/SCID Mäuse und NMRI Foxn1nu Mäuse [103-105].

NOD/SCID Mäuse verfügen über keine funktionellen B- und T-Lymphozyten oder natürliche Killerzellen (NK-Zellen), die mit dem erfolgreichen Anwachsen des Xenografts interferieren könnten [104]. Dahingegen fehlen bei NMRI Foxn1nu Mäuse lediglich funktionale T-Lymphozyten, B-Lymphozyten sowie NK-Zellen sind in diesem Mausstamm funktional vorhanden [105].

Ein direkter Vergleich zwischen NOD/SCID Mäusen und NMRI Foxn1nu Mäusen zeigte leicht höhere Erfolgsraten bei der PDX-Etablierung in NOD/SCID Mäusen [106]. GBM-Gewebe von 18 Fällen wurde für diesen Vergleich subkutan in die Flanken beider Mausstämme implantiert [106]. Dabei zeigte sich, dass die Erfolgsrate bei NOD/SCID Mäusen (38,8%) etwas höher war als beim Einsatz von NMRI Foxn1nu Mäusen (27,7%) [106]. Aufgrund der übersichtlichen Fallzahl sind diese Ergebnisse jedoch mit Vorsicht zu betrachten.

Dennoch wäre der Trend durch die immunologischen Eigenschaften der beiden Mausstämme erklärbar. So könnte das Vorhandensein des angeborenen Immunsystems bei NMRI Foxn1nu Mäusen zur geringeren Erfolgsrate bei der GBM PDX Etablierung beitragen [105,106].

Die Existenz eines intakten angeborenen Immunsystems ist allerdings auch ein Argument für die Verwendung von NMRI Foxn1nu Mäusen für GBM-PDX Studien. Insbesondere im Hinblick auf den Einsatz von PDX Modellen in der Erforschung der Wirksamkeit neuer Therapien oder Wirkstoffe gegen Glioblastome erlauben NMRI Foxn1nu Mäuse die Berücksichtigung möglicher Einflüsse des angeborenen Immunsystems.

Ein generell wichtiger Punkt ist eine möglichst hohe Übereinstimmung in den Eigenschaften des ursprünglichen GBMs und dem PDX das daraus hervorgegangen ist. Dabei ist zum einen die histologische Ähnlichkeit zwischen Originaltumor und PDX auch über mehrere *in vivo* Passagen hinweg wichtig.

In unserer Kohorte von erfolgreich etablierten GBM-PDX wurden zwei Fälle sowie zwei *in vivo* Passagen der dazugehörigen PDX-Tumoren histologisch verglichen [106]. Dazu wurden Gewebeschnitte angefertigt und mit Hämatoxylin und Eosin (HE) angefärbt [106]. In beiden Fällen finden sich histologische Charakteristika von Glioblastomen sowohl im Originaltumor als auch in den entsprechenden Xenografts [106]. In beiden Fällen stimmten auch wichtige Merkmale wie der Anteil mitotischer Zellen innerhalb des Gewebes und auftretende Nekrosen, die für Glioblastome typisch sind, zwischen Originaltumor und PDX überein [106].

Zudem konnten beide PDX Modelle von einem erfahrenen Neuropathologen auch formal als Glioblastom diagnostiziert werden [106]. Außerdem zeigte ein positiver immunhistochemischer Nachweis von GFAP bei PDX-Gewebeschnitten, dass diese einen neuronalen Charakter aufweisen [106].

Darüber hinaus zeigte auch eine vergleichende Mutationsanalyse zwischen Originaltumoren und ihren entsprechenden PDX-Modellen, dass im Originaltumor auftretende Mutationen in den Xenografts über mehrere *in vivo* Passagen erhalten blieben [106].

Auch eine im ursprünglichen GBM vorhandene Amplifikation des EGFR Gens konnte auch in den entsprechenden PDX Modellen nachgewiesen werden [55,56,106]. Jedoch ist der Grad der EGFR-Amplifikation in diesen *in vivo* Modellen variabel [56,106].

In unserer Kohorte von GBM-Fällen, bei denen erfolgreich heterotope Mausmodelle etabliert werden konnten (n=8), wurde ebenfalls eine EGFR-Amplifikation in jenen Fällen nachgewiesen, in denen diese auch beim ursprünglichen Tumor vorlag (n=6) [106]. Dabei schwankte der Grad der EGFR-Amplifikation über mehrere Passagen *in vivo* allerdings teilweise beträchtlich [106]. Tendenziell wurde aber eine Steigerung der EGFR-Amplifikation im Vergleich zum jeweiligen Ursprungstumor beobachtet. Jedoch war diese Steigerung bei den zwei Fällen, in denen die Xenografts über fünf *in vivo* Passagen im Verlauf analysiert werden konnten, nicht kontinuierlich [106].

Das wurde bei dem GBM-PDX Modell HROG59 besonders deutlich: der Ursprungstumor wies eine 12-fache Erhöhung der EGFR-Genkopiezahl auf, die im PDX Modell in Passage

3 auf 92-fach anstieg, jedoch in Passage 5 nur noch eine 36-fache EGFR-Amplifikation aufwies [106].

Es ist naheliegend, dass die Ursache dafür in klonalen Selektionsprozessen liegt.

Da Tumorzellen, die eine EGFR-Amplifikation tragen nicht gleichmäßig innerhalb des Tumorgewebes verteilt sind, wäre es möglich bei einer (Weiter-)Transplantation ein Stück Gewebe mit einer höheren Dichte an EGFR-amplifizierten Tumorzellen zu implantieren [106,110]. Dies könnte zu einer höheren EGFR-Kopiezahl im PDX führen. Umgekehrt könnte die Transplantation eines Gewebestücks mit vergleichsweise geringerer Dichte EGFR-amplifizierter Tumorzellen zu einem PDX mit geringerer EGFR-Kopiezahl führen [106].

Dennoch sind heterotope PDX Modelle wertvolle Ressourcen, die die Entwicklung personalisierter Therapiekonzepte voranbringen können [111,112]. Die technisch einfache Umsetzung dieser Modelle sowie die Möglichkeit der Generierung größerer Mengen Tumorgewebe, als dies bei einem orthotopen Modell möglich wäre, sind große Vorteile subkutaner GBM-Modelle.

Jedoch kann in diesen Modellen das für Glioblastome typische invasive Wachstum in umliegendes Gewebe nicht suffizient nachgebildet werden [106]. Dazu braucht es orthotope GBM-Modelle.

Dennoch können heterotope GBM-PDX Modelle durch die zügige Gewinnung von Tumorgewebe für die systematische und standardisierte Testung therapeutischer Substanzen *in vivo* genutzt werden.

Die standardisierte Testung verschiedener Therapeutika, die auch in der Klinik bereits Anwendung finden, anhand von 5 GBM-PDX zeigte wie erwartet heterogene Ergebnisse [106]. Dies steht im Einklang mit den Ergebnissen anderen GBM-PDX Studien und der Erfahrung aus dem klinischen Umfeld [112, 113].

Innerhalb unserer Kohorte wurde eine gute therapeutische Wirksamkeit von Temozolomid, dem Standardtherapeutikum zur Behandlung von GBM, dem Topoisomerase-Hemmer Irinotecan sowie dem Angiogenese-Hemmer Bevacizumab beobachtet [106]. Eine Kombination aus diesen Medikamenten wurde in einer klinischen Phase II Studie getestet und zeigte in einigen Fällen von inoperablen GBM Wirkung [114].

Somit darf davon ausgegangen werden, dass Studien zur Wirksamkeit (neuer) Medikamente auch in heterotopen GBM-Modellen aussagekräftige Ergebnisse liefern können.

Jedoch gilt es auch in PDX-Modellen, ganz wie bei *in vitro* Zellkultur-Modellen, die Passagenzahl für eine möglichst repräsentative Analyse so gering wie möglich zu halten. Denn auch bei PDX Modellen akkumulieren genetische Veränderungen mit steigender *in vivo* Passagenanzahl [111].

Eine Analyse der Veränderung von Genkopie-Zahlen (CNA; copy number alterations) in PDX verschiedener Tumorentitäten zeigte, dass CNAs mit steigender Zahl der *in vivo* Transfers zügig akkumulieren [111]. Das ist zum Teil durch klonale Selektion erklärbar, da die festgestellte CNA Akkumulation in den PDX mit der spezifischen Aneuploidie und genetischen Heterogenität der jeweiligen Ausgangstumoren korreliert [111].

Jedoch wurden auch CNAs identifiziert, die mit steigender Zahl der *in vivo* Passagen in den PDX Modellen akkumulieren, jedoch nicht mit der Tumorentwicklung im Patienten übereinstimmen [111]. Weiterhin verschwanden CNAs die in den Tumoren und im Verlauf der Tumorentwicklung beobachtet wurden mit der Zeit in den entsprechenden PDX Modellen [111].

Das verdeutlicht, dass CNAs – und potentiell auch weitere genetische Aberrationen – die während der Tumorentwicklung im Patienten einem positiven Selektionsdruck unterliegen, in der PDX-Umgebung keine Rolle mehr spielen und entsprechend negativ selektiert werden [111].

Das kann unter Umständen durchaus auch Effekte auf die Wirksamkeit verschiedener Therapeutika und damit auch Auswirkungen auf die Aussagekraft von präklinischen Studien haben [111].

Dennoch sind patientenindividuelle Tumormodelle, *in vitro* und *in vivo*, unerlässlich um personalisierte Therapieverfahren aus dem Labor in die Kliniken zu bringen.

2. Literatur

[1] Dolecek TA, Propp JM, Stroup NE, Kruchko C. CBTRUS Statistical Report: Primary Brain and Central Nervous System Tumors Diagnosed in the United States in 2005-2009. Neuro-Oncology 2012;14: v1-v49.

[2] Lima FR, Kahn SA, Soletti RC, Biasoli D, Alves T, da Fonseca AC, et al. Glioblastoma: Therapeutic challenges, what lies ahead. Biochim Biophys Acta. 2012;1826(2): 338-49.

[3] Ohgaki H, Kleihues P. Population-Based Studies on Incidence, Survival Rates, and Genetic Alterations in Astrocytic and Oligodendroglial Gliomas. J Neuropathol Exp Neurol. 2005;64(6): 479-89.

[4] Pollo B. Neuropathological diagnosis of brain tumours. Neurological Sciences 2011;32: 209–11.

[5] Levin V. High-Grade Gliomas: Diagnosis and Treatment. Neuro-Oncology 2007;9(3): 378.

[6] Zülch KJ, Bailey P. Brain tumors: Their biology and pathology, 3rd ed. Berlin: Springer, 1986.

[7] Tso CL, Freije WA, Day A, Chen Z, Merriman B, Perlina A, et al. Distinct transcription profiles of primary and secondary glioblastoma subgroups. Cancer Res. 2006;66(1): 159-67.

[8] Verhaak RG, Hoadley KA, Purdom E, Wang V, Qi Y, Wilkerson MD, Miller CR, et al. Integrated genomic analysis identifies clinically relevant subtypes of glioblastoma characterized by abnormalities in PDGFRA, IDH1, EGFR, and NF1. Cancer Cell. 2010;17(1): 98-110.

[9] Aldape K, Zadeh G, Mansouri S, Reifenberger G, von Deimling A. Glioblastoma: pathology, molecular mechanisms and markers. Acta Neuropathol. 2015;129(6): 829-48.

[10] Stupp R, Hegi ME, Mason WP, van den Bent MJ, Taphoorn MJ, Janzer RC, et al. Effects of radiotherapy with concomitant and adjuvant temozolomide versus radiotherapy alone on survival in glioblastoma in a randomised phase III study: 5-year analysis of the EORTC-NCIC trial. Lancet Oncol. 2009;10(5): 459-66.

[11] Hjelmeland AB, Rich JN. The Quest for Self-Identity: Not All Cancer Stem Cells Are the Same. Clin Cancer Res. 2012;18(13): 3495-8.

[12] Meacham CE, Morrison SJ. Tumour heterogeneity and cancer cell plasticity. Nature. 2013;501(7467): 328-37.

[13] Easwaran H, Tsai HC, Baylin SB. Cancer epigenetics: tumor heterogeneity, plasticity of stem-like states, and drug resistance. Mol Cell. 2014;54(5): 716-27.

[14] Furnari FB, Cloughesy TF, Cavenee WK, Mischel PS. Heterogeneity of epidermal growth factor receptor signalling networks in glioblastoma. Nat Rev Cancer. 2015;15(5): 302-10.

[15] Marusyk A, Tabassum DP, Altrock PM, Almendro V, Michor F, Polyak K. Non-cell-autonomous driving of tumour growth supports sub-clonal heterogeneity. Nature. 2014;514(7520): 54-8.

[16] Cleary AS, Leonard TL, Gestl SA, Gunther EJ. Tumour cell heterogeneity maintained by cooperating subclones in Wnt-driven mammary cancers. Nature. 2014;508(7494): 113-7.

[17] Inda MM, Bonavia R, Mukasa A, Narita Y, Sah DW, Vandenberg S, et al. Tumor heterogeneity is an active process maintained by a mutant EGFR-induced cytokine circuit in glioblastoma. Genes Dev. 2010;24: 1731–1745.

[18] Bhat KP, Balasubramaniyan V, Vaillant B, Ezhilarasan R, Hummelink K, Hollingsworth F, et al. Mesenchymal differentiation mediated by NF-kappaB promotes radiation resistance in glioblastoma. Cancer Cell. 2013;24(3): 331-46.

[19] Phillips HS, Kharbanda S, Chen R, Forrest WF, Soriano RH, Wu TD, et al. Molecular subclasses of high-grade glioma predict prognosis, delineate a pattern of disease progression, and resemble stages in neurogenesis. Cancer Cell. 2006;9(3): 157-73.

[20] Patel AP, Tirosh I, Trombetta JJ, Shalek AK, Gillespie SM, Wakimoto H, et al. Single-cell RNA-seq highlights intratumoral heterogeneity in primary glioblastoma. Science. 2014;344(6190): 1396-401.

[21] Shackleton M, Quintana E, Fearon ER, Morrison SJ. Heterogeneity in cancer: cancer stem cells versus clonal evolution. Cell. 2009;138: 822-829.

[22] Persano L, Rampazzo E, Basso G, Viola G. Glioblastoma cancer stem cells: role of the microenvironment and therapeutic targeting. Biochem Pharmacol. 2013;85(5): 612-22.

[23] Reya T, Morrison SJ, Clarke MF, Weissman IL. Stem cells, cancer, and cancer stem cells. Nature. 2001;414(6859): 105-11.

[24] Dirks PB. Brain tumor stem cells: The cancer stem cell hypothesis writ large. Molecular Oncology. 2010;4: 420-430.

[25] Chen R, Nishimura MC, Bumbaca SM, Kharbanda S, Forrest WF, Kasman IM, et al. A hierarchy of self-renewing tumor-initiating cell types in glioblastoma. Cancer Cell. 2010;17(4): 362-75.

[26] Lathia JD, Mack SC, Mulkearns-Hubert EE, Valentim CL, Rich JN. Cancer stem cells in glioblastoma. Genes Dev. 2015;29(12): 1203-17.

[27] Auffinger B, Spencer D, Pytel P, Ahmed AU, Lesniak MS. The role of glioma stem cells in chemotherapy resistance and glioblastoma multiforme recurrence. Expert Rev Neurother. 2015;15(7): 741-52.

[28] Reardon DA, Ligon KL, Chiocca EA, Wen PY. One size should not fit all: advancing toward personalized glioblastoma therapy. Discov Med. 2015;19(107): 471-7.

[29] Lee EQ, Kaley TJ, Duda DG, Schiff D, Lassman AB, Wong ET, et al. A Multicenter, Phase II, Randomized, Noncomparative Clinical Trial of Radiation and Temozolomide with or without Vandetanib in Newly Diagnosed Glioblastoma Patients. Clin Cancer Res. 2015; 21(16): 3610-8.

[30] Chen C, Ravelo A, Yu E, Dhanda R, Schnadig I. Clinical outcomes with bevacizumab-containing and non-bevacizumab-containing regimens in patients with recurrent glioblastoma from US community practices. J Neurooncol. 2015;122(3): 595-605.

[31] Westphal M, Heese O, Steinbach JP, Schnell O, Schackert G, Mehdorn M, et al. A randomised, open label phase III trial with nimotuzumab, an anti-epidermal growth factor receptor monoclonal antibody in the treatment of newly diagnosed adult glioblastoma. Eur J Cancer 2015;51(4): 522-32.

[32] Schuster JM, Friedman HS, Bigner DD. Therapeutic analysis of in vitro and in vivo brain tumor models. Neurol Clin. 1991;9(2): 375-82.

[33] Farias-Eisner G, Bank AM, Hwang BY, Appelboom G, Piazza MA, Bruce SS, et al. Glioblastoma biomarkers from bench to bedside: advances and challenges. Br J Neurosurg. 2012;26(2): 189-94.

[34] Voskoglou-Nomikos T, Pater JL, Seymour L. Clinical predictive value of the in vitro cell line, human xenograft, and mouse allograft preclinical cancer models. Clin Cancer Res. 2003;9(11): 4227-39.

[35] Romaguera-Ros M, Peris-Celda M, Oliver-De La Cruz J, Carrión-Navarro J, Pérez-García A, García-Verdugo JM, et al. Cancer-initiating enriched cell lines from human glioblastoma: preparing for drug discovery assays. Stem Cell Rev. 2012;8(1): 288-98.

[36] Bigner SH, Humphrey PA, Wong AJ, Vogelstein B, Mark J, Friedman HS, et al. Characterization of the epidermal growth factor receptor in human glioma cell lines and xenografts. Cancer Res. 1990;50(24): 8017-22.

[37] Piaskowski S, Bienkowski M, Stoczynska-Fidelus E, Stawski R, Sieruta M, Szybka M, et al. Glioma cells showing IDH1 mutation cannot be propagated in standard cell culture conditions. Br J Cancer. 2011;104(6): 968-70.

[38] Turner KM, Deshpande V, Beyter D, Koga T, Rusert J, Lee C, et al. Extrachromosomal oncogene amplification drives tumour evolution and genetic heterogeneity. Nature. 2017;543(7643): 122-125.

[39] Nikolaev S, Santoni F, Garieri M, Makrythanasis P, Falconnet E, Guipponi M, et al. Extrachromosomal driver mutations in glioblastoma and low-grade glioma. Nat Commun. 2014;5: 5690.

[40] Furnari FB, Fenton T, Bachoo RM, Mukasa A, Stommel JM, Stegh A, et al. Malignant astrocytic glioma: genetics, biology, and paths to treatment. Genes Dev. 2007;21(21): 2683-2710.

[41] Thorne AH, Zanca C, Furnari F. Epidermal growth factor receptor targeting and challenges in glioblastoma. Neuro Oncol. 2016;18(7): 914-8.

[42] Shinojima N, Tada K, Shiraishi S, Kamiryo T, Kochi M, Nakamura H, et al. Prognostic value of epidermal growth factor receptor in patients with glioblastoma multiforme. Cancer Res. 2003;63(20): 6962-70.

[43] Hill CS, Treisman R. Transcriptional regulation by extracellular signals: mechanisms and specificity. Cell. 1995;80(2): 199-211.

[44] Vivanco I, Sawyers CL. The phosphatidylinositol 3-Kinase AKT pathway in human cancer. Nat Rev Cancer. 2002;2(7): 489-501.

[45] Haura EB, Turkson J, Jove R. Mechanisms of disease: Insights into the emerging role of signal transducers and activators of transcription in cancer. Nat Clin Pract Oncol. 2005;2(6): 315-24.

[46] Huang HS, Nagane M, Klingbeil CK, Lin H, Nishikawa R, Ji XD, et al. The enhanced tumorigenic activity of a mutant epidermal growth factor receptor common in human cancers is mediated by threshold levels of constitutive tyrosine phosphorylation and unattenuated signaling. J Biol Chem. 1997;272(5): 2927-35.

[47] Wong AJ, Ruppert JM, Bigner SH, Grzeschik CH, Humphrey PA, Bigner DS, et al. Structural alterations of the epidermal growth factor receptor gene in human gliomas. Proc Natl Acad Sci U S A. 1992;89(7): 2965-9.

[48] Karpel-Massler G, Schmidt U, Unterberg A, Halatsch ME. Therapeutic inhibition of the epidermal growth factor receptor in high-grade gliomas: where do we stand? Mol Cancer Res 2009;7: 1000–12.

[49] Padfield E, Ellis HP, Kurian KM. Current therapeutic advances targeting EGFR and EGFRvIII in glioblastoma. Front Oncol. 2015;5: 5.

[50] Roth P and Weller M. Challenges to targeting epidermal growth factor receptor in glioblastoma: escape mechanisms and combinatorial treatment strategies. Neuro Oncol. 2014;16 Suppl 8:viii14-9.

[51] Reardon DA, Wen PY, Mellinghoff IK. Targeted molecular therapies against epidermal growth factor receptor: past experiences and challenges. Neuro Oncol. 2014;16 Suppl 8:viii7-13.

[52] Pillay V, Allaf L, Wilding AL, Donoghue JF, Court NW, Greenall SA, et al. The plasticity of oncogene addiction: implications for targeted therapies directed to receptor tyrosine kinases. Neoplasia. 2009;11(5): 448-58, 2 p following 458.

[53] Clark PA, Iida M, Treisman DM, Kalluri H, Ezhilan S, Zorniak M, et al. Activation of multiple ERBB family receptors mediates glioblastoma cancer stem-like cell resistance to EGFR-targeted inhibition. Neoplasia. 2012;14(5): 420-8.

[54] Nathanson DA, Gini B, Mottahedeh J, Visnyei K, Koga T, Gomez G, et al. Targeted therapy resistance mediated by dynamic regulation of extrachromosomal mutant EGFR DNA. Science. 2014; 343(6166): 72-6.

[55] **William D**, Mokri P, Lamp N, Linnebacher M, Classen CF, Erbersdobler A, et al. Amplification of the EGFR gene can be maintained and modulated by variation of EGF concentrations in in vitro models of glioblastoma multiforme. PLoS ONE. 2017;12(9): e0185208.

[56] Stockhausen MT, Broholm H, Villingshøj M, Kirchhoff M, Gerdes T, Kristoffersen K, et al. „Maintenance of EGFR and EGFRvIII expressions in an in vivo and in vitro model of human glioblastoma multiforme. Exp Cell Res. 2011;317(11): 1513–26.

[57] Gomez-Roman N, Stevenson K, Gilmour L, Hamilton G, Chalmers AJ. A novel 3D human glioblastoma cell culture system for modeling drug and radiation responses. Neuro-Oncology. 2017;19(2): 229-241.

[58] Fernandez-Fuente G, Mollinedo P, Grande L, Vazquez-Barquero A, Fernandez-Luna JL. Culture dimensionality influences the resistance of glioblastoma stem-like cells to multikinase inhibitors. Mol Cancer Ther. 2014;13(6): 1664-72.

[59] Hasselbach LA, Irtenkauf SM, Lemke NW, Nelson KK, Berezovsky AD, Carlton ET, et al. Optimization of high grade glioma cell culture from surgical specimens for use in clinically relevant animal models and 3D immunochemistry. J Vis Exp. 2014;(83): e51088.

[60] Schulte A, Gunther HS, Martens T, Zapf S, Riethdorf S, Wulfing C, et al. Glioblastoma stem-like cell lines with either maintenance or loss of high-level EGFR amplification, generated via modulation of ligand concentration. Clin Cancer Res 2012; 18(7): 1901–13.

[61] Laks DR, Crisman TJ, Shih MY, Mottahedeh J, Gao F, Sperry J, et al. Large-scale assessment of the gliomasphere model system. Neuro Oncol. 2016;18(10): 1367-78.

[62] Mazzoleni S, Politi LS, Pala M, Cominelli M, Franzin A, Sergi Sergi L, et al. Epidermal growth factor receptor expression identifies functionally and molecularly distinct tumor-

initiating cells in human glioblastoma multiforme and is required for gliomagenesis. Cancer Res. 2010;70(19): 7500–13.

[63] Pandita A, Aldape KD, Zadeh G, Guha A, James CD. Contrasting in vivo and in vitro fates of glioblastoma cell subpopulations with amplified EGFR. Genes Chromosomes Cancer. 2004;39: 29–36.

[64] Soeda A, Inagaki A, Oka N, Ikegame Y, Aoki H, Yoshimura S, et al. Epidermal growth factor plays a crucial role in mitogenic regulation of human brain tumor stem cells. J Biol Chem. 2008;283: 10958–66.

[65] Emlet DR, Gupta P, Holgado-Madruga M, Del Vecchio CA, Mitra SS, Han SY, et al. Targeting a glioblastoma cancer stem-cell population defined by EGF receptor variant III. Cancer Res. 2014;74(4): 1238-49.

[66] Beier D, Hau P, Proescholdt M, Lohmeier A, Wischhusen J, Oefner PJ, et al. CD133(þ) and CD133(-) glioblastoma-derived cancer stem cells show differential growth characteristics and molecular profiles. Cancer Res. 2007;67: 4010–5.

[67] Kemper K, Sprick MR, de Bree M, Scopelliti A, Vermeulen L, Hoek M, et al. The AC133 epitope, but not the CD133 protein, is lost upon cancer stem cell differentiation. Cancer Res. 2010;70: 719–29.

[68] Nishide K, Nakatani Y, Kiyonari H, Kondo T. Glioblastoma formation from cell population depleted of Prominin1-expressing cells. PLoS ONE 2009;4: e6869.

[69] Stockhausen MT, Kristoffersen K, Stobbe L, Poulsen HS. Differentiation of glioblastoma multiforme stem-like cells leads to downregulation of EGFR and EGFRvIII and decreased tumorigenic and stem-like cell potential. Cancer Biol Ther. 2014;15(2): 216-24.

[70] Campos B, Wan F, Farhadi M, Ernst A, Zeppernick F, Tagscherer KE, et al. Differentiation therapy exerts antitumor effects on stem-like glioma cells. Clin Cancer Res. 2010;16: 2715-28.

[71] Ying M, Wang S, Sang Y, Sun P, Lal B, Goodwin CR, et al. Regulation of glioblastoma stem cells by retinoic acid: role for Notch pathway inhibition. Oncogene. 2011;30: 3454-67.

[72] Devarasetty M, Mazzocchi AR, Skardal A. Applications of Bioengineered 3D Tissue and Tumor Organoids in Drug Development and Precision Medicine: Current and Future. BioDrugs. 2018; doi: 10.1007/s40259-017-0258-x. [Epub ahead of print]

[73] Lamb R, Harrison H, Hulit J, Smith DL, Lisanti MP, Sotgia F. Mitochondria as new therapeutic targets for eradicating cancer stem cells: Quantitative proteomics and functional validation via MCT1/2 inhibition. Oncotarget. 2014;5(22): 11029-37.

[74] Lamb R, Ozsvari B, Lisanti CL, Tanowitz HB, Howell A, Martinez-Outschoorn UE, et al. Antibiotics that target mitochondria effectively eradicate cancer stem cells, across multiple tumor types: Treating cancer like an infectious disease. Oncotarget. 2015;6(7): 4569-84.

[75] Beier D, Rohrl S, Pillai DR, Schwarz S, Kunz-Schughart LA, Leukel P et al. Temozolomide preferentially depletes cancer stem cells in glioblastoma. Cancer Res. 2008;68: 5706–5715.

[76] Rosso L, Brock CS, Gallo JM, Saleem A, Price PM, Turkheimer FE et al. A new model for prediction of drug distribution in tumor and normal tissues: pharmacokinetics of temozolomide in glioma patients. Cancer Res. 2009;69: 120–127.

[77] Brada M, Judson I, Beale P, Moore S, Reidenberg P, Statkevich P et al. Phase I doseescalation and pharmacokinetic study of temozolomide (SCH 52365) for refractory or relapsing malignancies. Br J Cancer. 1999;81: 1022–1030.

[78] Ostermann S, Csajka C, Buclin T, Leyvraz S, Lejeune F, Decosterd LA et al. Plasma and cerebrospinal fluid population pharmacokinetics of temozolomide in malignant glioma patients. Clin Cancer Res. 2004;10: 3728–3736.

[79] **William D**, Walther M, Schneider B, Linnebacher M, Classen CF. Temozolomide-induced increase of tumorigenicity can be diminished by targeting of mitochondria in in vitro models of patient individual glioblastoma. PLoS One. 2018;13(1): e0191511.

[80] Moullan N, Mouchiroud L, Wang X, Ryu D, Williams EG, Mottis A et al. Tetracyclines Disturb Mitochondrial Function across Eukaryotic Models: A Call for Caution in Biomedical Research. Cell Rep. 2015;pii: S2211-1247(15)00180-1.

[81] Wang-Gillam A, Siegel E, Mayes DA, Hutchins LF, Zhou Y. Anti-Tumor Effect of Doxycycline on Glioblastoma Cells. Journal of Cancer Molecules 2007;3(5): 147-153.

[82] Burbulla LF, Fitzgerald JC, Stegen K, Westermeier J, Thost AK, Kato H, et al. Mitochondrial proteolytic stress induced by loss of mortalin function is rescued by Parkin and PINK1. Cell Death Dis. 2014;5: e1180.

[83] Schneider HC, Berthold J, Bauer MF, Dietmeier K, Guiard B, Brunner M, et al. Mitochondrial Hsp70/MIM44 complex facilitates protein import. Nature. 1994;371: 768–774.

[84] Deocaris CC, Kaul SC, Wadhwa R. On the brotherhood of the mitochondrial chaperones mortalin and heat shock protein 60. Cell Stress Chaperones. 2006;11: 116–128.

[85] Yaguchi T, Aida S, Kaul SC, Wadhwa R. Involvement of mortalin in cellular senescence from the perspective of its mitochondrial import, chaperone, and oxidative stress management functions. Ann NY Acad Sci. 2007;1100: 306–311.

[86] Jin J, Hulette C, Wang Y, Zhang T, Pan C, Wadhwa R, et al. Proteomic identification of a stress protein, mortalin/mthsp70/GRP75: relevance to Parkinson disease. Mol Cell Proteomics. 2006; 5: 1193–1204.

[87] Palacino JJ, Sagi D, Goldberg MS, Krauss S, Motz C, Wacker M, et al. Mitochondrial dysfunction and oxidative damage in parkin-deficient mice. J Biol Chem. 2004;279: 18614–18622.

[88] Valente EM, Abou-Sleiman PM, Caputo V, Muqit MM, Harvey K, Gispert S, et al. Hereditary early-onset Parkinson's disease caused by mutations in PINK1. Science. 2004;304: 1158–1160.

[89] De VT, Knegtel RM, Holmes EH, Macher BA. Fucosyltransferases: structure/function studies. Glycobiology. 2001;11: 119–128.

[90] Yang XS, Liu S, Liu YJ, Liu JW, Liu TJ, Wang XQ, et al. Overexpression of fucosyltransferase IV promotes A431 cell proliferation through activating MAPK and PI3K/Akt signaling pathways. J Cell Physiol. 2010;225(2): 612–9.

[91] Cheng L, Luo S, Jin C, Ma H, Zhou H, Jia L. FUT family mediates the multidrug resistance of human hepatocellular carcinoma via the PI3K/Akt signaling pathway. Cell Death Dis. 2013;4: e923.

[92] Cancer Genome Atlas Research Network. Comprehensive genomic characterization defines human glioblastoma genes and core pathways. Nature 2008; 455(7216): 1061–8.

[93] Lattova E, Tomanek B, Bartusik D, Perreault H. N-glycomic changes in human breast carcinoma MCF7 and T-lymphoblastoid cells after treatment with herceptin and herceptin/Lipoplex. J Proteome Res 2010; 9: 1533–1540.

[94] Shu H, Zhang S, Kang X, Li S, Qin X, Sun C, et al. Protein expression and fucosylated glycans of the serum haptoglobin-{beta} subunit in hepatitis B virus-based liver diseases. Acta Biochim Biophys Sin (Shanghai) 2011; 43: 528–534.

[95] Mejías-Luque R, López-Ferrer A, Garrido M, Fabra A, de Bolós C. Changes in the invasive and metastatic capacities of HT-29/M3 cells induced by the expression of fucosyltransferase 1. Cancer Sci 2007; 98: 1000–1005.

[96] Vasseur JA, Goetz JA, Alley WR, Novotny MV. Smoking and lung cancer-induced changes in N-glycosylation of blood serum proteins. Glycobiology 2012; 22: 1684–1708.

[97] Giordano G, Febbraro A, Tomaselli E, Sarnicola ML, Parcesepe P, Parente D, et al. Cancer-related CD15/FUT4 overexpression decreases benefit to agents targeting EGFR or VEGF acting as a novel RAF-MEK-ERK kinase downstream regulator in metastatic colorectal cancer. J Exp Clin Cancer Res. 2015;34: 108.

[98] Gao J, Aksoy BA, Dogrusoz U, Dresdner G, Gross B, Sumer SO, et al. Integrative analysis of complex cancer genomics and clinical profiles using the cBioPortal. Sci Signal. 2013;6(269): pl1.

[99] Cerami E, Gao J, Dogrusoz U, Gross BE, Sumer SO, Aksoy BA, et al. The cBio Cancer Genomics Portal: An Open Platform for Exploring Multidimensional Cancer Genomics Data. Cancer Discov. 2012;2(5): 401-4.

[100] Huszthy PC, Daphu I, Niclou SP, Stieber D, Nigro JM, Sakariassen PØ, Miletic H, Thorsen F, Bjerkvig R. In vivo models of primary brain tumors: pitfalls and perspectives. Neuro-oncology. 2012;14: 979–93.

[101] Siolas D and Hannon GJ. Patient Derived Tumor Xenografts: transforming clinical samples into mouse models. Cancer Res. 2013;73(17): 5315–5319.

[102] Park D, Wang D, Chen G, Deng X. Establishment of Patient-derived Xenografts in Mice. Bio-protocol. 2016;6(22): e2008.

[103] Joo KM, Kim J, Jin J, Kim M, Seol HJ, Muradov J, et al. Patient-specific orthotopic glioblastoma xenograft models recapitulate the histopathology and biology of human glioblastomas in situ. Cell Rep. 2013;3: 260–73.

[104] Shultz LD, Schweitzer PA, Christianson SW, Gott B, Schweitzer IB, Tennent B, et al. Multiple defects in innate and adaptive immunologic function in NOD/LtSz-scid mice. J Immunol. 1995;154(1): 180-91.

[105] Kelland LR. Of mice and men: values and liabilities of the athymic nude mouse model in anticancer drug development. Eur J Cancer. 2004;40(6): 827-36.

[106] **William D**, Mullins CS, Schneider B, Orthmann A, Lamp N, Krohn M, et al. Optimized creation of glioblastoma patient derived xenografts for use in preclinical studies. J Transl Med. 2017;15(1): 27.

[107] Linnebacher M, Maletzki C, Ostwald C, Klier U, Krohn M, Klar E, Prall F. Cryopreservation of human colorectal carcinomas prior to xenografting. BMC Cancer. 2010;8: 362.

[108] Carlson BL, Pokorny JL, Schroeder MA, Sarkaria JN. Establishment, maintenance and in vitro and in vivo applications of primary human glioblastoma multiforme (GBM) xenograft models for translational biology studies and drug discovery. Curr Protoc Pharmacol. 2011 Mar;Chapter 14:Unit 14.16.

[109] Mullins CS, Bock S, Krohn M, Linnebacher M. Generation of xenotrans- plants from human cancer biopsies to assess anti-cancer activities of HDACi. Methods Mol Biol. 2017;1510: 217–29.

[110] Hatanpaa KJ, Burma S, Zhao D, Habib AA. Epidermal growth factor receptor in glioma: signal transduction, neuropathology, imaging, and radioresistance. Neoplasia. 2010;12(9): 675–84.

[111] Ben-David U, Ha G, Tseng YY, Greenwald NF, Oh C, Shih J, et al. Patient-derived xenografts undergo mouse-specific tumor evolution. Nat Genet. 2017 Nov;49(11): 1567-1575.

[112] Cloughesy TF, Paul S, Mischel PS. Molecular targeting of Glioblastoma— how do you hit a moving target? Clin Cancer Res. 2011;17(1): 6–11.

[113] Reardon DA, Wen PY. Therapeutic advances in the treatment of glioblastoma: rationale and potential role of targeted agents. Oncologist. 2006;11(2): 152–64.

[114] Peters KB, Lou E, Desjardins A, Reardon DA, Lipp ES, Miller E, Herndon JE 2nd, McSherry F, Friedman HS, Vredenburgh JJ. Phase II trial of upfront bevacizumab,

irinotecan, and temozolomide for unresectable glioblastoma. Oncologist. 2015;20(7): 727–8.

3. Eigenanteil an den zur Dissertation eingereichten Publikationen

Amplification of the EGFR gene can be maintained and modulated by variation of EGF concentrations in in vitro models of glioblastoma multiforme.

William D, Mokri P, Lamp N, Linnebacher M, Classen CF, Erbersdobler A, Schneider B

PLoS ONE (2017) 12(9): e0185208. https://doi.org/10.1371/journal.pone.0185208

- Verfassung des Manuskripts, Corresponding Author
- Maßgebliche Beteiligung an der Studienplanung
- Beteiligung an der Durchführung der experimentellen Arbeiten (Western Blots, Unterstützung bei Probenvorbereitung für PCR, Western Blot, IHC und CISH. Statistische Auswertung)
- Bearbeitung der Kommentare von Gutachtern und Überarbeitung des Manuskripts nach Revision des Manuskripts gemeinsam mit Dr. B. Schneider

Optimized creation of glioblastoma patient derived xenografts for use in preclinical studies.

William D, Mullins CS, Schneider B, Orthmann A, Lamp N, Krohn M, Hoffmann A, Classen CF, Linnebacher M

J Transl Med (2017) 15:27 DOI 10.1186/s12967-017-1128-5

- Verfassung des Manuskripts
- Beteiligung an der Durchführung der experimentellen Arbeiten (Implantation von Tumorgewebe in Mäusen, Probenaufbereitung für molekularbiologische Analysen, IHC und STR-Analysen, statistische Asuwertung)

- Bearbeitung der Kommentare von Gutachtern und Überarbeitung des Manuskripts nach Revision des Manuskripts gemeinsam mit PD Dr. M. Linnebacher

Temozolomide-induced increase of tumorigenicity can be diminished by targeting of mitochondria in in vitro models of patient individual glioblastoma

William D, Walther M, Schneider B, Linnebacher M, Classen CF

PLoS ONE 13(1):e0191511. https://doi.org/10.1371/ journal.pone.0191511

- Verfassung des Manuskripts, Corresponding Author
- Planung der Studie
- Durchführung der experimentellen Arbeiten (Zellkultur, Behandlungder Zellen *in vitro*, Western Blots, Immunfluoreszenzfärbung von Mitochondrien, Aufbereitung von Proben für PCR Analysen, statistische Auswertung)
- Bearbeitung der Kommentare von Gutachtern und Überarbeitung des Manuskripts nach Revision des Manuskripts gemeinsam mit Prof Dr. C.F. Classen und Dr. B. Schneider

4. Publikationen

4.1. Amplification of the EGFR gene can be maintained and modulated by variation of EGF concentrations in in vitro models of glioblastoma multiforme.

William D, Mokri P, Lamp N, Linnebacher M, Classen CF, Erbersdobler A, Schneider B

PLoS ONE (2017) 12(9): e0185208. https://doi.org/10.1371/journal.pone.0185208

PLOS ONE

RESEARCH ARTICLE

Amplification of the *EGFR* gene can be maintained and modulated by variation of EGF concentrations in *in vitro* models of glioblastoma multiforme

Doreen William[1]*, Poroshista Mokri[1], Nora Lamp[2], Michael Linnebacher[3], Carl Friedrich Classen[1], Andreas Erbersdobler[2], Björn Schneider[2]

1 University Medicine Rostock, Children and Adolescents Hospital, Rostock, Germany, **2** University Medicine Rostock, Institute of Pathology, Rostock, Germany, **3** University Medicine Rostock, Department of General Surgery, Molecular Oncology and Immunotherapy, Rostock, Germany

* doreen.william@med.uni-rostock.de

OPEN ACCESS

Citation: William D, Mokri P, Lamp N, Linnebacher M, Classen CF, Erbersdobler A, et al. (2017) Amplification of the *EGFR* gene can be maintained and modulated by variation of EGF concentrations in *in vitro* models of glioblastoma multiforme. PLoS ONE 12(9): e0185208. https://doi.org/10.1371/journal.pone.0185208

Editor: Helen Fillmore, University of Portsmouth, UNITED KINGDOM

Received: April 4, 2017

Accepted: September 10, 2017

Published: September 21, 2017

Data Availability Statement: All relevant data are within the paper.

Funding: The authors received no specific funding for this work.

Competing interests: The authors have declared that no competing interests exist.

Abstract

Glioblastoma multiforme (GBM) is the most common and lethal brain tumor in adults. It is known that amplification of the epidermal growth factor receptor gene (*EGFR*) occurs in approximately 40% of GBM, leading to enhanced activation of the EGFR signaling pathway and promoting tumor growth. Although GBM mutations are stably maintained in GBM *in vitro* models, rapid loss of *EGFR* gene amplification is a common observation during cell culture. To maintain *EGFR* amplification *in vitro*, heterotopic GBM xenografts with elevated *EGFR* copy number were cultured under varying serum conditions and EGF concentrations. *EGFR* copy numbers were assessed over several passages by quantitative PCR and chromogenic *in situ* hybridization. As expected, in control assays with 10% FCS, cells lost *EGFR* amplification with increasing passage numbers. However, cells cultured under serum free conditions stably maintained elevated copy numbers. Furthermore, EGFR protein expression positively correlated with genomic amplification levels. Although elevated *EGFR* copy numbers could be maintained over several passages *in vitro*, levels of *EGFR* amplification were variable and dependent on the EGF concentration in the medium. *In vitro* cultures of GBM cells with elevated *EGFR* copy number and corresponding EGFR protein expression should prove valuable preclinical tools to gain a better understanding of *EGFR* driven glioblastoma and assist in the development of new improved therapies.

Introduction

Glioblastoma multiforme (GBM) is the most common brain tumor in adults with a very dismal prognosis, despite a multimodal, intensive treatment regimen consisting of surgery, radio- and chemotherapy. Therapies are neither particularly effective nor durable with mean survival times of 12–15 months [1–3]. GBMs display a high intratumoral heterogeneity and are

characterized by invasive growth into surrounding tissue, making complete resection nearly impossible and favoring development of chemotherapy resistance [3,4].

The EGFR signaling pathway is a prominent regulator of proliferation, growth and survival of mammalian cells [5]. Upon binding of its extracellular ligand EGF or transforming growth factor α (TGFα), EGFR is activated, resulting in enhanced cell proliferation.

Alterations of the *EGFR* gene are considered as frequent driver mutations and are present in approximately 50% of GBM [6,7].

The most common *EGFR* aberration is genomic amplification (40%) [6], often due to extrachromosomal material (double minutes) [8,9], leading to overexpression and enhanced signaling [6]. A multitude of signaling pathway cascades activated by EGFR are associated with GBM progression, e.g. activation of Cyclooxygenase-2 [10,11], K-RAS and AKT signaling [12], and mammalian target of rapamycin (mTOR) together with phosphatidyl-inositol-3-kinase (PI3K) pathways [13–16]. Hence, EGFR or components of its signaling pathway may be promising therapy targets, as shown for tyrosine kinase inhibitors (TKIs) in lung cancer or antibody therapies in colorectal cancer [17,18]. However, substances targeting EGFR or its downstream targets have yet to prove effective in clinical GBM trials [19–21]. Although genomic *EGFR* amplification can be well maintained in *in vivo* models of glioblastoma [22,23], research in a preclinical setting *in vitro* is hampered by the fact that common cell culture models of GBM lack *EGFR* gene amplification [24,25].

Our work shows that this major cell culture disadvantage may be circumvented by culturing the cells under serum free conditions with varying EGF concentrations, leading to the maintenance of *EGFR* gene copy numbers. Although *EGFR* amplification is lost according to EGF concentration, it can subsequently be restored by EGF depletion. This enables further studying of this important signaling pathway in cell lines with the same genetic background and either high or low *EGFR* amplification levels.

Material & methods

Cell culture

Cell lines were established from GBM tissue of three different heterotopic patient derived xenograft (PDX) tumors with varying *EGFR* copy numbers [22]. All PDX models were established by implanting GBM tissue received from the operation theater at the department of neurosurgery at the university medicine of Rostock subcutaneously into the flanks of immunodeficient NMRI Foxn^1 nu mice [22]. Specimen collection was conducted in accordance with the ethics guidelines for the use of human material, approved by the Ethics Committee of the University of Rostock (Reference number: A 2009/34) and with informed written consent from all patients prior to surgery. Prior to cell line establishment, the PDX underwent 2 (xHROG33 and xHROG59) or 5 (xHROG22) serial *in vivo* passages in NMRI Foxn^1 nu mice. Serial passaging *in vivo* was performed by excision of the subcutaneous xenograft tumors and implanting small pieces of tumor tissue (approximately 3 mm^3) subcutaneously in the flanks of other NMRI Foxn^1 nu mice [22]. The obtained GBM PDX tissue was minced using sterile scalpels and passed through a 70 μm cell strainer to obtain single cell suspensions. Cells were divided equally among standard medium control (DMEM/Ham's F12, 2mM L-Glutamine, 10% FCS) and serum free media cultures (DMEM/Ham's F12, 2mM L-Glutamine, 1x B-27, 10ng/ml bFGF) with varying amounts of rhEGF (0 ng/ml, 0.5 ng/ml, 1 ng/ml, 1.5 ng/ml, 2 ng/ml, 2.5 ng/ml, 10 ng/ml and 30 ng/ml). Subsequently, all cultures were incubated at 37˚C, 5% CO_2 and 95% relative humidity. Multicellular spheroid cultures were passaged *in vitro* by passing the spheroids through a 70 μM cell strainer. When possible, cultures were sampled at every passage for further analysis.

Isolation of genomic DNA and PCR analysis

Genomic DNA was isolated using a commercial Kit (Wizard® Genomic DNA Purification Kit, Promega, Mannheim, Germany) following the manufacturer's instructions. DNA concentration was determined with a spectrophotometer (NanoDrop 1000, Peqlab, Erlangen, Germany). *EGFR* copy numbers were determined by quantitative PCR using 30 ng DNA as template on a StepOne Plus Realtime PCR system (Applied Biosystems, Darmstadt, Germany) with SensiFastSYBR Hi-Rox-Kit (Bioline, Luckenwalde, Germany) (EGFR-for: 5′-TCCCATGATGATCTGTCCCTCACA-3′; EGFR-rev: 5′-CAGGAAAATGCTGGCTGACCTAAG-3′). Commercially available normal Human Genomic DNA (Promega) served as calibrator and the repetitive element LINE1 as endogenous control (LINE1-for: 5′-TGCTTTGAATGCGTCCCAGAG-3′; LINE1-rev: 5′-AAAGCCGCTCAACTACATGG-3′). All reactions were performed in triplicate. The *EGFR* copy number was calculated with the ΔΔCt-algorithm.

Potential cross contamination of the samples with rodent genes was analyzed by PCR (94˚C 3min, 35 cycles of 94˚C 1min, 65˚C 2min, 72˚C 1min, final extension at 72˚C 4min) using the DFS–Taq polymerase supplied by Bioron (Bioron GmbH, Ludwigshafen, Germany) following manufacturer's instructions with primers specific for murine *MLH1* (for: 5′-TGTCAATAGGCTGCCCTAGG-3′, rev: 5′-TTTTCAGTGCAGCCTATGCTC-3′) [26]. Human origin of the samples was verified by PCR with primers specific for human cytochrome B (for: 5′- TAGCAATAATCCCCATCCTCCATATTAT-3′, rev: 5′- ACTTGTCCAATGATGGTAAAAGG-3′ [27]) Results were analyzed by gel electrophoresis.

Paraffin embedding of GBM cells

Cells were harvested and washed with PBS twice. The cells were fixed immediately by resuspending the pellets in 4% buffered formalin (Formafix; Grimm, Torgelow, Germany). Cells were subsequently processed following established standard procedures [28] to form a conglomerate and then embedded in paraffin using the automated Excelsior AS system (Thermo Scientific, Dreieich, Germany) following standard procedures.

Tissue microarray

Hematoxylin and Eosin (H&E) stained sections of FFPE cell lines were reviewed by an experienced pathologist and regions suitable for analysis were chosen. Tissue microarrays (TMA) were created using a Manual Tissue Arrayer MTA-1 (Beecher Instruments, Sun Prairie, WI, USA) with 1mm diameter punches. From the donor blocks, 3 punches per sample were taken from the selected regions and transferred to an empty acceptor block. The block was heated to 50˚C and the correct placement depth of the punches confirmed by microscopic examination. A section from the block was stained with H&E to confirm the presence of a sufficient amount of cells for further analysis.

Chromogenic *in situ* hybridization

In addition to quantitative PCR analysis, the *EGFR* amplification status was assessed by two-colored chromogenic *in situ* hybridization (2C CISH). 4 μM sections of FFPE tissue samples and TMAs were mounted to coated slides and *EGFR*-specific 2C CISH was performed using the ZytoDot 2C CISH implementation Kit with the ZytoDot 2C SPEC EGFR/CEN 7 Probe (Zytomed Systems, Berlin, Germany) according to manufacturer's protocols. Processed samples were analyzed by bright field microscopy. Red signals specifically represent the centromere of chromosome 7 for reference and ploidy, whereas green signals are specific for the

EGFR gene. A cell was considered to carry an *EGFR* amplification if the green / red ratio was >2 or the green signals occurred in clusters.

Immunohistochemistry

EGFR immunohistochemistry (IHC) was performed using a mouse derived anti-EGFR primary antibody (Zytomed Systems, clone 3G143, dilution 1:200). Slides were processed on an automatic IHC system, AutostainerLink48 (Dako, Hamburg, Germany), according to routine protocols.

Statistics

Statistical analysis was done using SigmaPlot 10.0 (Systat Software GmbH, Erkrath, Germany). A Kruskal-Wallis one way analysis of variance on ranks in combination with a Tukey test was used for statistical analysis of qPCR data.

Results

GBM PDX derived cell lines

In order to identify cell culture conditions, which would allow sustained *EGFR* amplification of GBM cells *in vitro*, cell lines were established from 3 different GBM PDX with varying *EGFR* copy numbers as determined by qPCR and 2C CISH (Fig 1). Prior to cell line establishment, HROG33 and HROG59 PDX underwent 2 serial passages *in vivo*, HROG22 PDX underwent 5 serial passages in NMRI Foxn^{1} nu mice.

HROG33 and HROG59 PDX showed high genomic *EGFR* amplification levels (Fig 1C and 1E), whereas *EGFR* amplification was absent from HROG22 PDX (Fig 1A). The HROG22 PDX also showed a weaker staining in immunohistochemistry analysis of EGFR protein expression, compared to the two *EGFR* amplified PDX, HROG33 and HROG59 (Fig 1B, 1D and 1E). Nevertheless, HROG22 was included in the study to determine if *in vitro* EGF exposure could select for HROG22 cells carrying *EGFR* amplifications. Cell line establishment of xHROG22 and xHROG33 was successful for all conditions tested (serum free with 0, 0.5, 1, 1.5, 2, 2.5, 10, 30 ng/ml EGF and 10% FCS controls). In the case of xHROG59, cell line establishment failed at 2 ng/ml EGF and the 10% FCS control, but was otherwise successful. Contamination of the cell lines with murine DNA was excluded by PCR specific for murine *MLH1* and their human origin was verified by PCR specific for human cytochrome B (S1 Fig, [26,27]). All cell lines established under serum free conditions grew as non-adherent multicellular spheroids regardless of EGF concentration, whereas the 10% FCS controls grew as adherent monolayers. Establishment of spheroid cultures with 10% FCS supplemented medium using anti-adhesive tissue culture dishes failed in all three cases. Although initial spheroid formation was observed, the cells failed to reform spheroids after splitting. Cells from all successful conditions were further analyzed over several passages. In the case of multicellular spheroid cultures, a passage was defined as the time required for single cells growing in suspension to form spheroids. Spheroid formation was considered as complete when they appeared solid in form with no lose single cells attached to the sphere and reached a diameter of approximately 100μM.

EGFR amplification is maintained in serum-free *in vitro* models of GBM and correlates with EGFR protein expression

Amplification of the *EGFR* gene was analyzed by qPCR over several *in vitro* passages for all culture conditions tested. As expected, *EGFR* amplification was lost in the 10% FCS control of

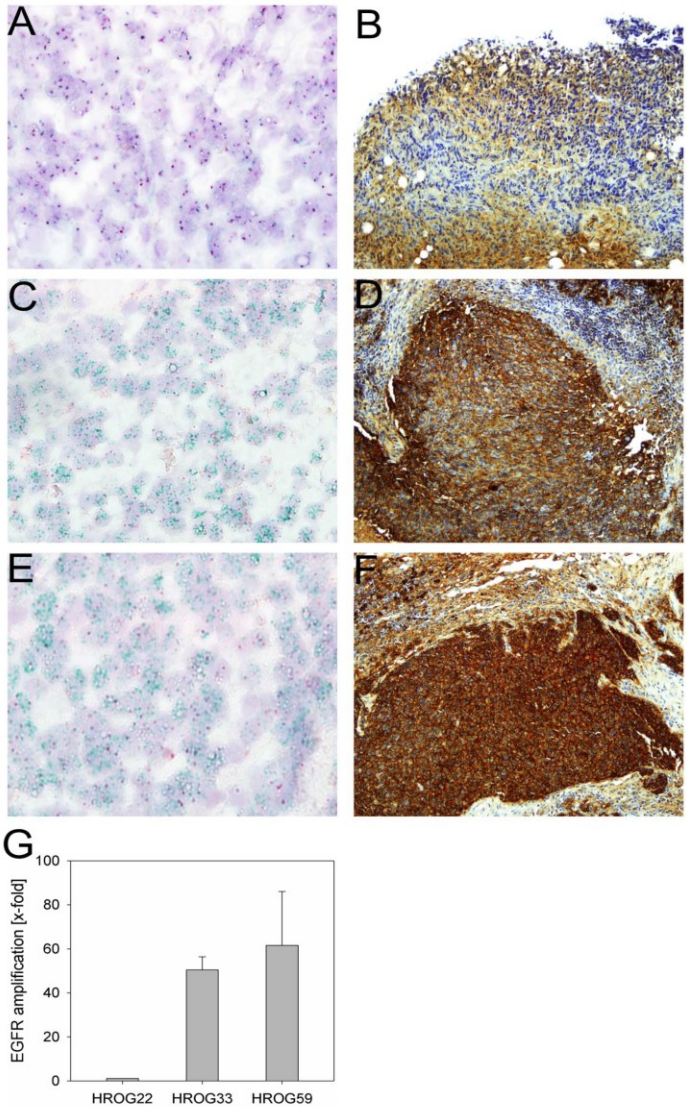

Fig 1. Analysis of *EGFR* amplification by 2C CISH and qPCR and corresponding EGFR protein expression by immunohistochemistry in GBM PDX tissue of HROG22, HROG33 and HROG59. A) 2C CISH of HROG22 (400x magnification), B) EGFR IHC of HROG22 (200x magnification), C) 2C CISH of HROG33 (400x magnification), D) EGFR IHC of HROG33 (200x magnification), E) 2C CISH of HROG59 (400x magnification), F) EGFR IHC of HROG59 (200x magnification); red signals: centromere of chr. 7; green signals: *EGFR* in the 2C CISH analyses; G) qPCR analysis of GBM PDX tissue, error bars represent the standard deviation of triplicate analyses.

https://doi.org/10.1371/journal.pone.0185208.g001

xHROG33 after few passages (Fig 2D, S2 Fig). However, under serum free conditions, *EGFR* amplification was maintained in xHROG33 and xHROG59 over at least 10 *in vitro* passages, although at varying degrees in dependence on the EGF concentration (Fig 2B and 2C, S2 Fig). Of note, GBM cells cultured with high amounts of EGF (30 ng/ml) showed the same rapid loss

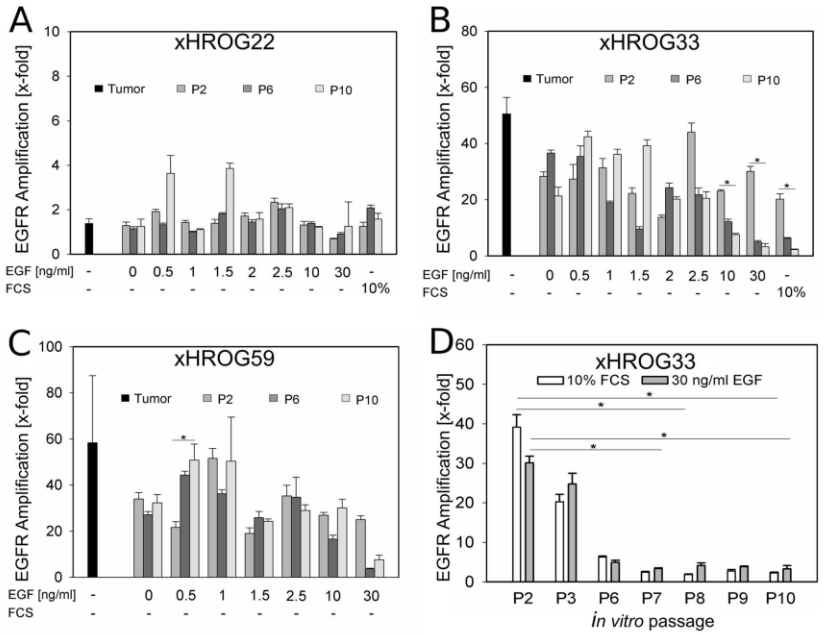

Fig 2. *EGFR* amplification is maintained over several *in vitro* passages, but lost in the 10% FCS control and with high EGF concentrations. qPCR analysis of A) xHROG22, B) xHROG33, C) x HROG59 cell lines grown under all culture conditions at passage 2 (grey bars), passage 6 (dark grey bars) and passage 10 (light grey bars). Black bars represent the respective PDX prior to cell culture establishment. D) qPCR analysis of the 10% FCS control (white bars) and the 30 ng/ml EGF cell line (grey bars) of xHROG33 over several *in vitro* passages. Error bars represent the standard deviation of triplicate analyses. * p<0.05, Tukey test.

https://doi.org/10.1371/journal.pone.0185208.g002

of *EGFR* amplification as the 10% FCS control (Fig 2D). In case of xHROG22, no marked differences in *EGFR* amplification were observed under all conditions applied with copy numbers below four (Fig 2A, S2 Fig).

To further confirm the qPCR data, cells at passage 10 were fixed in formalin and embedded in paraffin for *EGFR* specific CISH analyses (Fig 3). The 2C CISH analyses showed a high number of *EGFR* gene copies in xHROG33 cell lines cultured serum free with low amounts of EGF, whereas culture at 10 ng/ml EGF was accompanied by lowered amplification levels. Parity of chromosome 7 specific and *EGFR* specific signals indicating the loss of *EGFR* amplification was observed in xHROG33 cells cultured with 30 ng/ml EGF in the medium and the 10% FCS control (Fig 3). Similar results were obtained in xHROG59 (Fig 3). As expected, there was no increase of *EGFR* signal in xHROG22 (Fig 3). Thus, the 2C CISH results are well in line with the results obtained by qPCR analyses of *EGFR* amplification.

In order to determine if *EGFR* amplification levels also result in increased EGFR protein expression, TMA sections of embedded GBM cells were subjected to EGFR IHC staining (Fig 4). In all cases, the obtained results accorded with the 2C CISH and qPCR data (Figs 2 and 3).

Loss of *EGFR* amplification can be restored by EGF withdrawal

Genomic amplification of *EGFR* appears to be dependent on the EGF concentration present in the medium (Figs 2 and 3, S2 Fig). We observed a decrease in *EGFR* amplification with 10 ng/

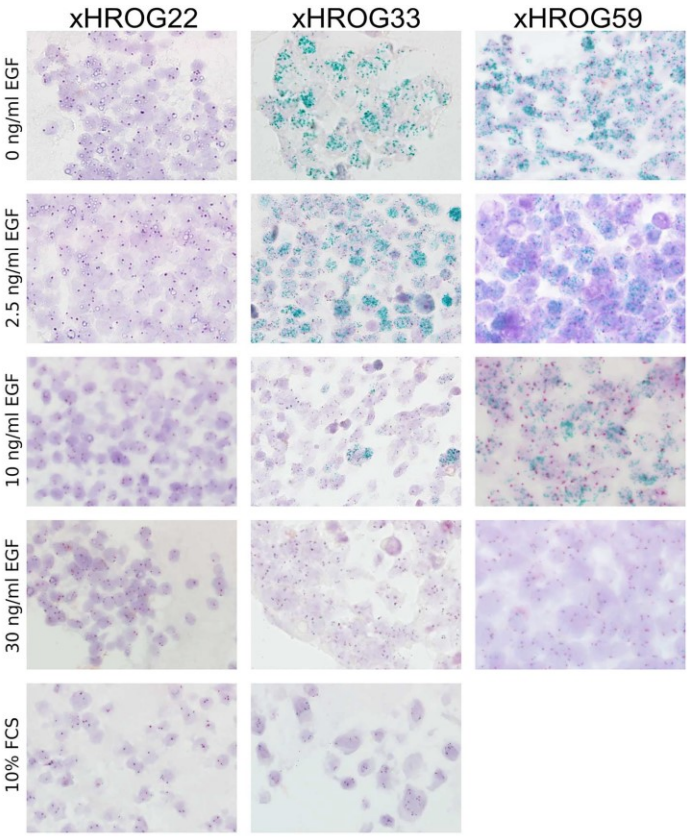

Fig 3. 2C CISH analysis confirms qPCR data of *EGFR* amplification. 2C CISH analyses of xHROG22, xHROG33 and xHROG59 cell lines established under different conditions as indicated at passage 10 of cell culture; 400x magnification.

https://doi.org/10.1371/journal.pone.0185208.g003

ml EGF in xHROG33 and xHROG59 and, additionally, for xHROG33 an almost complete loss of *EGFR* amplification with 30 ng/ml EGF approaching the level of the 10% FCS control. In both cases, after culture with 30 ng/ml EGF for 10 passages, EGF was withdrawn and *EGFR* amplification was analyzed by qPCR, 2C CISH and EGFR IHC staining after 5 *in vitro* passages post EGF depletion. *EGFR* amplification and protein expression were gradually restored after EGF withdrawal (Fig 5). In the case of the 10% FCS control of xHROG33, the cells failed to adapt to the change from 10% FCS to serum free without EGF followed by cell death.

Discussion

Glioblastoma multiforme remains a lethal brain tumor despite intensified treatment strategies, highlighting the need for more effective therapies [1,2]. Nearly half of GBM cases display a genomic amplification of *EGFR* and subsequent hyperactivation of the PI3K/AKT/mTOR signaling pathways [5,13,14]. However, preclinical *in vitro* studies are complicated by the rapid loss of genomic *EGFR* amplification under standard cell culture conditions [24,25]. GBM *in vitro* models with stable *EGFR* amplification would represent an experimental system more

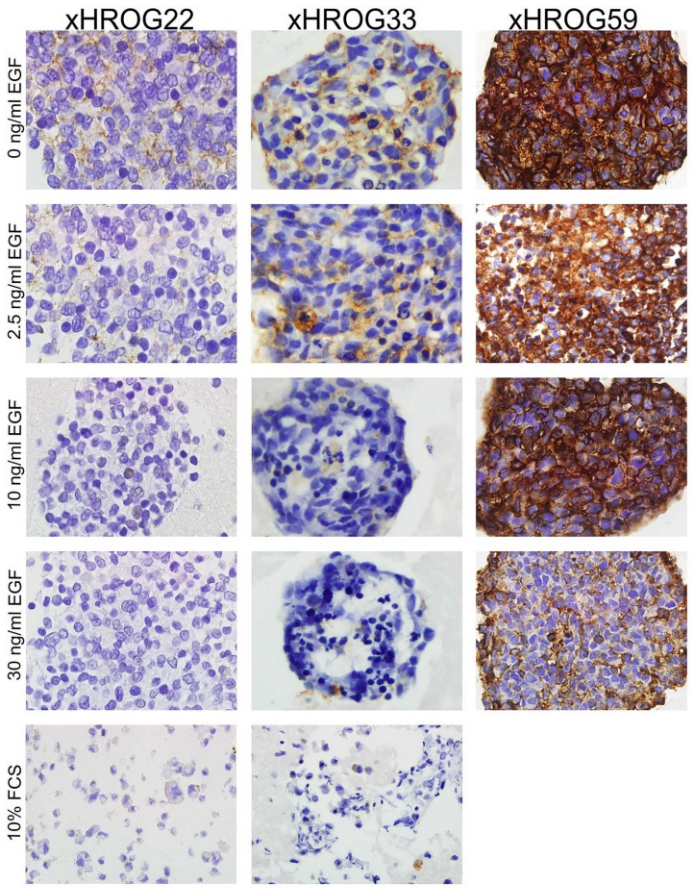

Fig 4. EGFR protein expression is concordant with genomic *EGFR* amplification. EGFR immunohistochemistry staining of paraffin embedded xHROG22, xHROG33 and xHROG59 cells grown under different conditions as indicated at passage 10 of cell culture; 200x magnification.

https://doi.org/10.1371/journal.pone.0185208.g004

faithfully representing the original tumor. The *in vitro* models in this study were established from GBM PDX instead of directly patient derived GBM tissue. We confirmed the human origin of all PDX models as well as their resemblance to the primary GBM in a previous study [22]. All PDX models were histologically analyzed by a neuropathologist and found to fulfill requirements for a GBM diagnosis [22]. Additionally, the human origin of the established cell lines was verified (S1 Fig), suggesting that the findings of this study would likely be translatable to directly patient derived *in vitro* models.

Although the exact doubling times of the established cell lines were not determined, we did not observe distinct differences in cell proliferation between cell lines cultivated with low EGF and high EGF concentrations. However, other studies observed higher proliferation rates with primary GBM cell cultures established under high EGF concentrations compared to cell lines of the same origin cultured without EGF supplementation [29].

We observed spontaneous spheroid formation in all cell lines under all applied serum free conditions independent on the EGF concentration in the media. Since the culture method

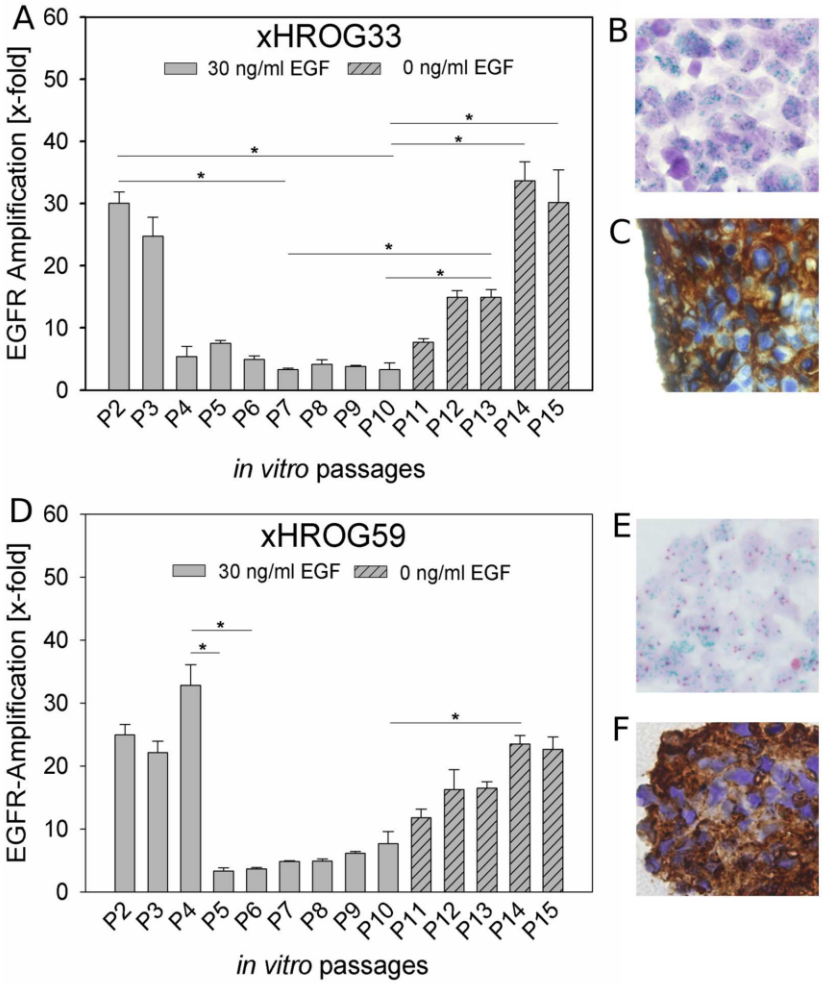

Fig 5. EGF withdrawal restores *EGFR* amplification. A and D) qPCR analysis of xHROG33 (A) and xHROG59 (D) cultured with 30 ng/ml EGF until passage 10 (grey bars) and without EGF for 5 additional passages (dashed bars), respectively. Error bars represent the standard deviation of triplicate analyses; B and E) 2C CISH analysis of paraffin embedded samples of xHROG33 (B) and xHROG59 (E) after 5 passages post EGF withdrawal (P15), C and F) EGFR immunohistochemistry staining of paraffin embedded samples of xHROG33 (C) and xHROG59 (F) after 5 passages post EGF withdrawal (P15). 400x magnification. * $p<0.05$, Tukey test.

https://doi.org/10.1371/journal.pone.0185208.g005

applied in this study (serum free media supplemented with B27 and FGF) is often used to enrich cancer stem-like cells (CSCs) of GBM we hypothesized that the spontaneous spheroid formation we observed under those conditions may be attributable to CSCs [30,31].

In the case of the *EGFR* unamplified xHROG22, obtaining *EGFR* amplified cells under the applied *in vitro* conditions proved unsuccessful. It is likely that an initial event to establish extrachromosomal *EGFR* amplification, like unscheduled DNA synthesis and replication or inverted duplications, occurs during tumorigenesis [32]. In case of HROG22 such an event

apparently did not occur, suggesting that this tumor is not dependent on *EGFR* amplification but rather on other mechanisms and pathways. It was not possible to induce *EGFR* amplification *in vitro* under the conditions applied in this study, suggesting that the xHROG22 cell line is similarly not dependent on *EGFR* amplification.

Two cell lines analyzed in this study (xHROG33 and xHROG59) stably maintained *EGFR* amplification under low EGF conditions ranging from 0 to 2.5 ng/ml over at least 10 *in vitro* passages in long-term cell culture (12 to 15 months). *EGFR* amplification levels decreased rapidly with higher EGF concentrations in both cases.

These results are well in line with previous studies, demonstrating maintained *EGFR* amplification under serum free conditions without EGF supplementation as well as decreased *EGFR* amplification with high EGF concentrations in primary GBM cell lines [23,29,33]. Hence, *EGFR* amplification levels appear to be directly influenced by the EGF concentration *in vitro*.

However, Schulte *et al*. reported an almost complete loss of *EGFR* amplification in primary GBM cell lines cultivated with 10 ng/ml EGF [29]. In the case of xHROG33 a decrease in *EGFR* amplification was observed in qPCR results, but 2C CISH analysis confirmed the presence of *EGFR* amplified cells. However, in the case of xHROG59 cells established under serum free conditions with 10 ng/ml EGF, we did not observe a major decrease of *EGFR* amplification in qPCR, 2C CISH or EGFR IHC analysis.

In case of xHROG33 we observed a rapid decrease of *EGFR* amplification in the 10% FCS control similar to the serum free culture with 30 ng/ml EGF. Although the morphology of the cells is different–spheroids in the serum free culture and adherent monolayer with 10% FCS–we deemed it unlikely that the morphology plays a significant role for decreased *EGFR* amplification of the 10% FCS cell line of xHROG33. Would the loss of *EGFR* amplification be attributable to cell attachment, we would have expected no similarly rapid decrease of *EGFR* amplification in the spheroid culture of xHROG33. Although not further investigated, we hypothesize that the variety of growth factors present in FCS has a similar effect on the *EGFR* amplification of the cells as the supplementation of high EGF amounts.

Our qPCR and 2C CISH data are concordant with EGFR protein expression as determined by IHC staining of EGFR, indicating that the genomic amplification is functional.

Furthermore, restoration of genomic *EGFR* amplification after high *in vitro* EGF-induced loss was possible by complete EGF withdrawal in both cases analyzed (xHROG33 and xHROG59). Previous studies demonstrated restoration of *EGFR* amplification in primary GBM cell lines by reducing EGF concentrations from 20 ng/ml to 5 ng/ml EGF [33]. However, other studies failed to restore *EGFR* amplification after withdrawal of EGF in primary GBM cell lines with high EGF-induced *EGFR* amplification loss [29,31]. Interestingly, similar restoration effects have been described in a model of EGFR inhibitor resistance [34]. Nathanson *et al* found extrachromosomal *EGFR* present in untreated GBM cells, which was lost under erlotinib treatment, but restored subsequently to drug removal [34]. Although in our study the withdrawal of EGF and not discontinued treatment with an EGFR inhibitor lead to restoration of *EGFR* amplification *in vitro*, the underlying mechanism might be similar. A marker chromosome including *EGFR* positive homogeneous staining regions (HSR) might serve as *EGFR* reservoir, enabling tumor cells to regain extrachromosomal *EGFR* amplification in response to microenvironmental stimuli like discontinued EGFR inhibitor exposure or, possibly, EGF withdrawal [34–36].

However, this was not further investigated in our study and thus remains speculative.

In sum, the GBM *in vitro* models described here stably maintain *EGFR* amplification under low EGF conditions. Furthermore exposure of cell lines that were initially derived from the same PDX tissue showed decreased *EGFR* amplification when high amounts of EGF were

supplemented. Thus, these *in vitro* models are a useful tool for in depth analysis of EGFR expression level dependent effects in an isogenic background.

Supporting information

S1 Fig. PCR analysis of murine *MLH1* and human specific *cytochrome B*. A) Analysis of gDNA pools of xHROG22 (xH.22), xHROG33 (xH.33) and xHROG59 (xH.59) at passage 2 (P2) and passage 10 (P10). Ctr M: DNA derived from mouse tail tissue as positive control for murine *MLH1* (~350bp), Ctr H: DNA derived from a GBM cell line established from patient derived GBM tissue B) Verification of human origin of the cell lines by human specific *cytochrome B* PCR (~130bp product).
(TIF)

S2 Fig. qPCR analysis of *EGFR* amplification of all successfully established cell lines. Tukey test, * $p<0.05$.
(TIF)

Acknowledgments

The authors thank the following colleagues for technical assistance: Mrs. J. Kölbel and Mrs. K. Grodno (cell and tissue embedding), Mrs. K. Westphal, Mrs. H. Clasen and Mrs. B. Krause (IHC), Mrs. S. Stegemann and Mrs. M. Schmidtgen (CISH and qPCR).

Author Contributions

Conceptualization: Doreen William, Björn Schneider.

Data curation: Doreen William, Björn Schneider.

Formal analysis: Doreen William, Björn Schneider.

Investigation: Doreen William, Poroshista Mokri, Nora Lamp, Björn Schneider.

Methodology: Doreen William, Poroshista Mokri, Nora Lamp, Björn Schneider.

Project administration: Doreen William, Poroshista Mokri, Björn Schneider.

Resources: Doreen William, Michael Linnebacher, Carl Friedrich Classen, Andreas Erbersdobler, Björn Schneider.

Supervision: Doreen William, Michael Linnebacher, Carl Friedrich Classen, Andreas Erbersdobler, Björn Schneider.

Validation: Doreen William, Björn Schneider.

Writing – original draft: Doreen William, Björn Schneider.

Writing – review & editing: Doreen William, Poroshista Mokri, Nora Lamp, Michael Linnebacher, Carl Friedrich Classen, Andreas Erbersdobler, Björn Schneider.

References

1. Dolecek TA, Propp JM, Stroup NE, Kruchko C. CBTRUS Statistical Report: Primary Brain and Central Nervous System Tumors Diagnosed in the United States in 2005–2009. Neuro-Oncology 2012; 14: 1–49.
2. Pollo B. Neuropathological diagnosis of brain tumours. Neurological Sciences 2011; 32: 209–11.
3. Stupp R, Hegi ME, Mason WP, van den Bent MJ, Taphoorn MJ, Janzer RC et al. Effects of radiotherapy with concomitant and adjuvant temozolomide versus radiotherapy alone on survival in glioblastoma in a

randomised phase III study: 5-year analysis of the EORTC-NCIC trial. The Lancet Oncology 2009; 10: 459–66. https://doi.org/10.1016/S1470-2045(09)70025-7 PMID: 19269895

4. Lima FR, Kahn SA, Soletti RC, Biasoli D, Alves T, da Fonseca AC et al. Glioblastoma: Therapeutic challenges, what lies ahead. Biochimica et Biophysica Acta (BBA)—Reviews on Cancer 2012; 1826: 338–49.
5. Thorne AH, Zanca C, Furnari F. Epidermal growth factor receptor targeting and challenges in glioblastoma. Neuro Oncol. 2016; 18(7): 914–8. https://doi.org/10.1093/neuonc/nov319 PMID: 26755074
6. Furnari FB, Fenton T, Bachoo RM, Mukasa A, Stommel JM, Stegh A, et al. Malignant astrocytic glioma: genetics, biology, and paths to treatment. Genes Dev. 2007; 21(21): 2683–2710. https://doi.org/10.1101/gad.1596707 PMID: 17974913
7. Shinojima N, Tada K, Shiraishi S, Kamiryo T, Kochi M, Nakamura H, et al. Prognostic value of epidermal growth factor receptor in patients with glioblastoma multiforme. Cancer Res. 2003 Oct 15; 63(20): 6962–70. PMID: 14583498
8. Muleris M, Almeida A, Dutrillaux AM, Pruchon E, Vega F, Delattre JY et al. Oncogene amplification in human gliomas: a molecular cytogenetic analysis. Oncogene 1994; 9(9): 2717–22. PMID: 8058336
9. Nikolaev S, Santoni F, Garieri M, Makrythanasis P, Falconnet E, Guipponi M, et al. Extrachromosomal driver mutations in glioblastoma and low-grade glioma. Nat Commun. 2014; 5: 5690. https://doi.org/10.1038/ncomms6690 PMID: 25471132
10. Lo HW, Cao X, Zhu H, Ali-Osman F. Cyclooxygenase-2 is a novel transcriptional target of the nuclear EGFR-STAT3 and EGFRvIII-STAT3 signaling axes. Mol Cancer Res. 2010; 8(2): 232–245. https://doi.org/10.1158/1541-7786.MCR-09-0391 PMID: 20145033
11. Shono T, Tofilon PJ, Bruner JM, Owolabi O, Lang FF. Cyclooxygenase-2 expression in human gliomas: prognostic significance and molecular correlations. Cancer Res. 2001; 61(11): 4375–4381. PMID: 11389063
12. Lyustikman Y, Momota H, Pao W, Holland EC. Constitutive activation of Raf-1 induces glioma formation in mice. Neoplasia 2008; 10(5): 501–10. PMID: 18472967
13. Parsons DW, Jones S, Zhang X, Lin JC, Leary RJ, Angenendt P, et al. An integrated genomic analysis of human glioblastoma multiforme. Science 2008; 321(5897): 1807–12. https://doi.org/10.1126/science.1164382 PMID: 18772396
14. Cancer Genome Atlas Research Network. Comprehensive genomic characterization defines human glioblastoma genes and core pathways. Nature 2008; 455(7216): 1061–8. https://doi.org/10.1038/nature07385 PMID: 18772890
15. Akhavan D, Cloughesy TF, Mischel PS. mTOR signaling in glioblastoma: lessons learned from bench to bedside. Neuro Oncol. 2010; 12(8): 882–889. https://doi.org/10.1093/neuonc/noq052 PMID: 20472883
16. Nicholas MK, Lukas RV, Jafri NF, Faoro L, Salgia R. Epidermal growth factor receptor—mediated signal transduction in the development and therapy of gliomas. Clin Cancer Res. 2006; 12(24): 7261–70. https://doi.org/10.1158/1078-0432.CCR-06-0874 PMID: 17189397
17. McCoach CE, Jimeno A. Osimertinib, a third-generation tyrosine kinase inhibitor targeting non-small cell lung cancer with EGFR T790M mutations. Drugs Today (Barc). 2016; 52(10): 561–568.
18. Kircher SM, Nimeiri HS, Benson AB 3rd. Targeting Angiogenesis in Colorectal Cancer: Tyrosine Kinase Inhibitors. Cancer J. 2016; 22(3): 182–9. https://doi.org/10.1097/PPO.0000000000000192 PMID: 27341596
19. Lee EQ, Kaley TJ, Duda DG, Schiff D, Lassman AB, Wong ET, et al. A Multicenter, Phase II, Randomized, Noncomparative Clinical Trial of Radiation and Temozolomide with or without Vandetanib in Newly Diagnosed Glioblastoma Patients. Clin Cancer Res. 2015; 21(16): 3610–8. https://doi.org/10.1158/1078-0432.CCR-14-3220 PMID: 25910950
20. Chen C, Ravelo A, Yu E, Dhanda R, Schnadig I. Clinical outcomes with bevacizumab-containing and non-bevacizumab-containing regimens in patients with recurrent glioblastoma from US community practices. J Neurooncol. 2015; 122(3): 595–605. https://doi.org/10.1007/s11060-015-1752-y PMID: 25773061
21. Westphal M, Heese O, Steinbach JP, Schnell O, Schackert G, Mehdorn M, et al. A randomised, open label phase III trial with nimotuzumab, an anti-epidermal growth factor receptor monoclonal antibody in the treatment of newly diagnosed adult glioblastoma. Eur J Cancer 2015; 51(4): 522–32. https://doi.org/10.1016/j.ejca.2014.12.019 PMID: 25616647
22. William D, Mullins CS, Schneider B, Orthmann A, Lamp N, Krohn M, et al. Optimized creation of glioblastoma patient derived xenografts for use in preclinical studies. J Transl Med. 2017; 15(1): 27. https://doi.org/10.1186/s12967-017-1128-5 PMID: 28183348

23. Stockhausen MT, Broholm H, Villingshøj M, Kirchhoff M, Gerdes T, Kristoffersen K, et al. „Maintenance of EGFR and EGFRvIII expressions in an in vivo and in vitro model of human glioblastoma multiforme. Exp Cell Res. 2011; 317(11): 1513–26. https://doi.org/10.1016/j.yexcr.2011.04.001 PMID: 21514294

24. Humphrey PA, Wong AJ, Vogelstein B, Friedman HS, Werner MH, Bigner DD, et al. Amplification and expression of the epidermal growth factor receptor gene in human glioma xenografts. Cancer Res 1988; 48: 2231–8. PMID: 3258189

25. Pandita A, Aldape KD, Zadeh G, Guha A, James CD. Contrasting in vivo and in vitro fates of glioblastoma cell subpopulations with amplified EGFR. Genes Chromosomes Cancer 2004; 39: 29–36. https://doi.org/10.1002/gcc.10300 PMID: 14603439

26. Maletzki C, Beyrich F, Hühns M, Klar E, Linnebacher M. The mutational profile and infiltration pattern of murine MLH1-/- tumors: concurrences, disparities and cell line establishment for functional analysis. Oncotarget 2016; 7(33): 53583–53598. https://doi.org/10.18632/oncotarget.10677 PMID: 27447752

27. Matsuda H, Seo Y, Kakizaki E, Kozawa S, Muraoka E, Yukawa N. Identification of DNA of human origin based on amplification of human-specific mitochondrial cytochrome b region. Forensic Sci Int. 2005; 152(2–3): 109–14. https://doi.org/10.1016/j.forsciint.2004.07.019 PMID: 15978336

28. Dijkstra JR, Opdam FJ, Boonyaratanakornkit J, Schönbrunner ER, Shahbazian M, Edsjö A, et al. Implementation of formalin-fixed, paraffin-embedded cell line pellets as high-quality process controls in quality assessment programs for KRAS mutation analysis. J Mol Diagn. 2012; 14(3): 187–91. https://doi.org/10.1016/j.jmoldx.2012.01.002 PMID: 22414609

29. Schulte A, Gunther HS, Martens T, Zapf S, Riethdorf S, Wulfing C et al. Glioblastoma stem-like cell lines with either maintenance or loss of high-level EGFR amplification, generated via modulation of ligand concentration. Clin Cancer Res 2012; 18(7): 1901–13. https://doi.org/10.1158/1078-0432.CCR-11-3084 PMID: 22316604

30. Ernst A, Hofmann S, Ahmadi R, Becker N, Korshunov A, Engel F, et al. Genomic and expression profiling of glioblastoma stem cell-like spheroid cultures identifies novel tumor-relevant genes associated with survival. Clin Cancer Res. 2009; 15(21): 6541–50. https://doi.org/10.1158/1078-0432.CCR-09-0695 PMID: 19861460

31. Soeda A, Inagaki A, Oka N, Ikegame Y, Aoki H, Yoshimura S-I et al. Epidermal growth factor plays a crucial role in mitogenic regulation of human brain tumor stem cells. J Biol Chem 2008; 283(16): 10958–66. https://doi.org/10.1074/jbc.M704205200 PMID: 18292095

32. Stark G. R., Debatisse M., Giulotto E. & Wahl G. M. Recent progress in understanding mechanisms of mammalian DNA amplification. Cell 1989; 57: 901–908 PMID: 2661014

33. Mazzoleni S, Politi LS, Pala M, Cominelli M, Franzin A, Sergi Sergi L et al. Epidermal growth factor receptor expression identifies functionally and molecularly distinct tumor-initiating cells in human glioblastoma multiforme and is required for gliomagenesis. Cancer Res 2010; 70(19): 7500–13. https://doi.org/10.1158/0008-5472.CAN-10-2353 PMID: 20858720

34. Nathanson DA, Gini B, Mottahedeh J, Visnyei K, Koga T, Gomez G, et al. Targeted therapy resistance mediated by dynamic regulation of extrachromosomal mutant EGFR DNA. Science. 2014; 343(6166): 72–6. https://doi.org/10.1126/science.1241328 PMID: 24310612

35. Turner KM, Deshpande V, Beyter D, Koga T, Rusert J, Lee C, et al. Extrachromosomal oncogene amplification drives tumour evolution and genetic heterogeneity. Nature 2017; 543(7643): 122–125. https://doi.org/10.1038/nature21356 PMID: 28178237

36. Windle B., Draper B. W., Yin Y. X., O'Gorman S. & Wahl G. M. A central role for chromosome breakage in gene amplification, deletion formation, and amplicon integration. Genes Dev. 1991; 5: 160–174. PMID: 1995414

S1 Fig PCR analysis of murine MLH1 and human specific cytochrome B.

A) Analysis of gDNA pools of xHROG22 (xH.22), xHROG33 (xH.33) and xHROG59 (xH.59) at passage 2 (P2) and passage 10 (P10). Ctr M: DNA derived from mouse tail tissue as positive control for murine MLH1 (~350bp), Ctr H: DNA derived from a GBM cell line established from patient derived GBM tissue B) Verification of human origin of the cell lines by human specific cytochrome B PCR (~130bp product).

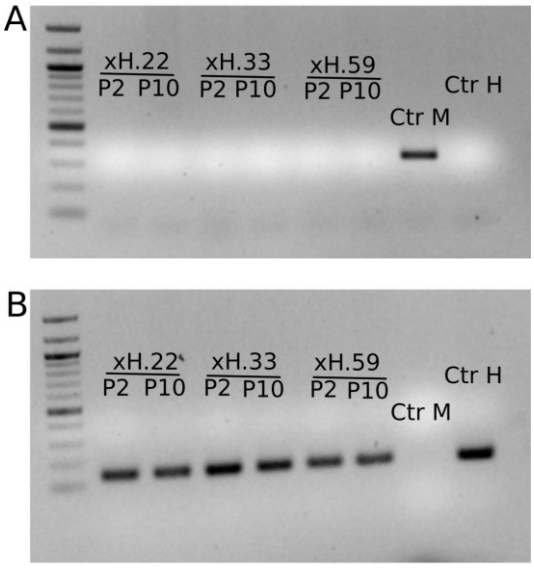

S2 Fig qPCR analysis of EGFR amplification of all successfully established cell lines. Tukey test, * $p<0.05$.

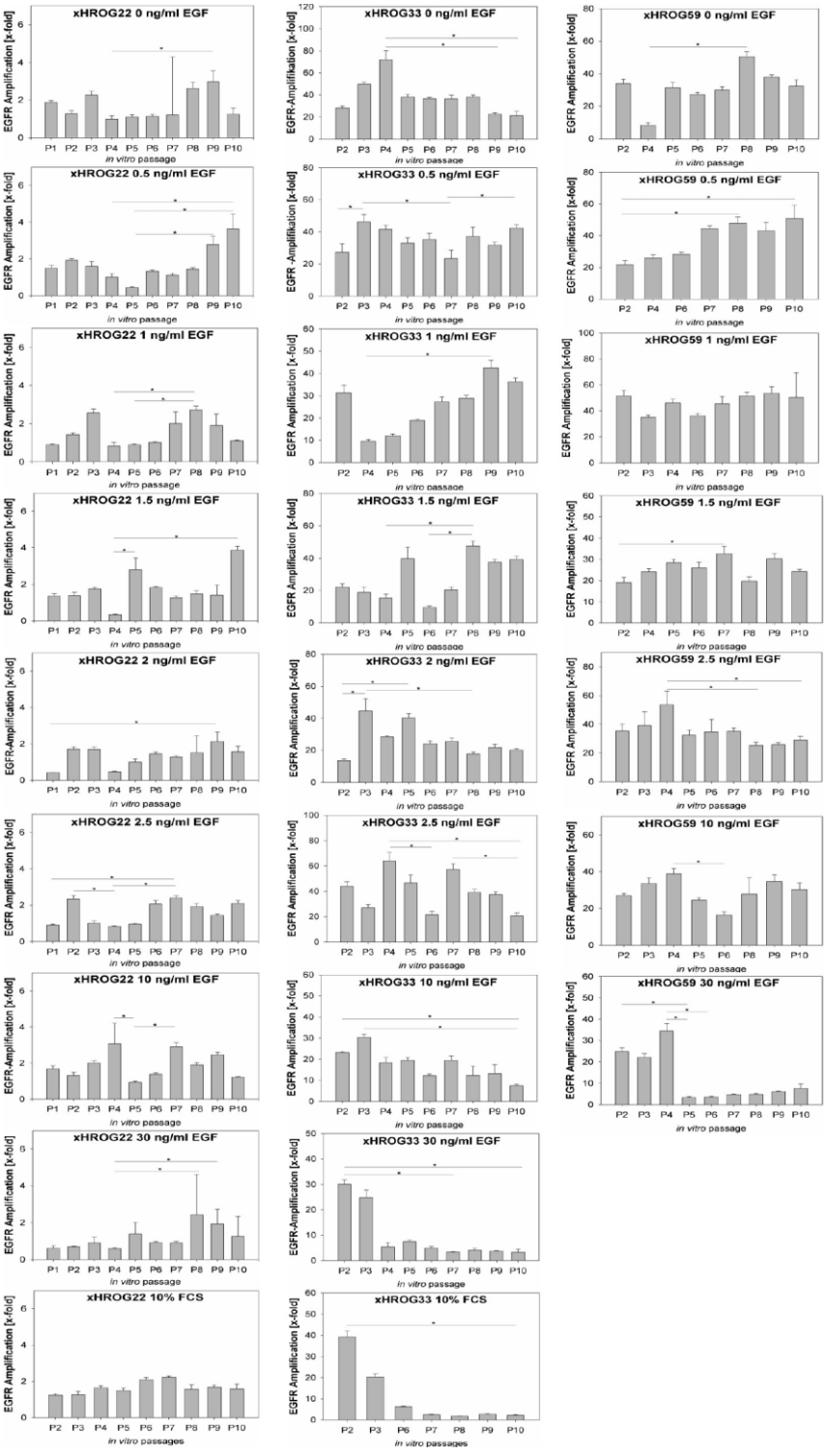

4.2. Temozolomide-induced increase of tumorigenicity can be diminished by targeting of mitochondria in in vitro models of patient individual glioblastoma

William D, Walther M, Schneider B, Linnebacher M, Classen CF

PLoS ONE 13(1):e0191511. https://doi.org/10.1371/ journal.pone.0191511

PLOS ONE

RESEARCH ARTICLE

Temozolomide-induced increase of tumorigenicity can be diminished by targeting of mitochondria in *in vitro* models of patient individual glioblastoma

Doreen William[1]*, Madlin Walther[1], Björn Schneider[2], Michael Linnebacher[3], Carl Friedrich Classen[1]

1 University Children's and Adolescents' Hospital, University Medicine of Rostock, Rostock, Germany, **2** Institute of Pathology, University Medicine of Rostock, Rostock, Germany, **3** Department of Surgery, University Medicine of Rostock, Schillingallee Rostock, Germany

* doreenwilliam@web.de

OPEN ACCESS

Citation: William D, Walther M, Schneider B, Linnebacher M, Classen CF (2018) Temozolomide-induced increase of tumorigenicity can be diminished by targeting of mitochondria in *in vitro* models of patient individual glioblastoma. PLoS ONE 13(1): e0191511. https://doi.org/10.1371/journal.pone.0191511

Editor: Ilya Ulasov, Northwestren University, UNITED STATES

Received: October 2, 2017

Accepted: January 6, 2018

Published: January 19, 2018

Data Availability Statement: All relevant data are within the paper.

Funding: The authors received no specific funding for this work.

Competing interests: The authors have declared that no competing interests exist.

Abstract

Glioblastoma multiforme (GBM) is a highly heterogeneous and aggressive brain tumor with a dismal prognosis. Development of resistance towards cytostatic drugs like the GBM standard drug temozolomide is a severe problem in GBM treatment. One potential source of GBM relapse could be so called cancer stem like cells (CSCs). These represent an undifferentiated subpopulation of cells with high potential for tumor initiation. Furthermore, it has been shown that differentiated GBM cells can regain CSC properties when exposed to continuous temozolomide treatment *in vitro*. In this study, treatment of several primary GBM cell lines with clinically relevant doses of temozolomide increased their tumorigenicity as determined by colony formation assays in soft agar. Increased tumorigenicity is a known property of CSCs. Hence, therapy options that specifically target CSCs are under investigation. CSCs appear to be particularly dependent on mitochondria biogenesis which may represent a useful target for CSC elimination. Toxicity towards mitochondria is a known side effect of several antibiotics. Thus, addition of antibiotics like doxycycline may represent a useful tool to inhibit CSCs in GBM. Here, we show that combining temozolomide treatment of primary GBM cells with doxycycline could counteract the increase of tumorigenicity induced by temozolomide treatment.

Introduction

Glioblastoma multiforme (GBM) is a highly malignant brain tumor associated with a median survival of only 12 to 15 months despite aggressive multimodal standard treatment, consisting of resection followed by radio- and chemotherapy [1,2]. The development of resistance towards cytostatic drugs like the first line drug temozolomide is a problem for GBM treatment, and relapses of the disease are common [3]. One potential source of resistance and relapses are the so-called cancer stem-like cells (CSCs) within those tumors [4,5]. CSCs are a subpopulation of cells with the capability of self-renewal, increased drug resistance and potential of

tumor (re-)initiation [6–8]. CSCs show expression of proteins associated with a physiological stem or progenitor cell state, for example CD133, CD15 and nestin [9]. The higher drug resistance of CSCs appears to be attributable to several different factors. There is evidence that CSCs show increased expression of MGMT [10] and multidrug resistance related proteins (MDRs) [11]. Furthermore, tumor cells can undergo dedifferentiation processes to acquire a CSC phenotype [12]. It has been shown that clinically relevant doses of temozolomide (TMZ) lead to enrichment of CSCs in a non-CSC population *in vitro*, which is not only caused by selection processes but also by conversion of non-CSCs into CSCs [12]. Hence, the direct targeting of CSCs might be a promising strategy for GBM treatment.

An Achilles heel of CSCs in several different tumor entities seems to be their increased dependence on mitochondria [13,14]. Mitochondria are essential for a variety of tumor functions [15]. Altered mitochondria function in cancer can lead to increased proliferation of tumor cells, apoptosis inhibition and induce a switch from catabolic to anabolic state [15]. It was reported that especially CSCs show an anabolic metabolism, supporting tumor initiation and proliferation [13].

Toxicity towards mitochondria is a known side effect of several antibiotics including tetracyclines [14]. Tetracyclines inhibit bacterial protein biosynthesis by reversibly binding the aminoacetyl-tRNA of the 30S subunit of 70S ribosomes. The 30S subunit of bacterial ribosomes is structurally very similar to the 28S subunit of mitochondrial ribosomes, enabling tetracyclines to bind and inhibit mitochondrial function [14]. Previous studies showed that treatment of GBM cells with doxycycline (Dox), a tetracycline derivate, inhibits spheroid formation of GBM-CSCs *in vitro*, which may indicate CSC inhibition [14]. Furthermore, CSCs of several tumor entities displayed an increased susceptibility towards treatment with antibiotics that are toxic towards mitochondria, compared to non-CSCs of the respective tumor entities *in vitro* [14].

In this study, four patient derived primary GBM cell lines were analyzed with regard to tumorigenicity upon TMZ treatment. We could show that continuous treatment of non-CSCs with therapeutic doses of TMZ lead to increased tumorigenicity *in vitro*, which can be counteracted by combined treatment with Dox.

Materials & methods

Cell culture

The primary GBM cell lines used in this study were previously established from patient individual GBM tissue in our laboratory [16]. Specimen collection was conducted in accordance with the ethics guidelines for the use of human material, approved by the Ethics Committee of the University of Rostock (Reference number: A 2009/34). Cells were cultured in DMEM/Ham's F12 (Biochrom, Berlin, Germany) supplemented with 10% FCS (PAN-Biotech, Aidenbach, Germany) and 2mM L-Glutamine (Biochrom) and cultivated at 37˚C, 5% CO_2 and 95% relative humidity.

Treatment with temozolomide and doxycycline

TMZ (MSD SHARP & DOHME GMBH, Haar, Germany) stock and Dox (AppliChem, Darmstadt, Germany) solutions were prepared at a concentration of 175mM (TMZ) and 39mM (Dox) in DMSO, aliquoted and stored at -30˚C. Cells were treated with TMZ (50μM) alone, Dox (50μM) alone or a combination of both drugs (50μM each) for 2 cycles of 72h each. After 72h the medium was changed to freshly prepared medium containing the respective drugs and the cells were incubated for another 72h. Control cells were treated with DMSO only. Determination of cell viability after treatment was done by Calcein AM assay (Thermo Fisher Scientific).

Colony formation assay

To determine the tumorigenic potential of the primary GBM cell lines, colony formation assays were performed in soft agar [17]. 96-Well plates were coated with 0.4% Agar dissolved in medium (100μl per well) and allowed to solidify.

Cells were harvested by trypsination and resuspended in 0.35% Agar dissolved in medium tempered to 40˚C in a water bath. The cells were seeded in the pre-coated 96-well plates at a concentration of 500 cells per well and allowed to solidify. The cells were fed regularly by addition of 50μl medium per well and cultivated in a CO_2 incubator at 37˚C. After 14 days, the cells were stained with calcein AM viability dye (Thermo Fisher Scientific) and formed colonies were counted using an Elispot-reader (CTL Europe GmbH, Bonn, Germany).

Western blot

Proteins were isolated from GBM cell lines by lysis of GBM cells with ripa buffer supplemented with protease inhibitor cocktail (Roche, Basel, Switzerland) following manufacturer's instructions. Protein concentrations were determined via BCA assay kit (Merck Millipore, Massachusetts, USA). 30μg of protein per sample were separated on 8% SDS-polyacrylamide gels and subsequently transferred on polyvinylidene fluoride membranes using a tank blot system with Towbin buffer (25mM Tris, 192mM Glycine, 10% methanol, 0.1% SDS). After transfer, membranes were incubated in blocking solution (5% dry milk in tris buffered saline, pH 7.4) for 2h at room temperature (RT). Afterwards membranes were incubated with primary antibodies against CD15 (immunotools; 1:1000), nestin (Merck Millipore, 1:1000) and β-actin (Abcam, 1:1000) diluted in blocking solution for 2h. Prior to detection membranes were incubated with horseradish peroxidase-conjugated secondary antibodies (rabbit α-mouse-hrp, antibodies-online; 1:1000 in blocking solution) for 1h at RT. Detection was done with the Super Signal West Femto Kit (Thermo Fisher scientific) in a GelLogic 1500 Imaging System (Kodak, Berlin, Germany). Quantification was done by densitometric measurements of the digital images using ImageJ software [18]. The values were obtained by measuring the brightness of the western blot signal and the same area size was used throughout one blot.

As Tubulin was used as control, the values obtained for CD15 and Nestin were divided by the corresponding Tubulin values. To obtain the relative expression after treatment, the quotients of the treated samples were divided by the quotients of the untreated samples.

Immunofluorescence staining of mitochondria

The cells were grown on cover slips in 24-well plates at 5000 cells per well and treated with temozolomide (50μM), doxycycline (50μM) or a combination of both drugs for 2 cycles at 72h each. For fluorescence staining of mitochondria the MITO-ID Red Detection Kit (Enzo) was used following manufacturer's instructions.

Quantification of mitochondria content

The relative amount of mitochondria in cell lines was determined by quantitative PCR. Therefore, total genomic DNA was isolated using the Genomic Wizard DNA extraction kit (Promega, Mannheim, Germany) following manufacturers' instructions. 30ng of genomic DNA were used as template for quantitative PCR on a StepOne Plus Realtime PCR system (Applied Biosystems, Darmstadt, Germany) with SensiFastSYBR Hi-Rox-Kit (Bioline, Luckenwalde, Germany). Primers specific for regions that are only present in the mitochondrial genome (tRNA-Leu(UUR); forward: `5′-CACCCAAGAACAGGGTTTGT-3′`, reverse: `5′-TGGCCAT GGGTATGTTGTTA-3′`) and primers specific for B2-microglobulin (forward: `5′-TGCTGTC`

TCCATGTTTGATGTATCT-3′, reverse: 5′-TCTCTGCTCCCCACCTCTAAGT-3′), which is specifically located on nuclear DNA were used [19].

Analysis of MGMT promoter methylation

Analysis of MGMT promoter methylation was done using the MethyLight method [20]. Briefly, genomic DNA was subject to bisulfite conversion using the Epitect Bisulfite Kit (Qiagen, Hilden, Germany) according to the manufacturer's recommendations. A primer / probe combination specific for the methylated MGMT promoter sequence was used (forward: 5′-GCGTTTCGACGTTCGTAGGT-3′; reverse: 5′-CACTCTTCCGAAAACGAAACG-3′; probe: 5′-6FAM-CGCAAACGATACGCACCGCGA-TMR-3′), with SensiFast Probe Kit (Bioline, Luckenwalde, Germany). Fully methylated CpG Methylase (SssI) treated DNA served as calibrator. The collagenase gene 2A1 (COL2A1), was used as endogenous control (forward: 5′-TCTAACAATTATAAACTCCAACCACCAA-3′; reverse: 5′-GGGAAGATGGGATAGAAGGGAATAT-3′; probe: 5′-6FAM-CCTTCATTCTAACCCAATACCTATCCCACCTCTAAA-TMR-3′). The percentage of methylated reference (PMR) value was calculated by dividing the MGMT / COL2A1 ratio of the sample by the MGMT / COL2A1 ratio of the SssI-treated DNA, and multiplying by 100. Samples with a PMR value > 4 were considered as methylated. All reactions were performed in triplicates.

Immunohistochemistry analysis of formalin fixed paraffin embedded GBM tissue samples

Immunohistochemistry (IHC) was performed using antibodies specific for nestin (Merck Millipore) and CD15 (immunotools). Slides were processed on an automatic IHC system, AutostainerLink48 (Dako, Hamburg, Germany), following routine protocols.

Statistics

Statistical analysis was performed using SigmaPlot 10.0 (Systat Software, Inc., Erkrath, Germany). A Mann-Whitney Rank Sum Test was performed to determine significant differences between treatment groups. P values of $p<0.05$ were considered as significant, $p<0.001$ was considered as highly significant.

Results

Clinically relevant doses of temozolomide increase tumorigenicity of GBM cells *in vitro*

Four previously in our laboratory established glioblastoma cell lines [16]–HROG06, HROG10, HROG36 and HROG38 –were treated with 50μM TMZ, 50μM Dox or a combination of both substances for 2 cycles of 72h to determine their sensitivity towards this treatment (Fig 1). All cell lines were derived from treatment naïve GBMs and showed an unmethylated MGMT-promoter (S1 Table). TMZ treatment had no effect on the viability of all cell lines at the applied dosis. Dox treatment was able to significantly reduce the amount of viable cells in all cases in comparison to untreated controls. Simultaneous treatment with both substances did not show additional effects compared to Dox monotherapy, indicating that the reduction of viable cells is solely attributable to Dox (Fig 1). The methylation status of the MGMT-promoter remained stable under all treatment conditions (S1 Table).

Surviving cells from each treatment condition and cell line were analyzed further regarding their tumorigenicity *in vitro* by colony formation assays in soft agar. TMZ treated cell lines

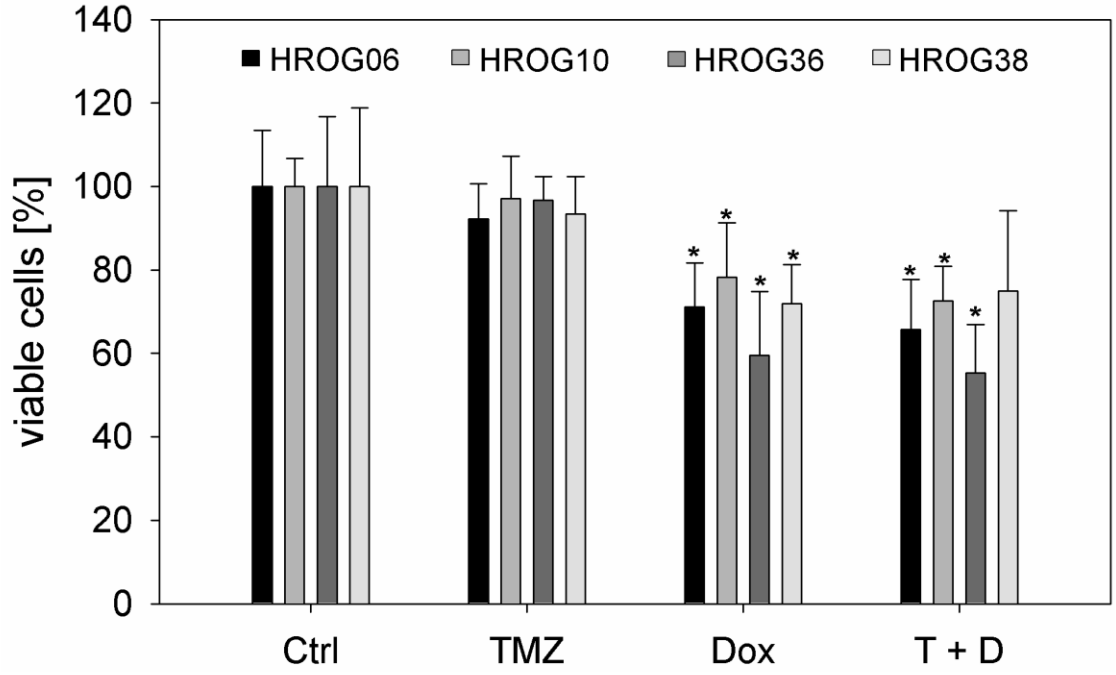

Fig 1. Sensitivity of patient individual GBM cell lines towards TMZ and Dox. Results are given as median values of 4 independent experiments in triplicates. Error bars represent the standard deviation, Ctrl: untreated cells, TMZ: 50μM temozolomide, Dox: 50μM doxycycline, T+D: combination treatment with temozolomide and doxycycline (50μM each), *$p<0.05$, Mann Whitney Rank sum test.

https://doi.org/10.1371/journal.pone.0191511.g001

HROG06, HROG10 and HROG36 showed significantly increased tumorigenicity *in vitro* compared to untreated cells. No difference was observed in case of HROG38 (Fig 2).

Targeting mitochondria with doxycycline counteracts TMZ induced *in vitro* tumorigenicity

A previous study demonstrated that non-CSCs can (re-)gain CSC properties after TMZ treatment [12]. The increased *in vitro* tumorigenicity after treatment with TMZ might be an indicator for a conversion of GBM cells into a CSC like cell type. Since it has been reported previously that CSCs show an increased dependence on mitochondrial biogenesis, they may be an attractive therapeutic target [14]. In order to determine if simultaneous treatment with Dox can prevent the TMZ induced increase of tumorigenicity *in vitro*, the four GBM cell lines were treated with 50μM Dox and 50μM TMZ alone and in combination. Three cell lines treated with a monotherapy of 50μM Dox showed *in vitro* tumorigenicity levels similar to the untreated controls (HROG06, HROG10 and HROG38), indicating that Dox itself does not influence *in vitro* tumorigenicity in those cell lines (Fig 2). However, in case of the HROG36 cell line, treatment with 50μM Dox alone lead to significantly decreased *in vitro* tumorigenicity compared to untreated controls ($p<0.001$; Fig 2). Upon combination treatment with TMZ and Dox, the *in vitro* tumorigenicity decreased significantly compared to TMZ treatment in HROG06 and HROG36 ($p = 0.004$ and $p<0.001$, respectively; Fig 2). In case of HROG10, we observed a trend towards a decreased *in vitro* tumorigenicity upon combination treatment

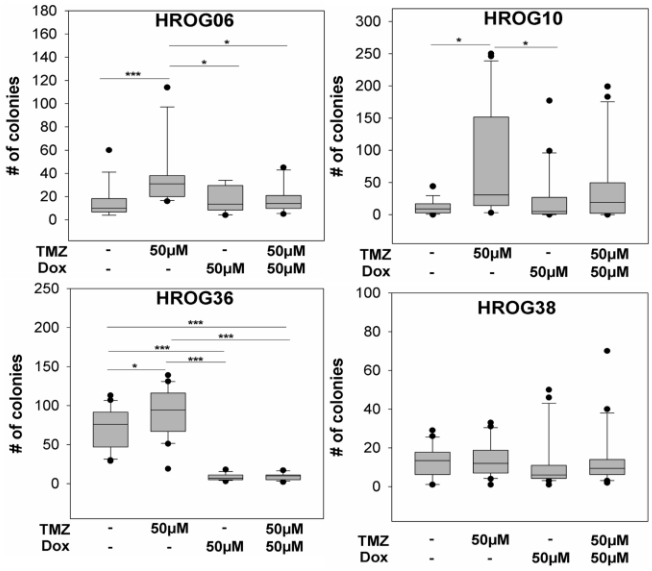

Fig 2. TMZ treatment of non-CSCs leads to increased tumorigenicity *in vitro* which can be diminished by combination treatment with Dox. Tumorigenicity of GBM cell lines after treatment with TMZ, Dox or a combination of both drugs in vitro, * $p<0.05$, *** $p<0.001$, Mann Whitney rank sum test.

https://doi.org/10.1371/journal.pone.0191511.g002

with TMZ and Dox which did not reach significance (p = 0.066). No treatment effects were observed in case of HROG38 (p = 0.386; Fig 2).

Expression of GBM-CSC markers nestin and CD15

GBM tumor cells show increased tumorigenicity *in vitro* after treatment with clinically relevant doses of TMZ. This could possibly be attributable to a conversion of non-CSCs into CSC like cells. Hence, expression of two GBM-CSC markers–CD15 and nestin [9]—was analyzed. CD15 was expressed at low levels (HROG06, HROG10, HROG36) or undetectable (HROG38) in untreated non-CSCs in all four analyzed cell lines. However, increased CD15 expression was observed after treatment with 50μM TMZ compared to untreated cells in HROG06, HROG10 and HROG36 cell lines (Fig 3). All cell lines treated with a combination of 50μM TMZ and 50μM Dox showed expression levels of CD15 comparable to untreated non-CSCs (Fig 3). Expression of the intracellular marker nestin was not affected by TMZ treatment in HROG06, HROG10 and HROG38. In case of HROG36, increased nestin expression was observed after TMZ treatment, but not after Dox or combination treatment (Fig 3).

Analysis of mitochondria content in GBM cell lines

In order to determine the effect of the different treatments on the amount of mitochondria in the GBM cell lines, we quantified the content of mitochondrial DNA in relation to nuclear DNA by qPCR using primer sets specific for mitochondrial DNA or nuclear DNA (Fig 4A). Additionally, mitochondria of all four cell lines treated with 50μM TMZ, 50μM Dox and a combination of both drugs were stained, using the MITO-ID Red Detection Kit (Enzo), and compared to untreated control cells (Fig 4B). In case of HROG06, a significant increase of the amount of mitochondria was observed upon treatment with TMZ and Dox as single agents,

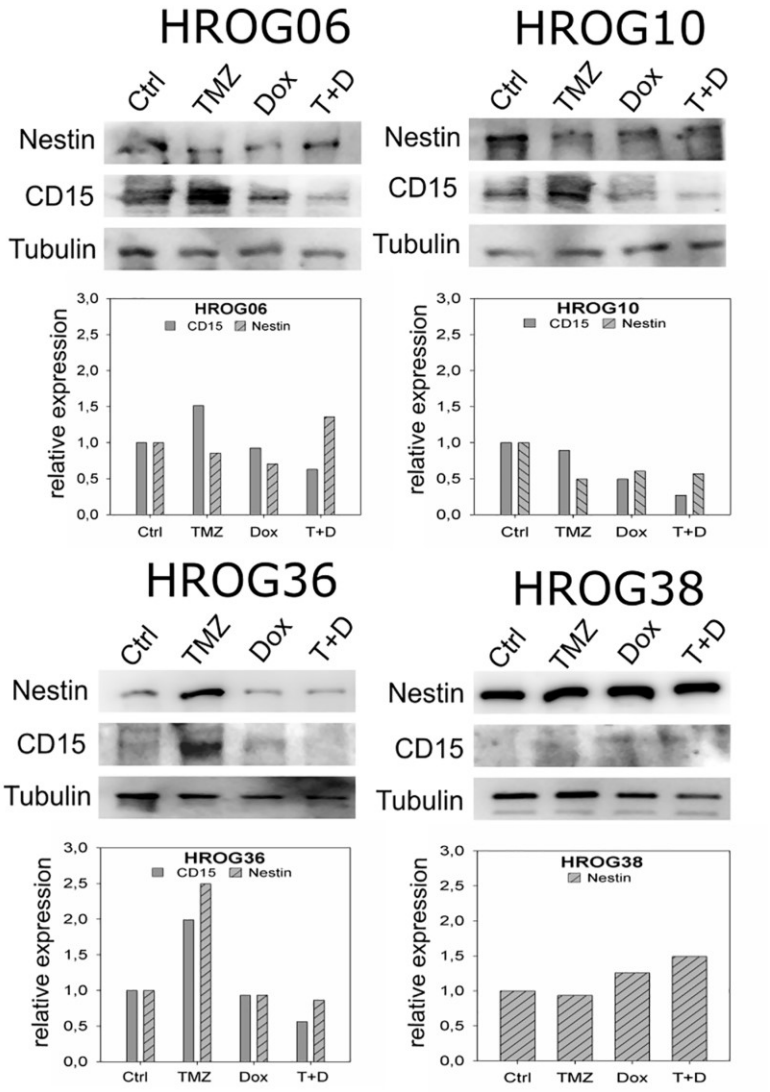

Fig 3. Nestin and CD15 expression after *in vitro* treatment with TMZ, Dox and a combination of both drugs. Upper panels show western blot analysis of GBM non-CSCs under different treatment conditions (50μM TMZ, 50μM Dox or 50μM each), Tubulin represents the loading control. Lower panels are results from densitometric scanning analyses of the western blot signals. Results are given as relative expression to untreated control cells.

https://doi.org/10.1371/journal.pone.0191511.g003

but not in combination, in comparison to untreated control cells (TMZ: p = 0.009, Dox: p = 0.017, combination: p = 0.31; Fig 4A). However, microscopic analysis of fluorescence stained mitochondria revealed no marked difference in mitochondria content in HROG06 cells under all treatment regimens and untreated control cells (Fig 4B). In case of HROG10 we observed a significant decrease of mitochondrial DNA by qPCR after Dox treatment compared to untreated control cells ($p<0.001$) and cells treated with 50μM TMZ ($p<0.001$; Fig 4A).

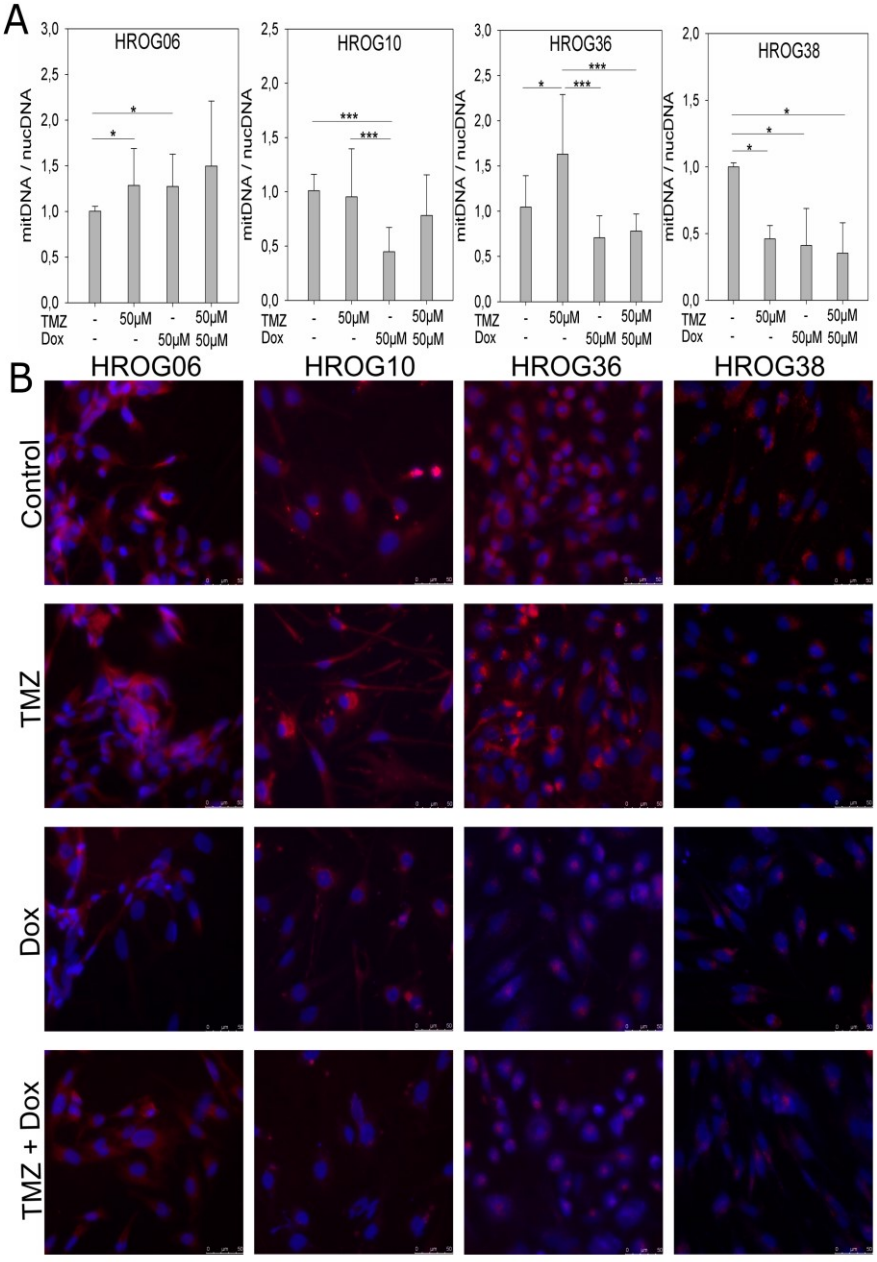

Fig 4. Mitochondria content of GBM non-CSCs can be affected by temozolomide and doxycycline treatment. A) Quantification of mitochondria amount in GBM cell lines via qPCR analysis of mitochondrial DNA in relation to nuclear DNA under different treatment conditions, results are depicted as mean values of 3 independent experiments in triplicates, error bars indicate the standard deviation; * $p<0.05$, *** $p<0.001$; B) Fluorescence staining of mitochondria in GBM cell lines under different treatment conditions.

https://doi.org/10.1371/journal.pone.0191511.g004

Direct staining of mitochondria showed a lower staining intensity after treatment with 50μM Dox alone or in combination with 50μM TMZ compared to untreated and TMZ treated cells (Fig 4B). In the HROG36 cell line the amount of mitochondria increased significantly upon treatment with TMZ compared to untreated controls ($p = 0.016$) in qPCR analysis, which was also observed by fluorescence microscopy of stained mitochondria (Fig 4A and 4B). Additionally we observed a significant decrease of mitochondrial DNA after treatment with Dox ($p<0.001$) or a combination of TMZ and Dox compared to TMZ treated cells in qPCR analysis ($p<0.001$; Fig 4A). Again, this effect was clearly visible by fluorescence staining of mitochondria of HROG36 cells (Fig 4B). In case of HROG38 decreased amounts of mitochondrial DNA were evident in all treatment conditions in comparison to untreated controls ($p = 0.002$), which was confirmed by microscopic analysis (Fig 4B).

CD15 expression is increased in clinical samples of relapsed GBM

We could confirm that treatment with 50μM TMZ enhances tumorigenicity *in vitro* and influences the expression of the two GBM CSC markers nestin and CD15. Within our cohort of GBM patients that were operated on at the department of neurosurgery in Rostock, we identified two cases that underwent surgery for both the primary GBM and the relapsed tumor. More importantly, both patients received a TMZ therapy prior to the excision of the relapsed GBM. In the first matched pair ("Primary GBM1" and "Relapsed GBM 1") TMZ was applied until three days before excision of the relapsed tumor, in case of the second pair ("Primary GBM 2" and "Relapsed GBM2") the patient received TMZ until 3 months prior to surgery. Formalin fixed paraffin embedded tissue samples of those tumors were analyzed by immunohistochemistry staining of CD15 and nestin (Fig 5, S1 Fig). There were no marked differences in nestin expression in both matched cases. However, increased expression of CD15 was evident in both relapsed GBM samples in comparison to the matched primary GBMs (Fig 5, S1 Fig).

Discussion

Despite multimodal treatment, GBM remains a lethal tumor with only few long-time survivors [1,2]. Drug resistance is a major challenge of GBM treatment. Several mechanisms of drug resistance, for example increased MGMT expression [21] and upregulation of ABC transporters [11] have been identified for GBM. Another proposed drug resistance mechanism is the loss of cellular hierarchy within a tumor [12], which we explored further in this study. The hypothesis of cellular hierarchy proposes the existence of a small subset of undifferentiated CSCs within a GBM which are capable of self-renewal and tumor growth initiation [6–8]. GBM-CSCs can also differentiate into several neural cell lineages like astrocytes, oligodendrocytes or glia cells, enhancing the tumor mass [22]. However, there is evidence that differentiated tumor cells can undergo dedifferentiation processes to (re-)gain a CSC phenotype and evade chemotherapy [12]. We could detect significantly increased *in vitro* tumorigenicity in 3 out of 4 patient derived GBM cell lines after treatment with clinically relevant TMZ doses (Fig 2), suggesting that TMZ possibly induced a conversion of non-CSCs to a CSC phenotype in those cell lines [12]. This is well in line with the results of the study by Auffinger *et al*., demonstrating conversion of GBM non-CSCs into CSCs after TMZ treatment *in vitro* [12]. However, this effect might also be caused by TMZ induced selection of CSCs in our study. To further investigate the possible conversion of non-CSCs into CSCs we analyzed expression of the two GBM CSC markers nestin and CD15 (Fig 3). We also aimed to target the supposed CSCs by treatment with Dox, because it has been reported that CSCs of several tumor entities–including GBM–show increased dependence on mitochondria [13,14]. The results we obtained lead us to conclude that a potential non-CSC conversion after TMZ therapy is not the only

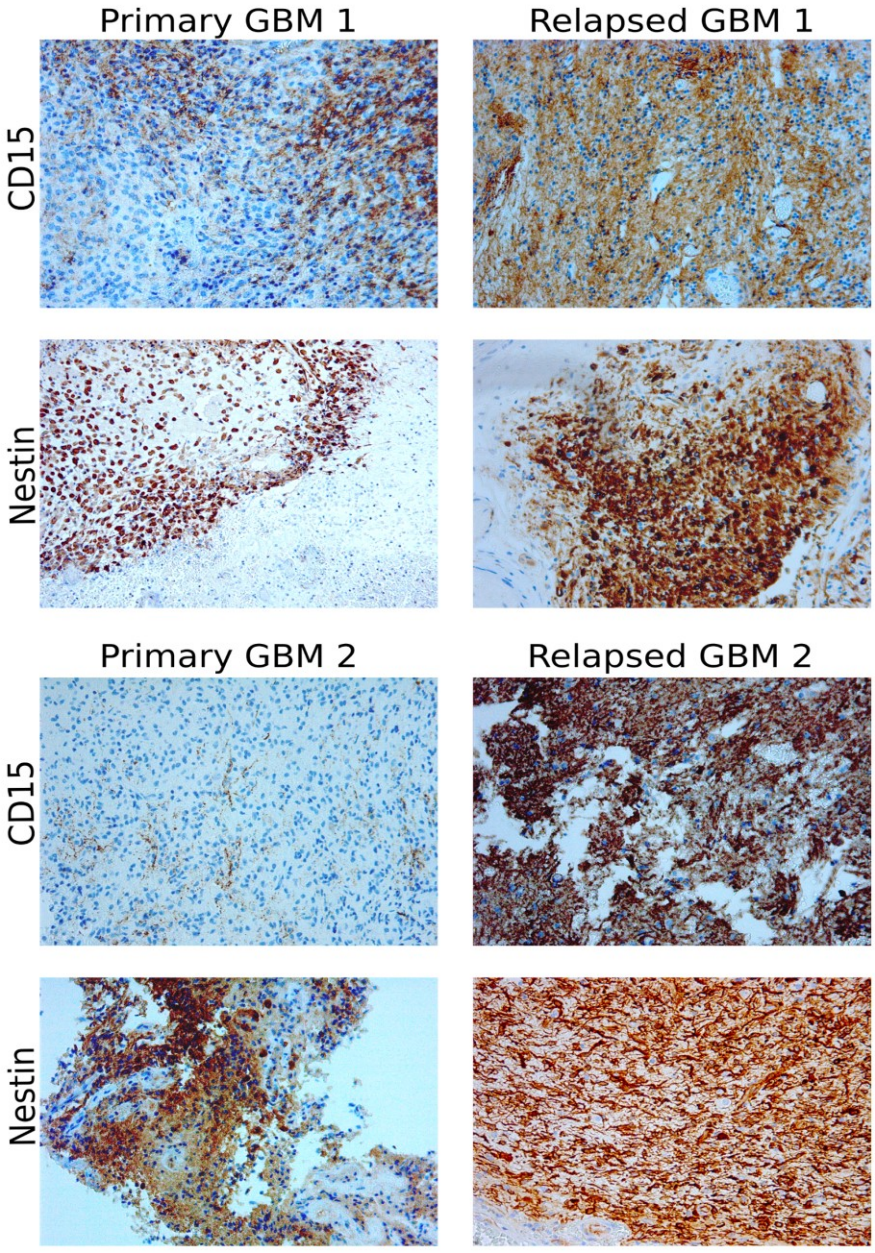

Fig 5. CD15 expression is increased in clinical samples of two relapsed GBM. IHC staining of nestin and CD15 in clinical samples of two cases pre and post chemotherapy with TMZ, 200x magnification.

https://doi.org/10.1371/journal.pone.0191511.g005

mechanism responsible for increased tumorigenicity *in vitro*. Only one cell line–HROG36 – showed results that were relatively consistent with the hypothesis of loss of cell hierarchy and conversion of non-CSCs into CSCs in our study: 1) increased tumorigenicity after treatment

with TMZ that was associated with a higher mitochondria content, 2) diminished tumorigenicity and lowered mitochondria content after Dox treatment and 3) higher expression of both analyzed GBM CSC markers nestin and CD15 after TMZ treatment but not after Dox or combination treatment. In case of HROG06, additional treatment with Dox diminished the TMZ induced increased tumorigenicity, but had no effect on mitochondria content. HROG10 also showed increased tumorigenicity *in vitro* after TMZ treatment, which was not significantly reduced by additional Dox treatment ($p = 0.066$), despite decreased mitochondria content after Dox treatment in this cell line. Although not investigated further, it seems possible that Dox treatment induced proteotoxic stress in mitochondria causing impaired functionality without decreasing the mitochondria amount [23].

We found increased CD15 expression in those three cell lines that also showed increased *in vitro* tumorigenicity after TMZ treatment (Figs 2 and 3). This result prompted us to analyze CD15 expression by immunohistochemistry staining of FFPE material from 2 patients that underwent surgery for the primary GBM as well as the relapsed tumor. Furthermore both patients received chemotherapy with TMZ until 3 days (case #1) or 3 months (case #2) prior to the second surgery. In both cases, CD15 expression was higher in the relapsed GBMs, whereas the difference in nestin expression was less pronounced (Fig 5, S1 Fig). CD15 is a proposed yet controversial CSC marker for GBM [24,25]. Despite the controversial role of CD15 as a GBM CSC marker surprisingly little is known about its exact function in GBM. CD15 is a member of the family of fucosyltransferases (FUT) that are involved in the generation of fucosylated carbohydrate structures [26]. Furthermore, CD15 promotes proliferation and cell cycle progression via crosstalk with PI3K/Akt and MAPK in A431 cells [27]. Members of the FUT family, including CD15, were linked to multidrug resistance in hepatocellular carcinoma cells via PI3K/Akt signaling [28]. The PI3K/Akt pathway is known to be often deregulated in GBM and might as well be influenced by fucosyltransferases to promote drug resistance [29,30]. There is also evidence of increased expression of fucosylated glycans in other cancers, like breast cancer, lung cancer or colon cancer [31–34]. Thus, analysis of fucosylated glycans and expression of fucosyltransferases could provide more insight in the development of drug resistance [28]. Little is known about the role of fucosyltransferases in drug resistance in GBM. Our *in vitro* data show increased expression of CD15 after chemotherapy with TMZ in those cell lines that also showed increased tumorigenicity after TMZ treatment. Furthermore, we observed increased CD15 expression in two clinical cases in the relapsed GBM in comparison to the respective *de novo* GBMs. Although we could only analyze two clinical cases pre and post chemotherapy with TMZ it seems possible that FUTs are involved in drug resistance and should be further investigated.

Taken together, our data support the conclusion that different resistance mechanisms occur in individual GBM cells *in vitro* and possibly complement one another. A conversion of non-CSCs to cells with a CSC like phenotype seems possible, but appears to be not the only explanation for diminished *in vitro* tumorigenicity upon combination therapy with TMZ and Dox. It is also possible that Dox induced proteotoxic stress in mitochondria of non-CSCs or the possible unspecific inhibition of matrix metalloproteinases by Dox treatment is contributing to the decreased tumorigenicity we observed [35]. Another factor appears to be CD15 whose role in drug resistance development in GBM is largely unknown and our data warrant further research into the influence of fucosyltransferases in GBM.

Supporting information

S1 Table. Patient / cell line characteristics and MGMT-promoter methylation status of the cell lines pre and post treatment with 50μM TMZ, 50μM Dox and a combination of both

drugs.
(PDF)

S1 Fig. Immunohistochemistry staining of several different regions of FFPE material of 2 paired primary and relapsed GBM cases in 100x magnification.
(TIF)

Acknowledgments

The authors thank Dr. Claudia Maletzki for advice and discussions during the project as well as Birgit Salewski and Anja Rahn for excellent technical assistance. Furthermore, the authors thank the histopathology lab at the institute for pathology in the University Medicine of Rostock for IHC staining of the clinical samples.

Author Contributions

Conceptualization: Doreen William.

Data curation: Doreen William.

Formal analysis: Doreen William, Madlin Walther, Björn Schneider.

Funding acquisition: Carl Friedrich Classen.

Investigation: Doreen William, Madlin Walther, Björn Schneider.

Methodology: Doreen William, Madlin Walther.

Project administration: Doreen William, Carl Friedrich Classen.

Resources: Michael Linnebacher, Carl Friedrich Classen.

Supervision: Michael Linnebacher, Carl Friedrich Classen.

Validation: Doreen William.

Visualization: Doreen William.

Writing – original draft: Doreen William.

Writing – review & editing: Doreen William, Madlin Walther, Björn Schneider, Michael Linnebacher, Carl Friedrich Classen.

References

1. Dolecek TA, Propp JM, Stroup NE, Kruchko C. CBTRUS Statistical Report: Primary Brain and Central Nervous System Tumors Diagnosed in the United States in 2005–2009. Neuro-Oncology 2012; 14: 1–49.
2. Stupp R, Hegi ME, Mason WP, van den Bent MJ, Taphoorn MJ, Janzer RC, et al. Effects of radiotherapy with concomitant and adjuvant temozolomide versus radiotherapy alone on survival in glioblastoma in a randomised phase III study: 5-year analysis of the EORTC-NCIC trial. The Lancet Oncology 2009; 10: 459–66. https://doi.org/10.1016/S1470-2045(09)70025-7 PMID: 19269895
3. Zhang J, Stevens MFG, Bradshaw TD. Temozolomide: mechanisms of action, repair and resistance. Current molecular pharmacology 2012; 5: 102–14. PMID: 22122467
4. Beier D, Schulz JB, Beier CP. Chemoresistance of glioblastoma cancer stem cells—much more complex than expected. Molecular cancer 2011; 10: 128 https://doi.org/10.1186/1476-4598-10-128 PMID: 21988793
5. Murat A, Migliavacca E, Gorlia T, Lambiv WL, Shay T, Hamou MF, et al. Stem cell-related "self-renewal" signature and high epidermal growth factor receptor expression associated with resistance to concomitant chemoradiotherapy in glioblastoma. J Clin Oncol. 2008; 26(18): 3015–24. https://doi.org/10.1200/JCO.2007.15.7164 PMID: 18565887

6. Lima FR, Kahn SA, Soletti RC, Biasoli D, Alves T, da Fonseca AC, et al. Glioblastoma: Therapeutic challenges, what lies ahead. Biochim Biophys Acta. 2012; 1826(2): 338–49. https://doi.org/10.1016/j.bbcan.2012.05.004 PMID: 22677165
7. Hanahan D. & Weinberg R. A. Hallmarks of cancer: the next generation. Cell. 2011; 144(5): 646–74. https://doi.org/10.1016/j.cell.2011.02.013 PMID: 21376230
8. Persano L., Rampazzo E, Basso G, Viola G. Glioblastoma cancer stem cells: role of the microenvironment and therapeutic targeting. Biochem Pharmacol. 2013; 85(5): 612–22. https://doi.org/10.1016/j.bcp.2012.10.001 PMID: 23063412
9. Bradshaw A, Wickremsekera A, Tan ST, Peng L, Davis PF, Itinteang T. Cancer Stem Cell Hierarchy in Glioblastoma Multiforme. Frontiers in Surgery. 2016; 3:21. https://doi.org/10.3389/fsurg.2016.00021 PMID: 27148537
10. Blough MD, Westgate MR, Beauchamp D, Kelly JJ, Stechishin O, Ramirez AL, et al. Sensitivity to temozolomide in brain tumor initiating cells. Neuro-Oncology 2010; 12:756–60. https://doi.org/10.1093/neuonc/noq032 PMID: 20388697
11. Tivnan A, Zakaria Z, O'Leary C, Kögel D, Pokorny JL, Sarkaria JN, et al. Inhibition of multidrug resistance protein 1 (MRP1) improves chemotherapy drug response in primary and recurrent glioblastoma multiforme. Frontiers in neuroscience 2015; 9: 218. https://doi.org/10.3389/fnins.2015.00218 PMID: 26136652
12. Auffinger B, Tobias AL, Han Y, Lee G, Guo D, Dey M, et al. Conversion of Differentiated Cancer Cells Into Cancer Stem-Like Cells in a Glioblastoma Model After Primary Chemotherapy. Cell death and differentiation 2014; 21: 1119–31. https://doi.org/10.1038/cdd.2014.31 PMID: 24608791
13. Lamb R, Harrison H, Hulit J, Smith DL, Lisanti MP, Sotgia F. Mitochondria as new therapeutic targets for eradicating cancer stem cells: Quantitative proteomics and functional validation via MCT1/2 inhibition. Oncotarget 2014; 5: 11029–37. https://doi.org/10.18632/oncotarget.2789 PMID: 25415228
14. Lamb R, Ozsvari B, Lisanti CL, Tanowitz HB, Howell A, Martinez-Outschoorn UE, et al. Antibiotics that target mitochondria effectively eradicate cancer stem cells, across multiple tumor types: Treating cancer like an infectious disease. Oncotarget 2015; 6: 4569–84. https://doi.org/10.18632/oncotarget.3174 PMID: 25625193
15. Wallace DC. Mitochondria and cancer. Nature Reviews Cancer 2012; 12: 685–98. https://doi.org/10.1038/nrc3365 PMID: 23001348
16. Mullins CS, Schneider B, Stockhammer F, Krohn M, Classen CF, Linnebacher M. Establishment and characterization of primary glioblastoma cell lines from fresh and frozen material: A detailed comparison. PLoS ONE 2013; 8: e71070 https://doi.org/10.1371/journal.pone.0071070 PMID: 23951083
17. Borowicz S, Van Scoyk M, Avasarala S, Karuppusamy Rathinam MK, Tauler J, Bikkavilli RK, et al. The Soft Agar Colony Formation Assay. J Vis Exp. 2014;(92):e51998. https://doi.org/10.3791/51998 PMID: 25408172
18. Schneider CA, Rasband WS, Eliceiri KW. (2012), NIH Image to ImageJ: 25 years of image analysis. Nature methods 2012; 9(7): 671–675. PMID: 22930834
19. Rooney JP, Ryde IT, Sanders LH, Howlett EH, Colton MD, Germ KE, et al. PCR Based Determination of Mitochondrial DNA Copy Number in Multiple Species. Methods Mol Biol. 2015; 1241: 23–38. https://doi.org/10.1007/978-1-4939-1875-1_3 PMID: 25308485
20. Eads CA, Danenberg KD, Kawakami K, Saltz LB, Blake C, Shibata D, et al. MethyLight: a high-throughput assay to measure DNA methylation. Nucl Acids Res. 2000; 28(8):E32 PMID: 10734209
21. Esteller M, Garcia-Foncillas J, Andion E, Goodman SN, Hidalgo OF, Vanaclocha V, et al. Inactivation of the DNA-repair gene MGMT and the clinical response of gliomas to alkylating agents. N Engl J Med. 2000; 343(19): 1350–4. https://doi.org/10.1056/NEJM200011093431901 PMID: 11070098
22. Reya T, Morrison SJ, Clarke MF, Weissman IL. Stem cells, cancer, and cancer stem cells. Nature 2001; 414: 105–11. https://doi.org/10.1038/35102167 PMID: 11689955
23. Moullan N, Mouchiroud L, Wang X, Ryu D, Williams EG, Mottis A et al. Tetracyclines Disturb Mitochondrial Function across Eukaryotic Models: A Call for Caution in Biomedical Research. Cell Rep. 2015; pii: S2211–1247(15)00180-1.
24. Kenney-Herbert E, Al-Mayhani T, Piccirillo SG, Fowler J, Spiteri I, Jones P, et al. CD15 Expression Does Not Identify a Phenotypically or Genetically Distinct Glioblastoma Population. Stem Cells Transl Med. 2015; 4(7): 822–31. https://doi.org/10.5966/sctm.2014-0047 PMID: 26019225
25. Yamamuro S, Okamoto Y, Sano E, Ochiai Y, Ogino A, Ohta T, et al. Characterization of glioma stem-like cells from human glioblastomas. Int J Oncol. 2015; 47(1): 91–6. https://doi.org/10.3892/ijo.2015.2992 PMID: 25955568
26. De VT, Knegtel RM, Holmes EH, Macher BA. Fucosyltransferases: structure/function studies. Glycobiology 2001; 11: 119–128.

27. Yang XS, Liu S, Liu YJ, Liu JW, Liu TJ, Wang XQ, et al. Overexpression of fucosyltransferase IV promotes A431 cell proliferation through activating MAPK and PI3K/Akt signaling pathways. J Cell Physiol. 2010; 225(2): 612–9. https://doi.org/10.1002/jcp.22250 PMID: 20506505

28. Cheng L, Luo S, Jin C, Ma H, Zhou H, Jia L. FUT family mediates the multidrug resistance of human hepatocellular carcinoma via the PI3K/Akt signaling pathway. Cell Death Dis. 2013; 4:e923 https://doi.org/10.1038/cddis.2013.450 PMID: 24232099

29. Furnari FB, Fenton T, Bachoo RM, Mukasa A, Stommel JM, Stegh A, et al. Malignant astrocytic glioma: genetics, biology, and paths to treatment. Genes Dev. 2007; 21(21): 2683–2710. https://doi.org/10.1101/gad.1596707 PMID: 17974913

30. Cancer Genome Atlas Research Network. Comprehensive genomic characterization defines human glioblastoma genes and core pathways. Nature 2008; 455(7216): 1061–8. https://doi.org/10.1038/nature07385 PMID: 18772890

31. Lattova E, Tomanek B, Bartusik D, Perreault H. N-glycomic changes in human breast carcinoma MCF-7 and T-lymphoblastoid cells after treatment with herceptin and herceptin/Lipoplex. J Proteome Res 2010; 9: 1533–1540. https://doi.org/10.1021/pr9010266 PMID: 20063903

32. Shu H, Zhang S, Kang X, Li S, Qin X, Sun C, et al. Protein expression and fucosylated glycans of the serum haptoglobin-{beta} subunit in hepatitis B virus-based liver diseases. Acta Biochim Biophys Sin (Shanghai) 2011; 43: 528–534.

33. Mejías-Luque R, López-Ferrer A, Garrido M, Fabra A, de Bolós C. Changes in the invasive and metastatic capacities of HT-29/M3 cells induced by the expression of fucosyltransferase 1. Cancer Sci 2007; 98: 1000–1005. https://doi.org/10.1111/j.1349-7006.2007.00484.x PMID: 17459061

34. Vasseur JA, Goetz JA, Alley WR, Novotny MV. Smoking and lung cancer-induced changes in N-glycosylation of blood serum proteins. Glycobiology 2012; 22: 1684–1708. https://doi.org/10.1093/glycob/cws108 PMID: 22781126

35. Wang-Gillam A, Siegel E, Mayes DA, Hutchins LF, Zhou Y. Anti-Tumor Effect of Doxycycline on Glioblastoma Cells. Journal of Cancer Molecules 2007; 3(5): 147–153.

S1 Table Patient / cell line characteristics and MGMT-promoter methylation status of the cell lines pre and post treatment with 50µM TMZ, 50µM Dox and a combination of both drugs.

Cell line	Diagnosis	Patient age/gender	MGMT-Promotor Methylation	
			untreated	treated
HROG06	GBM	53/M	unmethylated	unmethylated
HROG10	GBM	74/M	unmethylated	unmethylated
HROG36	GBM	80/F	unmethylated	unmethylated
HROG38	GBM	49/F	unmethylated	unmethylated

S1 Fig Immunohistochemistry staining of several different regions of FFPE material of 2 paired primary and relapsed GBM cases in 100x magnification.

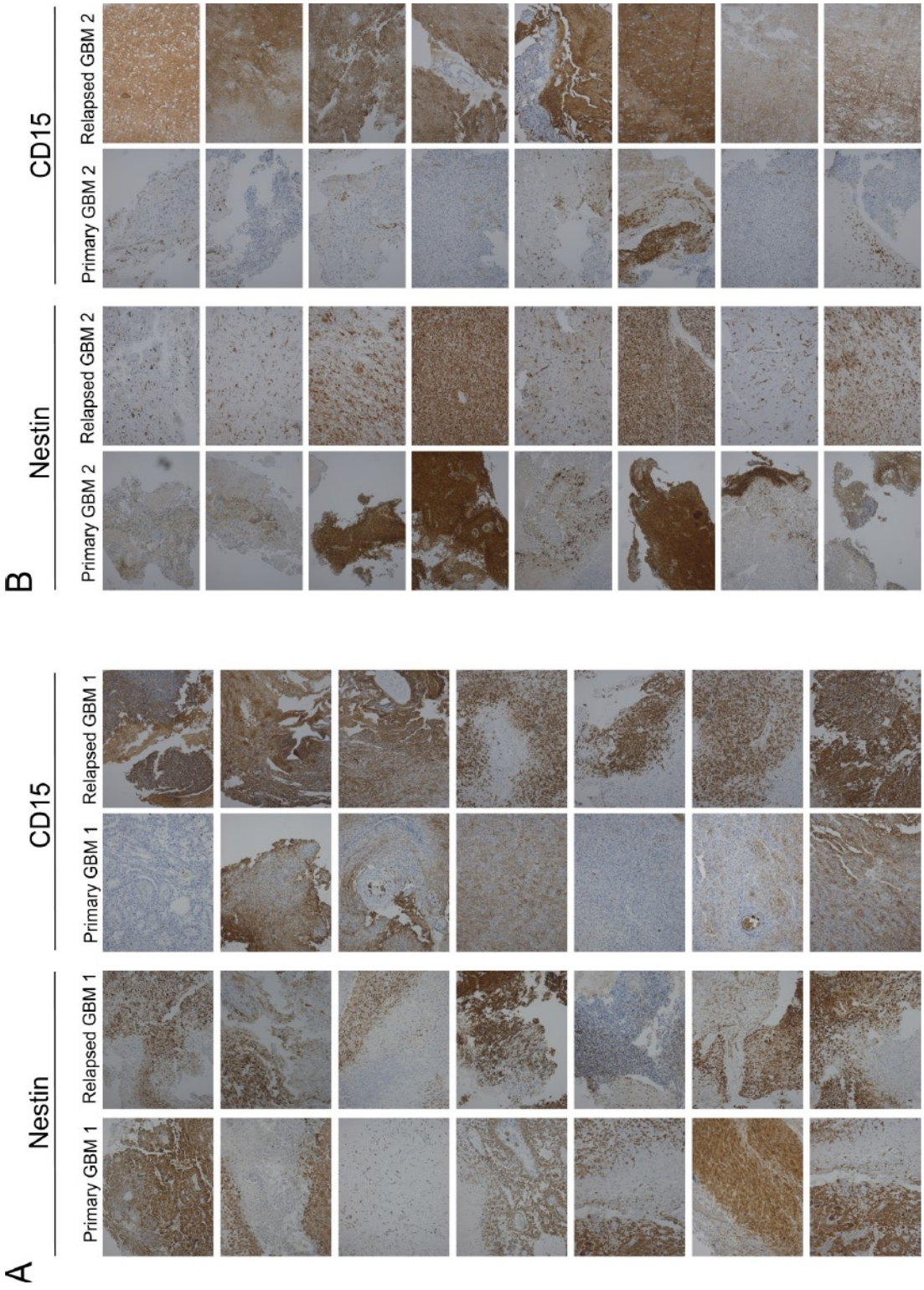

4.3. Optimized creation of glioblastoma patient derived xenografts for use in preclinical studies

William D, Mullins CS, Schneider B, Orthmann A, Lamp N, Krohn M, Hoffmann A, Classen CF and Linnebacher M

J Transl Med. 2017 Feb 9;15(1):27. doi: 10.1186/s12967-017-1128-5.

William et al. J Transl Med (2017) 15:27
DOI 10.1186/s12967-017-1128-5

Journal of Translational Medicine

RESEARCH Open Access

Optimized creation of glioblastoma patient derived xenografts for use in preclinical studies

Doreen William[1], Christina Susanne Mullins[2], Björn Schneider[3], Andrea Orthmann[4], Nora Lamp[3], Mathias Krohn[2], Annika Hoffmann[4], Carl-Friedrich Classen[1] and Michael Linnebacher[2*]

Abstract

Background: Glioblastoma multiforme (GBM) is the most common and lethal brain tumor in adults, highlighting the need for novel treatment strategies. Patient derived xenografts (PDX) represent a valuable tool to accomplish this task.

Methods: PDX were established by implanting GBM tissue subcutaneously. Engraftment success was compared between NMRI Foxn1^{nu} and NOD/SCID as well as between fresh and cryopreserved tissue. Established PDX were analyzed histologically and molecularly. Five PDX were experimentally treated with different drugs to assess their potential for preclinical drug testing.

Results: Establishment of PDX was attempted for 36 consecutive GBM cases with an overall success rate of 22.2% in NMRI Foxn1^{nu} mice. No difference was observed between fresh or cryopreserved (20–1057 days) tissue in direct comparison (n = 10 cases). Additionally, engraftment was better in NOD/SCID mice (38.8%) directly compared to NMRI Foxn1^{nu} mice (27.7%) (n = 18 cases). Molecular data and histology of the PDX compare well to the primary GBM. The experimental treatment revealed individual differences in the sensitivity towards several clinically relevant drugs.

Conclusions: The use of vitally frozen GBM tissue allows a more convenient workflow without efficiency loss. NOD/SCID mice appear to be better suited for initial engraftment of tumor tissue compared to NMRI Foxn1^{nu} mice.

Keywords: Glioblastoma multiforme, PDX, Preclinical mouse models, Therapy, Engraftment rate

Background

Glioblastoma multiforme (GBM) is the most common primary brain tumor in adults [1, 2]. With a median survival of 14–16 months from diagnosis, the prognosis for GBM patients is very dismal and novel therapeutic strategies are urgently needed to combat this disease [3–6]. A promising approach is to further facilitate personalized therapy regimens, which are tailored to specific molecular alterations of individual tumors. Besides methylation status of the MGMT promoter, established prognostic parameters for GBM are missing [7]. However, with next generation sequencing techniques on the rise, more detailed analyses of cancer genomes are becoming routinely available to clinicians and researchers worldwide [8, 9]. For example, previous analyses of GBM genomes revealed several common alterations in tyrosine kinase signaling (e.g. mutations or amplification of EGFR, ERBB2, PDGFRA, MET and PTEN) [10]. Several tyrosine kinase inhibitors and other targeted drugs entered clinical trials for GBM treatment (e.g. vandetanib, bevacizumab, nimotuzumab) however, with so far unsatisfying outcome [11–13].

In order to accomplish better personalized therapy strategies, individual models of GBM and sufficient amounts of tumor material for detailed molecular and functional analyses are required.

Although the generation of individual in vitro models of GBM is feasible with success rates of cell culture establishment of approximately 60% [14], in vitro models have

*Correspondence: michael.linnebacher@med.uni-rostock.de
[2] Department of Surgery, Molecular Oncology and Immunotherapy, University Medicine Rostock, Schillingallee 35, 18057 Rostock, Germany
Full list of author information is available at the end of the article

several disadvantages. Due to enhanced clonal selection in vitro, the use of (ultra-) low passage cell lines is mandatory to best preserve intratumoral heterogeneity [15]. Additionally, during in vitro culture, several genomic aberrations, e.g. amplification of *EGFR*, which are present in the primary tumor, are not maintained [16, 17]. In contrast, intratumoral heterogeneity and genomic aberrations are well maintained in heterotopic or orthotopic patient derived in vivo models of GBM [18, 19]. The establishment of such PDX models requires optimized logistics and standardized protocols; further the combined expertise from different fields (surgery, molecular biology and animal care facility) is imperative. In this study, we present a feasible method for the establishment of GBM PDX models from patient tumor material. First, we investigated the success rates of PDX establishment using cryopreserved GBM tissue (postoperative immediately frozen) compared to fresh tumor tissue. We could demonstrate that cryopreservation with subsequent long term storage of GBM tissue at ultra-low temperatures is a suitable and logistically convenient method for xenografting at a later time point. Furthermore, we compared the success rates of PDX establishment using two different immunocompromised mouse strains (NMRI Foxn1^{nu} and NOD/SCID) in order to further optimize PDX creation. Once established, PDX models may be a suitable tool for the prediction of therapy outcomes as well as planning of patient individual treatments in order to identify the best possible therapy option for patients suffering from GBM.

Methods

Tumor specimen collection and cryopreservation

Tumor tissue was collected directly from the operation theater at the department of neurosurgery at the University Medicine of Rostock. Specimen collection was conducted in accordance with the ethics guidelines for the use of human material, approved by the Ethics Committee of the University of Rostock (Reference number: A 2009/34) and with informed written consent from all patients prior to surgery. Tumor tissue was cut with sterile scalpels to small tissue cubes (approximately 3 × 3 × 3 mm). For cryopreservation, 4 tumor cubes were transferred to a sterile cryo-tube containing 1.5 mL freezing medium (fetal calf serum, 10% DMSO) and immediately frozen at −80 °C in a freezing container. Vitally frozen tumor material was transferred after overnight cooling at −80 °C into liquid nitrogen for long term storage at ultra-low temperatures.

Xenografting

Tumor tissue cubes were implanted subcutaneously into the flanks of female 6–8 weeks old NMRI Foxn1^{nu} or NOD/SCID mice under anaesthesia (Ketamine/Xylazin 90/6 mg/kg Bw) as previously described [20–22]. Briefly, cryopreserved tumor tissue was thawed at 37 °C and washed with PBS prior to subcutaneous implantation.

Care and housing of the animals was provided at the animal facilities of the University Medicine Rostock in accordance with recommendations from the Guide for the Care and Use of Laboratory Animals of the National Institutes of Health. The procedure was approved by the Committees on the Ethics of Animal Experiments (Landesamt für Landwirtschaft, Lebensmittelsicherheit und Fischerei Mecklenburg-Vorpommern; permission number: 7221.3-1.1-083/11). Mice were kept in a specific pathogen free environment and exposed to 12 h light/12 h darkness cycles with standard food and water (supplemented with Co-trimoxazol for 6 weeks after surgery) ad libitum. Mice were sacrificed when tumors grew to a volume of 1 cm^3 and tumor material was collected for further studies or passaged further in NMRI Foxn1^{nu} mice.

For the establishment of orthotopic GBM PDX, a single cell suspension derived from previously established GBM PDX was injected into the brain of NOD/SCID mice. Upon first signs of extracerebral tumors at place of cell injection or abnormal behavior, the mice were sacrificed and the brains were snap frozen for further analysis.

Experimental treatment of tumor bearing mice

The chemotherapeutic response of the PDX models was determined in female NMRI nu/nu mice (Janvier, Le Genest-Saint-Isle, France). Once tumors became palpable, tumor size and body weight were measured twice a week. Tumor volumes (V) were calculated by the formula V = (length × width^2)/2 and related to the values at the first day of treatment (relative tumor volume, RTV). Median treated to control (T/C) values of RTV was used for the evaluation of each treatment modality.

When the mean tumor volume reached the indicated starting volume (80–120 mm^3), mice were randomized to the six treatment arms (five mice per group) and treatment was started. If not mentioned otherwise, the following drugs and modalities were used in the single treatment studies: everolimus 5 mg/kg, orally, (days 1–5) × 2; sorafenib 80 mg/kg, orally, (days 1–5) × 2; bevacizumab 10 mg/kg, intraperitoneally, (three times a week) × 2; irinotecan 15 mg/kg, intraperitoneally, days 1–5; salinomycin 10 mg/kg, orally, days 1–14; temozolomide 90 mg/kg, orally, days 1–5. Control mice were treated with the vehicle alone (saline), orally. Doses and schedules were chosen according to previous experience in animal experiments and represent the maximum tolerated or efficient doses. The injection volume was 0.2 mL/20 g body weight.

EGFR copy number analysis

Genomic DNA (gDNA) from snap frozen tumor tissue was isolated using the Wizard Genomic DNA Purification Kit (Promega, Mannheim, Germany) according to the manufacturer's instructions. EGFR copy number was determined by quantitative PCR on a StepOne Realtime PCR system (Applied Biosystems, Darmstadt, Germany) with SensiFastSYBR Hi-Rox-Kit (Bioline, Luckenwalde, Germany) in triplicates. Commercial normal human gDNA (Promega) served as calibrator and the repetitive element LINE1 as endogenous control. The EGFR copy number was calculated with the $^{\Delta\Delta}C_t$-algorithm.

MGMT promoter methylation analysis

MGMT promoter methylation was analyzed with the MethyLight method [23]. Briefly, gDNA was subject to bisulfide conversion using the Epitect Bisulfite Kit (Qiagen, Hilden, Germany) according to the manufacturer's recommendations. Quantitative PCR was performed with the SensiFast Probe HiRox Kit (Bioline) and a primer/probe combination specific for the methylated MGMT promoter sequence (Additional file 1). Fully methylated SSSI treated DNA served as calibrator and the collagenase gene 2A1 (COL2A1) served as endogenous control. The percentage of methylated reference (PMR) value was calculated by dividing the MGMT/COL2A1 ratio of the sample by the MGMT/COL2A1 ratio of the SSSI-treated DNA multiplied by 100. Samples with a PMR value >4 were considered as methylated.

Mutation analysis

All samples were analyzed for mutations in the following loci: IDH1 R132 (exon 4), IDH2 R172 (exon 4), BRAF V600 (exon 15), KRAS G12, G13 (exon 2) and Q61 (exon 3) and TP53 exons 5–8. The desired genomic regions were amplified by PCR (Additional file 1). The PCR products were purified and used as template for Sanger sequencing using BigDye® Terminator v1.1 Cycle Sequencing Kit (Applied Biosystems) according to the manufacturer's protocol. The sequencing products were purified using the BigDye XTerminator® Purification Kit and analysed with the 3500 genetic analyzer system using the SeqScape® Software v2.7 (all Applied Biosystems).

Genetic fingerprint analysis

A genetic fingerprint analysis was performed by PCR using 9 different loci (D5S818, D7S820, D16S539, D13S317, Amelogenin, vWA, TPOX, TH01 and CSF1; Additional file 1) to verify the identity of the PDX in comparison to original GBM material [24]. Briefly, 25 ng DNA of each sample were used in 2 multiplex PCR reactions (cycling conditions: initial denaturation at 96 °C for 2 min, 30 cycles of 94 °C 30 s, 59 °C 2 min and 72 °C 1.5 min, 60 °C for 45 min). PCR products were diluted tenfold and subsequently analyzed by capillary electrophoresis.

Immunohistochemistry and H&E-staining

Formaldehyde fixed tissue samples were processed using the ExcelsiorAS system (ThermoScientific) according to the manufacturer's recommendations. For GFAP immunohistochemistry a ready to use anti-GFAP primary antibody (Dako, Hamburg, Germany) was used and the samples were processed on an automated system, EnVision™ FLEX (Dako), following manufacturer's instructions. Hematoxylin and Eosin staining was performed following established standard protocols [25].

Statistics

Statistical analysis was performed using SigmaPlot 10.0 (Systat Software). Tumor volumes were compared between treatment and control groups at the end of the experiment and analyzed by unpaired *t* test.

Results

Engraftment of primary tumor samples in immunocompromized mice

Overall, 42 tumor samples were collected and subsequently cryopreserved. Out of all samples 36 samples were classified as GBM (WHO°IV), 5 as astrocytomas (WHO°I–III) and 1 an anaplastic oligodendroglioma (WHO°III). Information on patient characteristics, diagnosis, and molecular alterations of the tumors is summarized in Table 1 and Additional file 2.

Cryopreserved tissue samples of all cases were implanted bilaterally subcutaneously in the flanks of female 6–8 weeks old NMRI Foxn1^{nu} mice. Cryopreservation periods of the tumor samples ranged from 20 to 1057 days. Engraftment of frozen GBM samples was successful in 8 out of 36 cases (22.2%) (Table 1). Engraftment of the 5 astrocytoma samples and the anaplastic oligodendroglioma sample was not successful (Additional file 2).

For 10 GBM cases, a direct comparison of tumor take rate between cryopreserved tumor tissue and tumor tissue freshly received from the operation theater was performed (Table 1). Engraftment of cryopreserved tumor tissue in NMRI Foxn1^{nu} mice was successful in one case out of 10 (HROG52, 10.0%); identical to engraftment of fresh tumor tissue (HROG59, 10.0%). In 2 cases the initial tumor growth of fresh GBM tissue was followed by complete spontaneous regression (HROG58 and HROG60). Thus, within this limited number of cases, there was no difference between engraftment success of cryopreserved

Table 1 Overview of GBM patient characteristics, molecular alterations, cryoperiod of the samples prior to subcutaneous implantation and outcome of PDX establishment attempts in NMRI Foxn1^{nu} mice

Sample ID	Sex/age	Molecular alterations	Cryoperiod (days)	Engraftment
HROG02	M/68	P53 (R248Q), 3xEGFR, MGMT(M)	305	–
HROG04	F/53	36xEGFR, MGMT(U)	270	–
			588	–
			826	–
HROG05	F/60	82xEGFR, K-ras (G12D), MGMT(M)	268	✓
HROG06	M/53	P53 (R273H, R306*), 82xEGFR, MGMT(U)	260	–
			570	✓
HROG07	M/55	12xEGFR, MGMT(U)	143	–
			699	–
HROG10	M/74	MGMT(U)	71	–
			627	–
HROG11	F/54	P53 (R248Q), 3xEGFR, MGMT(U)	56	–
HROG12	M/64	36xEGFR, MGMT(U)	307	✓
HROG13	F/77	MGMT(U)	318	–
			529	✓
HROG15	M/56	n.d.	240	–
HROG16	M/53	MGMT(U)	237	–
HROG17	M/70	3xEGFR, MGMT(M)	194	✓
HROG19	M/69	8xEGFR, MGMT(U)	217	–
HROG21	M/44	IDH1 (R132H), MGMT(U)	192	–
HROG22	M/66	MGMT(M)	167	–
HROG23	F/60	BRAF (V600E), MGMT(U)	191	–
			1057	–
HROG24	F/73	P53 (R273C), 42xEGFR, MGMT(U)	112	–
			350	–
HROG25	F/77	MGMT(U)	117	–
HROG31	F/59	MGMT(U)	55	–
			214	–
HROG32	F/76	44xEGFR, MGMT(U)	125	–
HROG33	F/46	31xEGFR, MGMT(U)	119	✓
HROG34	F/69	96xEGFR, MGMT(U)	133	–
HROG36	F/80	MGMT(U)	80	–
HROG38	F/49	MGMT(U)	58	–
			236	–
HROG41	M/71	IDH1 (R132H), MGMT(M)	31	–
			209	–
HROG42	F/70	MGMT(U)	30	–
			189	–
HROG49	M/45	MGMT(U)	Fresh	–
			360	–
HROG52	M/47	n.d.	Fresh	✓
			308	–
HROG54	M/58	MGMT(M)	Fresh	–
			281	–
HROG55	F/74	MGMT(M)	Fresh	–
			278	–
HROG56	F/76	MGMT(U)	Fresh	–
			222	–

Table 1 continued

Sample ID	Sex/age	Molecular alterations	Cryoperiod (days)	Engraftment
HROG58	F/57	MGMT(U)	Fresh	–
			165	–
HROG59	M/60	16xEGFR, MGMT(U)	Fresh	✓
			152	–
HROG60	M/51	2xEGFR, MGMT(U)	Fresh	–
			126	–
			513	–
HROG63	M/48	18xEGFR, MGMT(U)	Fresh	–
			20	–
HROG64	F/57	MGMT(M)	Fresh	–
			20	–

M male, *F* female, *xEGFR* EGFR gene amplification, *MGMT(M)* methylated MGMT promoter, *MGMT(U)* unmethylated MGMT promoter, *n.d.* not determined

and fresh GBM tissue samples. Furthermore, success rates of engraftment in NMRI Foxn1^{nu} mice or in NOD/SCID mice were compared on the basis of 18 cryopreserved GBM samples (Table 2). In NMRI Foxn1^{nu} mice, 5 out of 18 samples were successfully engrafted (27.7%). The success rate was higher in NOD/SCID mice (7 out of 18 samples; 38.8%). Four cases (HROG05, HROG06, HROG13 and HROG17) were successfully engrafted in both mouse strains, two cases could only be successfully engrafted in NOD/SCID mice and one case only engrafted in NMRI Foxn1^{nu} mice (Table 2).

Table 2 Direct comparison of PDX establishment success between NMRI Foxn1^{nu} and NOD/SCID mice

Sample ID	Cryoperiod (days)	NMRI Foxn1^{nu}	NOD/SCID
HROG02	305–1963	–	–
HROG04	270–1213	–	–
HROG05	268–1248	✓	✓
HROG06	260–1918	✓	✓
HROG07	143–1123	–	✓
HROG10	71–1763	–	–
HROG13	318–1634	✓	✓
HROG15	240–1570	–	–
HROG17	194–1555	✓	✓
HROG19	217–1570	–	–
HROG21	192–900	–	–
HROG22	167–875	–	✓
HROG23	191–1057	–	–
HROG24	112–1494	–	–
HROG25	177–912	–	–
HROG38	58–1500	–	✓
HROG49	0–638	–	–
HROG59	0–427	✓	–

Overview of PDX establishment success of 18 cases, checkmarks indicate successful engraftment

Long-term stability of GBM PDX models

All initially successfully engrafted cases, both in NMRI Foxn1^{nu} and NOD/SCID mice, were passaged in vivo to determine if these PDX models demonstrate stable growth behavior. PDX models initially established in NOD/SCID mice (Table 2) were transferred in NMRI Foxn1^{nu} mice (Additional file 3). 9 out of the 11 initially positive PDX cases (81.8%) were successfully engrafted in the first in vivo transfer and subsequently passaged further. Two initially positive cases (HROG12 and HROG52) were unable to form a tumor in subsequent in vivo transfers into NMRI Foxn1^{nu} mice. In the case of HROG12, a second in vivo transfer attempt also failed. To date, 6 GBM PDX cases reached a minimum of 5 in vivo passages and therefore are considered as long-term stable PDX models (Additional file 3). The remaining cases HROG17, HROG33 and HROG38 have reached 3 or 4 passages and thus will very likely become long-term stable PDX models as well. Overall, a strong trend towards accelerated tumor growth was observed with increasing in vivo passage number (Table 3).

Morphology of primary GBM and their PDX derivates is conserved over several in vivo passages

As shown for HROG33 and HROG59 in two consecutive in vivo passages (designated as "PDX-T1" and "PDX-T2"), the PDX models resemble the respective primary GBM closely (Fig. 1). The HROG33 PDX models show a slightly higher compactness of cell structure than the primary tumor, but important characteristics such as content of mitotic cells, degree of pleomorphy and necrosis compare well with the primary tumor. Albeit the limited sample size of the PDX, both passages of HROG33 PDX fulfilled formal requirements which would have allowed a correct GBM diagnosis. The HROG59 PDX models also show key characteristics of the primary tumor (high

Table 3 Analysis of MGMT promoter methylation and EGFR amplification of GBM tumors and corresponding PDX over several in vivo passages

Sample ID	MGMT promoter methylation (PMR)	EGFR amplification	Tumor volume >0.2 cm^3 at day
HROG05			
Tumor	M (34,5)	82×	–
PDX P2	U (0)	12×	60
HROG06			
Tumor	U (0)	82×	–
PDX P0	U (0)	75×	54
PDX P1	U (0)	69×	24
PDX P2	U (0)	103×	40
PDX P3	U (0)	123×	27
PDX P4	U (0)	144×	25
PDX P5	U (0)	147×	19
HROG07			
Tumor	U (0)	12×	–
PDX P2	U (0)	152×	82
PDX P4	U (0)	96×	98
HROG12			
Tumor	U (1,4)	37×	–
PDX P0	U (0)	52×	123
HROG13			
Tumor	U (3,9)	1×	–
PDX P1	M (4)	2×	25
PDX P2	M (5)	2×	31
PDX P3	M (15)	2×	46
HROG17			
Tumor	M (14)	4×	–
PDX P2	M (11)	1×	59
HROG22			
Tumor	M (22,2)	1×	–
PDX P0	M (6)	2×	158
PDX P1	M (22)	2×	54
PDX P3	M (73)	1×	46
PDX P5	M (97)	2×	26
HROG33			
Tumor	U (0)	31×	–
PDX P1	U (0)	67×	90
HROG59			
Tumor	U (0)	16×	–
PDX P2	U (0)	85×	68
PDX P3	U (0)	92×	31
PDX P4	U (0)	47×	31
PDX P5	U (0)	36×	54

M methylated, *U* unmethylated, *PMR* percentage of methylated reference

degree of pleomorphy, necrosis and content of hyperchromatic cells). Of the two HROG59 PDX transfers, only HROG59 PDX-T2 formally fulfils the requirements for a GBM diagnosis. The specific section of HROG59 PDX-T1 does–most likely due to the small sample size—not contain a thrombotic blood vessel and thus, does not fulfil all formally required characteristics for a GBM diagnosis; yet compares very well to the primary tumor otherwise.

In general, the PDX models show a highly similar morphology between first and second in vivo passage. As compared to the respective primary GBM, important characteristics were conserved in the PDX models in these low passages. However, the heterotopic PDX do not show invasive growth behavior, which is characteristic for GBM. Invasive growth into surrounding tissue was observed in orthotopic models of two exemplary cases (HROG06 and HROG59; Additional file 4). High expression of glial fibrillary acidic protein (GFAP), a marker for astrocytic cells, is evident in both primary tumors and the corresponding heterotopic PDX models in both passages (Additional file 5). This additionally verifies that the GBM PDX models conserve their neuronal character.

Comparison of molecular aberrations between primary GBM and corresponding PDX

The presence of mutations found in the primary tumor was analyzed in every corresponding PDX model (Table 1; Additional file 2). In all cases, the mutations in the genes K-RAS, P53 and IDH1 could be confirmed in the PDX models. However, analyses of MGMT promoter methylation status of primary GBM and derived PDX models revealed differences in 2 out of 9 cases (Table 3). Furthermore, genomic amplification of EGFR was variable in the PDX models over several in vivo passages as well as in comparison to the primary GBM in all cases with EGFR amplification in the primary tumor. GBM cases without EGFR amplification did not gain additional EGFR gene copies over the PDX passages. Identity of all PDX models was verified by genetic fingerprint analyses (Additional file 6) and matched in all cases.

Experimental therapy of GBM PDX models

Five different GBM PDX models were experimentally treated with monotherapies of temozolomide, everolimus, sorafenib, salinomycin, bevacizumab or irinotecan (5 mice per group). Control mice were treated with physiological saline solution. 4 out of 5 PDX models were highly susceptible to temozolomide monotherapy, only HROG05 showed intrinsic temozolomide resistance (Fig. 2). Good treatment results were also obtained with the anti-VEGF antibody bevacizumab, which had a positive effect in all cases tested. Irinotecan, a topoisomerase inhibitor, was effective in 3 cases (HROG05, HROG13 and HROG59). Treatment with the mTOR inhibitor everolimus had positive effects in 2 cases (HROG05 and HROG13). The multi-kinase inhibitor sorafenib was

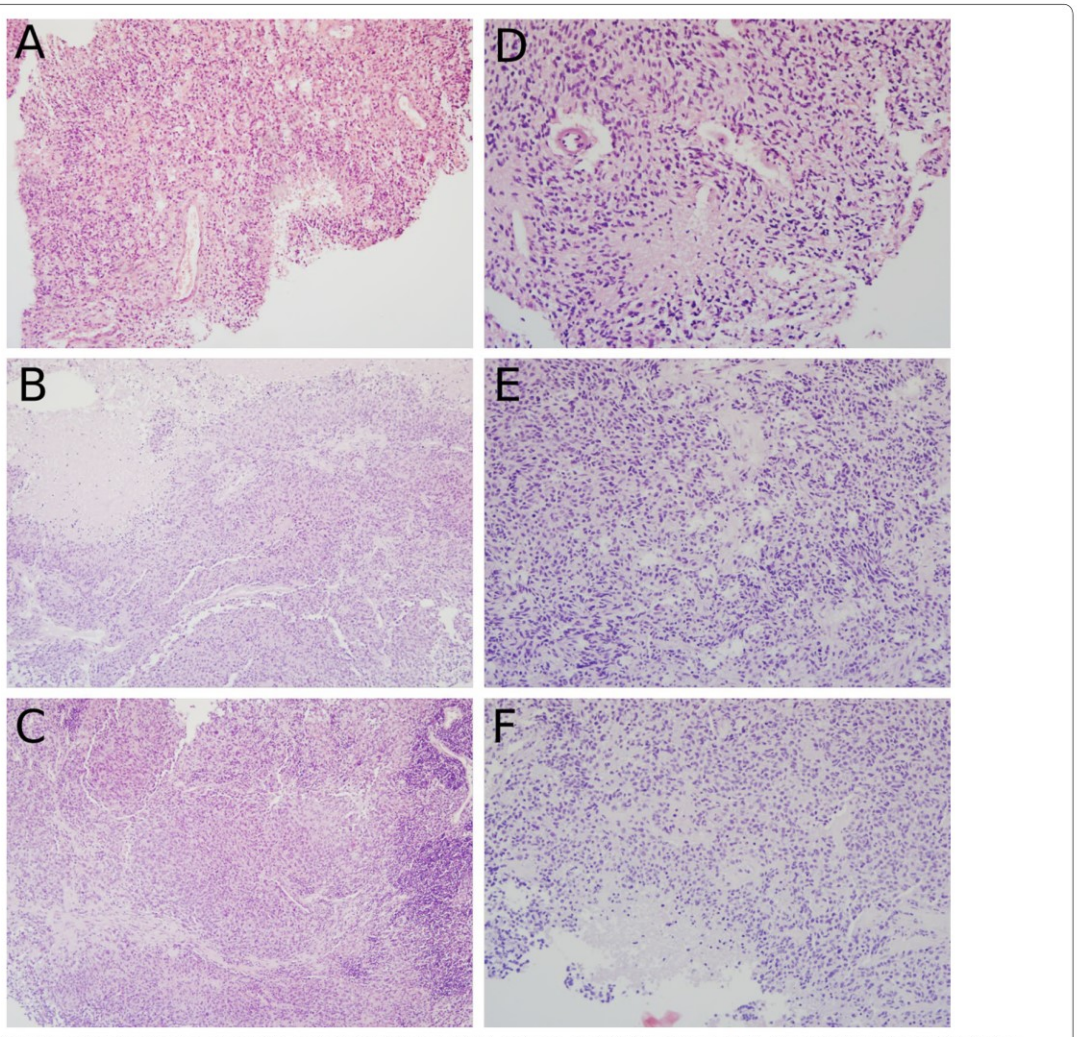

Fig. 1 Hematoxylin and eosin staining of paraffin embedded GBM and PDX sections. **A** HROG33 primary GBM, **B** HROG33 PDX after first in vivo transfer, **C** HROG33 PDX after second in vivo transfer, **D** HROG59 primary GBM, **E** HROG59 PDX after first in vivo transfer, **F** HROG59 PDX after second in vivo transfer. 200-fold magnification

effective only in one case (HROG22) and salinomycin treatment had no effect in all cases tested. Additionally, all experimentally treated PDX models were analyzed for potentially relevant mutations by panel sequencing covering 212 target regions in 48 cancer related genes (Table 4).

Discussion

Glioblastoma multiforme remains a tumor difficult to treat with a very dismal prognosis. Hence, gaining a better understanding of molecular characteristics of individual GBM is mandatory for the development of individualized therapy strategies. This task requires sufficient amounts of tumor material for analysis and—potentially—therapy response prediction approaches. Individual GBM PDX recommend themselves for this purpose, since tumor material can be propagated for further studies in an in vivo environment, while maintaining intratumoral heterogeneity as well as most genomic aberrations [26]. However, establishment of GBM PDX requires optimized logistics and standardized protocols. We demonstrate here that GBM tissue cryopreserved and subsequently stored for longer time periods enables xenografting at a later time point. Additionally, and to the best of our knowledge, this is the first study in which xenografting of fresh and vitally frozen GBM tissue was compared directly. We did not observe a difference of engraftment success between fresh and vitally frozen GBM tumor

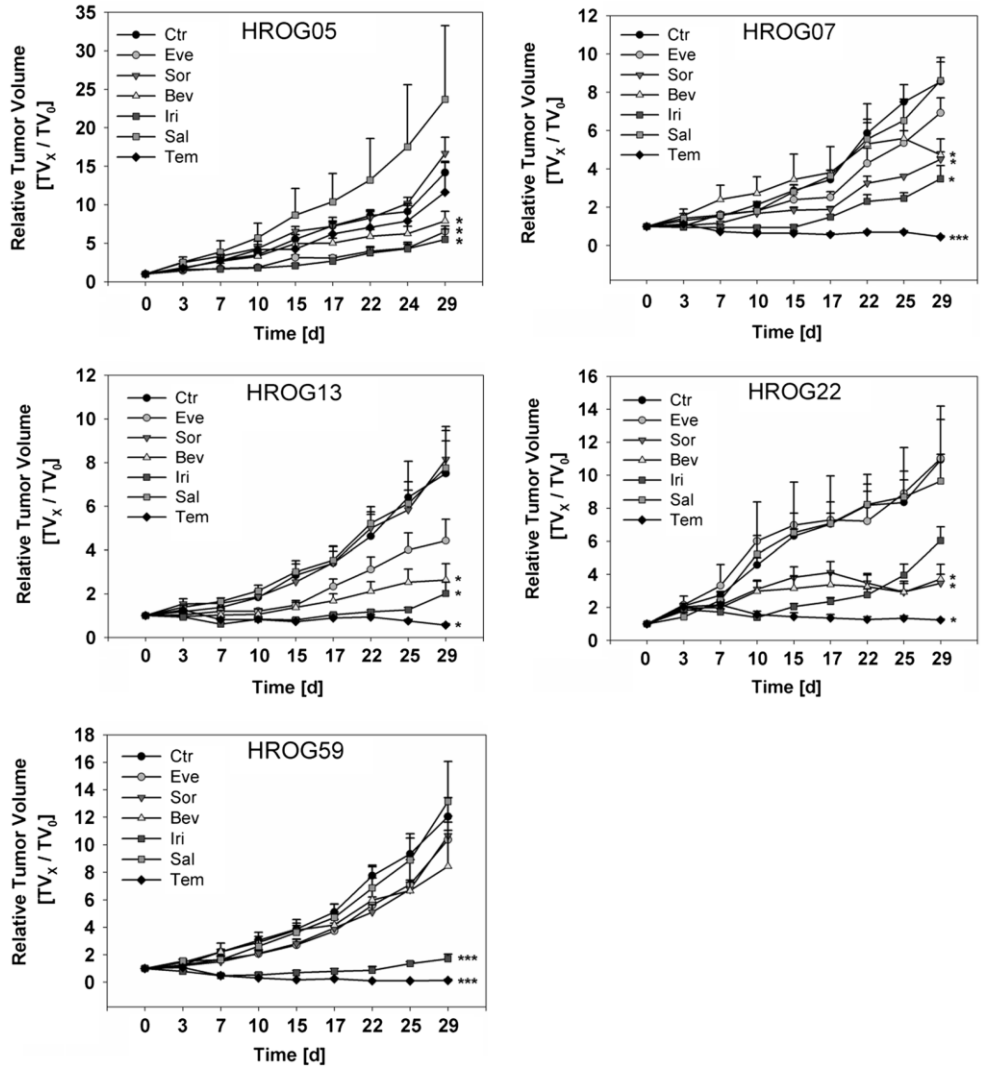

Fig. 2 Experimental treatment outcomes of 5 GBM PDX. Development of relative tumor volumes over time, error bars indicate the standard errors of the mean. *p < 0.005, ***p < 0.001, p-values were calculated with a t test at the end of the experiment in comparison to untreated controls. *ctr* control treated with PBS, *Eve* everolimus, *Sor* sorafenib, *Bev* bevacicumab, *Iri* irinotecan, *Sal* salinomycin, *Tem* temozolomide

Table 4 Mutations in PDX models used for in vivo therapy experiments

Sample ID	Mutations in PDX
HROG05	EGFR (R108K, Y626H), K-Ras (G12D), P53 (R280K)
HROG07	APC (A1340 V), FLT3 (V592I), PIK3CA (E545K), PTPN11 (S502L)
HROG13	ABL1 (A288S), ATM (F858L), ERBB2 (G748C), GNA11 (N336K), PTEN (S207C), VHL (E94*)
HROG22	PIK3CA (E545K), PTPN11 (S502L)
HROG59	ERBB2 (Del fs*), GNAQ (2x Del fs*), KDR (Q472H), PTEN (Q17L, M198I, L265I)

Mutations identified by amplicon panel sequencing covering 212 target regions in 48 cancer-related genes (Illumina MiSeq TSACP (Illumina Variant Caller 3.1.10.0)). Del: deletion, fs*: frame shift leading to stop, *: stop gain

material. Hence, many logistic obstacles (e.g. transport conditions and transport time of tumor tissue, availability of mice for xenografting, opening hours at laboratory animal facilities) can be circumvented by using this simple and feasible method of GBM tissue cryopreservation. However, we did not observe successful engraftment of both fresh and vitally frozen GBM tissue derived from an identical primary GBM tumor. Although this was not subject of further investigation, it seems likely that the quality of implanted tumor tissue—fresh or vitally frozen—as well as individual and yet unknown mouse factors have an influence on the success of an individual tumor graft [27].

Overall engraftment success in NMRI Foxn1^{nu} mice is with 22.2% rather low in comparison to successful establishment of GBM cell lines [14], orthotopic GBM PDX [18] or of PDX from other tumor entities [22], but well in line with previous reports from other studies on heterotopic GBM [28]. The GBM PDX establishment success rate appears to be higher in NOD/SCID mice, which lack B- and T-Lymphocytes as well as NK cells, than in NMRI Foxn1^{nu} mice (38.8 vs 27.7% in the directly compared 18 cases). Out of all 7 successfully engrafted cases in this cohort of 18 cases, 4 cases were positive in both mouse strains, 2 cases only engrafted in NOD/SCID mice and one case was only successful in NMRI Foxn1^{nu} mice. NMRI Foxn1^{nu} mice are a widely used host for tumor xenograft studies due to the complete absence of T-Lymphocytes, yet other components of the immune system (NK cells, granulocytes, monocytes/macrophages, dendritic cells and B-Lymphocytes) are still present. Although residual active immune cells in NMRI Foxn1^{nu} mice likely play a role in preventing tumor formation, other crucial parameters like the quality of the implanted tumor tissue, the biology of the individual tumors and the individual mice are likely to play an even greater role [27]. In three cases (HROG23, HROG58, HROG60), we observed initial tumor formation followed by complete regression of engrafted primary tumors in NMRI Foxn1^{nu} mice (data not shown) before material could be saved for subsequent in vivo passaging. In these cases, engrafting repetitions might still result in successful PDX generation as was the case for HROG06 and HROG13.

Mutations present in the primary GBM were maintained in all analyzed genes in all PDX models over several passages. However, genomic amplification of EGFR varied between primary GBM and their PDX in nearly all cases where EGFR amplification has been observed in the primary GBM. Although not further investigated, it seems likely that this effect is due to clonal selection processes as cells with high EGFR copy numbers are not evenly distributed throughout the whole tumor tissue [29]. However, we also observed variations in the EGFR copy numbers over the PDX passages, which implies that cell intrinsic factors are still active.

Nevertheless, PDX models of GBM are valuable tools for further studies, for development of novel therapeutics as well as response prediction attempts for individualized therapy approaches. Intratumoral heterogeneity is generally well maintained in these models and we could show that the morphology of a primary GBM tumor is comparable to its PDX over several passages. However, heterotopic PDX do not show invasive growth into surrounding tissue compared to orthotopic GBM models. Nevertheless, heterotopic (or orthotopic) GBM PDX models using cryopreserved tissue specimens are a suitable tool for therapy response prediction since this method is feasible to create sufficient amounts of tumor material by in vivo passaging in mice to allow systematic and standardized testing of several therapeutic substances in vivo. Responses towards clinically used therapeutics in our test series of GBM PDX models were as diverse as expected from previous studies but also from clinical experience [30, 31]. Generally good in vivo responses were obtained with temozolomide, irinotecan and bevacizumab. A combination of these drugs just recently proofed beneficial in some cases of unresectable GBM in the neoadjuvant setting in a clinical phase II trial [32]. Beside this, two out of five PDX models responded to sorafenib and one to everolimus. In total, these chemo-response data proof applicability and can be considered for targeted selection of these novel GBM PDX models in future preclinical studies either in the heterotopic or orthotopic setting.

Conclusions

Despite aggressive treatment regimen, GBM remains a lethal brain tumor and development of new therapy strategies is an urgent task to combat this disease. In order to achieve targeted therapy regimen, establishment an analysis of individual in vivo models of GBM is essential. Although orthotopic PDX have the advantage of an appropriate tumor microenvironment, heterotopic models, as presented in this study, are of high value for several reasons. Heterotopic PDX enable the production of sufficient amounts of tumor tissue for extensive molecular and functional analyses. Furthermore, heterotopic PDX histologically and molecularly resemble the primary GBM closely and the establishment of those PDX is technically easily feasible. We demonstrated that long term cryopreserved GBM tissue can be engrafted in mice without loss of engraftment efficiency, which allows for a convenient workflow and improved logistics. We also systematically compared the PDX establishment success between two widely used mouse models, NMRI Foxn1^{nu} and NOD/

SCID, for 18 GBM cases and found engraftment success to be higher in NOD/SCID mice (38.8 vs 27.7% in NMRI Foxn1^{nu} mice). However, factors such as quality of tumor tissue pieces and individual mice also play a role in overall engraftment success, but are not easily influenced by the user. Taken together, our data provide the means for optimized establishment of GBM PDX with regard to choice of mouse strain and use of cryopreserved tissue.

Additional files

Additional file 1. Sequences of oligonucleotides and probes.Nucleotide sequences and labeling of all oligonucleotides and probes used in this study.

Additional file 2. Overview of patient characteristics diagnosed with WHO°I–III tumors. Summary of molecular alterations, cryoperiod of the samples prior to implantation and the outcome of PDX establishment attempts.

Additional file 3. Overview of highest in vivo passages of engrafted samples. Given numbers indicate the highest in vivo passage reached for given samples, 0 indicates failure at regrafting after initially positive engraftment from primary GBM tissue.

Additional file 4. Cresyl violet staining of representative orthotopic GBM PDX samples. GBM cells were injected intracranially to establish orthotopic GBM PDX models. A-D) HROG06 31d post injection of 2 × 10^5 GBM cells, A & C) whole brain section for assessment of tumor volume and localization, B & D) 100× magnification for assessment of invasive growth of GBM cells into surrounding tissue; E & F) HROG59 34d post injection of 8.7 × 10^5 GBM cells, F) 100x magnification; G & H) HROG59 34d post injection of 3.5 × 10^5 GBM cells, H) 100x magnification.

Additional file 5. GFAP Immunohistochemistry staining of paraffin embedded GBM and PDX tissue sections. A) HROG33 primary GBM, stained with new fuchsine B) HROG33 PDX after first in vivo transfer, C) HROG33 PDX after second in vivo transfer, D) HROG59 primary GBM, E) HROG59 PDX after first in vivo transfer, F) HROG59 PDX after second in vivo transfer. 200-fold magnification B-F were stained with 3,3′-Diaminobenzidine.

Additional file 6. Results of genetic fingerprint analysis. Identity verification of all PDX cases over several in vivo passages by genetic fingerprint analysis.

Abbreviations

GBM: glioblastoma multiforme; PDX: patient derived xenograft; RTV: relative tumour value; Bw: bodyweight.

Authors' contributions

DW wrote the manuscript, performed fingerprint analyses, participated in subcutaneous implantation of tumor tissue in NMRI Foxn1^{nu} mice, prepared samples for paraffin embedding and molecular analyses. CSM and MK performed the majority of subcutaneous tissue implantation in NMRI Foxn1^{nu} mice. BS performed the mutation analyses, EGFR amplification analysis and MGMT promoter methylation analysis. NL analyzed all tissue sections of primary GBMs and PDX models. AO and AH performed the subcutaneous implantation of tumor tissue in NSG and NMRI Foxn1^{nu} mice as well as experimental treatment in vivo. CFC was involved in design and critical review of the manuscript. ML designed the study, analyzed the data and wrote the manuscript. All authors read and approved the final manuscript.

Author details

[1] Children's Hospital, University Medicine Rostock, Ernst-Heydemann-Str. 8, 18057 Rostock, Germany. [2] Department of Surgery, Molecular Oncology and Immunotherapy, University Medicine Rostock, Schillingallee 35, 18057 Rostock, Germany. [3] Institute of Pathology, University Medicine Rostock, Strempelstr. 14, 18057 Rostock, Germany. [4] Experimental Pharmacology and Oncology Berlin-Buch GmbH, Robert-Roessle-Str. 10, 13125 Berlin-Buch, Germany.

Acknowledgements

The authors thank all members of the histopathology lab of the Institute for Pathology at the University Medicine of Rostock for paraffin embedding of samples, providing tissue sections and immunohistochemistry staining.

Competing interests

The authors declare that they have no competing interests.

Availability of data and materials

All data generated or analyzed during this study are included in this published article [and its supplementary information files].

Ethics approval and consent to participate

Specimen collection was conducted in accordance with the ethics guidelines for the use of human material, approved by the Ethics Committee of the University of Rostock (Reference number: A 2009/34) and with informed written consent from all patients prior to surgery.

Animal experiments were approved by the Committee on the Ethics of Animal Experiments of the University of Rostock (Landesamt für Landwirtschaft, Lebensmittelsicherheit und Fischerei Mecklenburg-Vorpommern; permission number: 7221.3-1.1-083/11).

Funding

Monika Kutzner Stiftung, Berlin (D.W.), W. Vaillant Stiftung (C.M.)

Received: 22 November 2016 Accepted: 25 January 2017
Published online: 09 February 2017

References

1. Louis DN, Ohgaki H, Wiestler OD, Cavenee WK, Burger PC, Jouvet A, Scheithauer BW, Kleihues P. The 2007 WHO classification of tumours of the central nervous system. Acta Neuropathologica. 2007;114(2):97–109.
2. Ohgaki H, Kleihues P. Population-based studies on incidence, survival rates, and genetic alterations in astrocytic and oligodendroglial gliomas. J Neuropathol Exp Neurol. 2005;64(6):479–89.
3. Stupp R, Mason WP, van den Bent MJ, Weller M, Fisher B, Taphoorn MJ, Belanger K, Brandes AA, Marosi C, Bogdahn U, Curschmann J, Janzer RC, Ludwin SK, Gorlia T, Allgeier A, Lacombe D, Cairncross JG, Eisenhauer E, Mirimanoff RO. European Organisation for Research and Treatment of Cancer Brain Tumor and Radiotherapy Groups; National Cancer Institute of Canada Clinical Trials Group. Radiotherapy plus concomitant and adjuvant temozolomide for glioblastoma. N Engl J Med. 2005;352(10):987–96.
4. Kim SS, Harford JB, Pirollo KF, Chang EH. Effective treatment of glioblastoma requires crossing the blood–brain barrier and targeting tumors including cancer stem cells: the promise of nanomedicine. Biochem Biophys Res Commun. 2015;468(3):485–9.
5. Xu YY, Gao P, Sun Y, Duan YR. Development of targeted therapies in treatment of glioblastoma. Cancer Biol Med. 2015;12(3):223–37.
6. Reardon DA, Wen PY. Glioma in 2014: unravelling tumour heterogeneity-implications for therapy. Nat Rev Clin Oncol. 2015;12(2):69–70.
7. Cohen AL, Colman H. Glioma biology and molecular markers. Cancer Treat Res. 2015;163:15–30.
8. Parsons DW, Jones S, Zhang X, Lin JC, Leary RJ, Angenendt P, Mankoo P, Carter H, Siu IM, Gallia GL, Olivi A, McLendon R, Rasheed BA, Keir S, Nikolskaya T, Nikolsky Y, Busam DA, Tekleab H, Diaz LA Jr, Hartigan J, Smith DR, Strausberg RL, Marie SK, Shinjo SM, Yan H, Riggins GJ, Bigner DD, Karchin R, Papadopoulos N, Parmigiani G, Vogelstein B, Velculescu VE, Kinzler KW. An integrated genomic analysis of human glioblastoma multiforme. Science. 2008;321(5897):1807–12.

9. Thomas L, Di Stefano AL, Ducray F. Predictive biomarkers in adult gliomas: the present and the future. Curr Opin Oncol. 2013;25(6):689–94.
10. Duncan CG, Yan H. Genomic alterations and the pathogenesis of Glioblastoma. Cell Cycle. 2011;10(8):1174–5.
11. Lee EQ, Kaley TJ, Duda DG, Schiff D, Lassman AB, Wong ET, Mikkelsen T, Purow BW, Muzikansky A, Ancukiewicz M, Huse JT, Ramkissoon S, Drappatz J, Norden AD, Beroukhim R, Weiss SE, Alexander BM, McCluskey CS, Gerard M, Smith KH, Jain RK, Batchelor TT, Ligon KL, Wen PY. A multicenter, phase II, randomized, noncomparative clinical trial of radiation and temozolomide with or without vandetanib in newly diagnosed glioblastoma patients. Clin Cancer Res. 2015;21(16):3610–8.
12. Chen C, Ravelo A, Yu E, Dhanda R, Schnadig I. Clinical outcomes with bevacizumab-containing and non-bevacizumab-containing regimens in patients with recurrent glioblastoma from US community practices. J Neurooncol. 2015;122(3):595–605.
13. Westphal M, Heese O, Steinbach JP, Schnell O, Schackert G, Mehdorn M, Schulz D, Simon M, Schlegel U, Senft C, Geletneky K, Braun C, Hartung JG, Reuter D, Metz MW, Bach F, Pietsch T. A randomised, open label phase III trial with nimotuzumab, an anti-epidermal growth factor receptor monoclonal antibody in the treatment of newly diagnosed adult glioblastoma. Eur J Cancer. 2015;51(4):522–32.
14. Mullins CS, Schneider B, Stockhammer F, Krohn M, Classen CF, Linnebacher M. Establishment and characterization of primary GBM cell lines from fresh and frozen material: a detailed comparison. PloS ONE. 2013;8(8):e71070.
15. Voskoglou-Nomikos T, Pater JL, Seymour L. Clinical predictive value of the in vitro cell line, human xenograft, and mouse allograft preclinical cancer models. Clin Cancer Res. 2003;9:4227–39.
16. Bigner SH, Humphrey PA, Wong AJ, Vogelstein B, Mark J, Friedman HS, Bigner DD. Characterization of the epidermal growth factor receptor in human glioma cell lines and xenografts. Cancer Res. 1990;50:8017–22.
17. Romaguera-Ros M, Peris-Celda M, Oliver-De La Cruz J, Carrión-Navarro J, Pérez-García A, García-Verdugo JM, Ayuso-Sacido A. Cancer-initiating enriched cell lines from human glioblastoma: preparing for drug discovery assays. Stem Cell Rev. 2012;8:288–98.
18. Joo KM, Kim J, Jin J, Kim M, Seol HJ, Muradov J, Yang H, Choi YL, Park WY, Kong DS, Lee JI, Ko YH, Woo HG, Lee J, Kim S, Nam DH. Patient-specific orthotopic glioblastoma xenograft models recapitulate the histopathology and biology of human glioblastomas in situ. Cell Rep. 2013;3:260–73.
19. Huszthy PC, Daphu I, Niclou SP, Stieber D, Nigro JM, Sakariassen PØ, Miletic H, Thorsen F, Bjerkvig R. In vivo models of primary brain tumors: pitfalls and perspectives. Neuro-oncology. 2012;14:979–93.
20. Fichtner I, Slisow W, Gill J, Becker M, Elbe B, Hillebrand T, Bibby M. Anticancer drug response and expression of molecular markers in early-passage xenotransplanted colon carcinomas. Eur J Cancer. 2004;40:298–307.
21. Fichtner I, Rolff J, Soong R, Hoffmann J, Hammer S, Sommer A, Becker M, Merk J. Establishment of patient-derived non-small cell lung cancer xenografts as models for the identification of predictive biomarkers. Clin Cancer Res. 2008;14(20):6456–68.
22. Linnebacher M, Maletzki C, Ostwald C, Klier U, Krohn M, Klar E, Prall F. Cryopreservation of human colorectal carcinomas prior to xenografting. BMC Cancer. 2010;8:362.
23. Eads CA, Danenberg KD, Kawakami K, Saltz LB, Blake C, Shibata D, Danenberg PV, Laird PW. MethyLight: a high-throughput assay to measure DNA methylation. Nucl Acids Res. 2000;28(8):E32.
24. Masibay A, Mozer TJ, Sprecher C. Promega corporation reveals primer sequences in its testing kits. J Forensic Sci. 2000;45(6):1360–2.
25. Cardiff RD, Miller CH, Munn RJ. Manual hematoxylin and eosin staining of mouse tissue sections. Cold Spring Harb Protoc. 2014. doi:10.1101/pdb.prot073411.
26. Behrens D, Rolff J, Hoffmann J. Predictive in vivo models for oncology. Handb Exp Pharmacol. 2016;232:203–21.
27. Mullins CS, Bock S, Krohn M, Linnebacher M. Generation of xenotransplants from human cancer biopsies to assess anti-cancer activities of HDACi. Methods Mol Biol. 2017;1510:217–29.
28. Carlson BL, Pokorny JL, Schroeder MA, Sarkaria JN. Establishment, maintenance and in vitro and in vivo applications of primary human glioblastoma multiforme (GBM) xenograft models for translational biology studies and drug discovery. Curr Protoc Pharmacol. 2011. doi:10.1002/0471141755.ph1416s52.
29. Hatanpaa KJ, Burma S, Zhao D, Habib AA. Epidermal growth factor receptor in glioma: signal transduction, neuropathology, imaging, and radioresistance. Neoplasia. 2010;12(9):675–84.
30. Cloughesy TF, Paul S, Mischel PS. Molecular targeting of Glioblastoma—how do you hit a moving target? Clin Cancer Res. 2011;17(1):6–11.
31. Reardon DA, Wen PY. Therapeutic advances in the treatment of glioblastoma: rationale and potential role of targeted agents. Oncologist. 2006;11(2):152–64.
32. Peters KB, Lou E, Desjardins A, Reardon DA, Lipp ES, Miller E, Herndon JE 2nd, McSherry F, Friedman HS, Vredenburgh JJ. Phase II trial of upfront bevacizumab, irinotecan, and temozolomide for unresectable glioblastoma. Oncologist. 2015;20(7):727–8.

Additional file 1. Sequences of oligonucleotides and probes. Nucleotide sequences and labeling of all oligonucleotides and probes used in this study.

Additional File 1: Sequences of oligonucleotides and probes		
Target	**Forward Primer**	**Reverse Primer**
IDH1 exon 4	5'-GCACGGTCTTCAGAGAAGCC-3'	5'-CACATTATTGCCAACATGAC-3'
IDH2 exon 4	5'-GCCCACACATTTGCACTCTA-3'	5'-CAGAGACAAGAGGATGGCTAGG-3'
BRAF exon 15	5'-TCATAATGCTTGCTCTGATAGGA-3'	5'-CTTTCTAGTAACTCAGCAGC-3'
KRAS exon 2	5'-GTACTGGTGGAGTATTTGATAGTGTATTAA-3'	5'-TCAAAGAATGGTCCTGCACC-3'
KRAS exon 3	5'-CTTTGGAGCAGGAACAATGTCT-3'	5'-TACACAAAGAAAGCCCTCCCC-3'
TP53 exon 5	5'-(GC40)TTCCTCTTCCTACAGTACTC-3'	5'-CTGGGCAACCAGCCCTGTCGT-3'
TP53 exon 6	5'-(GC40)GACGACAGGGCTGGTTGCCCA-3'	5'-AGTTGCAAACCAGACCTCAG-3'
TP53 exon 7	5'-(GC40)TCTCCTAGGTTGGCTCT-3'	5'-GCAAGTGGCTCCTGACCTGG-3'
TP53 exon 8	5'-CCTATCCTGAGTAGTGGTAATC-3'	5'-(GC40)CCGCTTCTTGTCCTGCTTGCTT-3'
EGFR	5'-TCCCATGATGATCTGTCCCTCACA-3'	5'-CAGGAAAATGCTGGCTGACCTAAG-3'
LINE-1	5'-TGCTTTGAATGCGTCCCAGAG-3'	5'-AAAGCCGCTCAACTACATGG-3'
MGMT	5'-GCGTTTCGACGTTCGTAGGT-3'	5'-CACTCTTCCGAAAACGAAACG-3'
COL2A1	5'-TCTAACAATTATAAACTCCAACCACCAA-3'	5'-GGGAAGATGGGATAGAAGGGAATAT-3'
D5S818	5'-GGTGATTTTCCTCTTTGGTATCC-Hex-3'	5'-AGCCACAGTTTACAACATTTGTATCT-3'
D7S820	5'-ATGTTGGTCAGGCTGACTATG-Hex-3'	5'-GATTCCACATTTATCCTCATTGAC-3'
D13S317	5'-ATTACAGAAGTCTGGGATGTGGAGGA-Hex-3'	5'-GGCAGCCCAAAAAGACAGA-3'
D16S539	5'-GGGGGTCTAAGAGCTTGTAAAAAG-Hex-3'	5'-GTTTGTGTGTGCATCTGTAAGCATGTATC-3'
CSF1PO	5'-AACCTGAGTCTGCCAAGGACTAGG-FAM-3'	5'-TTCCACACACCACTGGCCATCTTC-3'
TPOX	5'-ACTGGCACAGAACAGGCACTTAGG-FAM-3'	5'-GGAGGAACTGGGAACCACACAGGTTA-3'
THO1	5'-ATTCAAAGGGTATCTGGGCTCTGG-FAM-3'	5'-GTGGGCTGAAAAGCTCCCGATTAT-3'
vWA	5'-GCCCTAGTGGATGATAAGAATAATCAGTATGTG-FAM-3'	5'-GGACAGATGATAAATACATAGGATGGATGG-3'
Amelogenin	5'-ACCTCATCCTGGGCACCCTGGTT-3'	5'-AGGCTTGAGGCCAACCATCAG-FAM-3'
MGMT – Probe	5'-6FAM-CGCAAACGATACGCACCGCGA-TMR-3'	
COL2A1 – Probe	5'-6FAM-CCTTCATTCTAACCCAATACCTATCCCACCTCTAAA-TMR-3'	

Additional file 2. Overview of patient characteristics diagnosed with WHO°I–III tumors. Summary of molecular alterations, cryoperiod of the samples prior to implantation and the outcome of PDX establishment attempts.

Additional File 2: Overview of patient characteristics diagnosed with WHO°I-III tumors					
Sample ID	**Sex / Age**	**Diagnosis**	**Molecular Alterations**	**Cryoperiod [d]**	**Engraftment**
HROG03	M / 50	AO (WHO° III)	IDH1 (R132H), MGMT(M)	291	—
HROG09	M / 66	AA (WHO° II-III)	n.d.	78	—
HROG20	M / 34	Astrocytoma (WHO° II)	n.d.	199	—
HROG26	M / 63	Astrocytoma (WHO° II)	MGMT(U)	126	—
HROG29	M / 39	OA (WHO°II)	IDH1 (R132H), MGMT(U)	141	—
HROG37	F / 20	PA (WHO°I)	BRAF (p.T599_V600insT), MGMT(U)	71	—
AO: Anaplastic Oligodendroglioma, AA: Anaplastic Astrocytoma, OA: Oligoastrocytoma, PA: Pilocytic Astrocytoma, MGMT(M): Methylated MGMT promoter, MGMT(U): unmethylated MGMT promoter, n.d.: not determined					

Additional file 3. Overview of highest in vivo passages of engrafted samples. Given numbers indicate the highest in vivo passage reached for given samples, 0 indicates failure at regrafting after initially positive engraftment from primary GBM tissue.

Additional File 3: Overview of highest *in vivo* passages of engrafted samples	
Sample ID	**Highest *in vivo* Passage**
HROG05	6
HROG06	7
HROG07	6
HROG12	0
HROG13	6
HROG17	4
HROG22	7
HROG33	3
HROG38	3
HROG52	0
HROG59	5

Additional file 4. Cresyl violet staining of representative orthotopic GBM PDX samples. GBM cells were injected intracranially to establish orthotopic GBM PDX models. A-D) HROG06 31d post injection of 2 × 105 GBM cells, A & C) whole brain section for assessment of tumor volume and localization, B & D) 100× magnification for assessment of invasive growth of GBM cells into surrounding tissue; E & F) HROG59 34d post injection of 8.7 × 105 GBM cells, F) 100x magnification; G & H) HROG59 34d post injection of 3.5 × 105 GBM cells, H) 100x magnification.

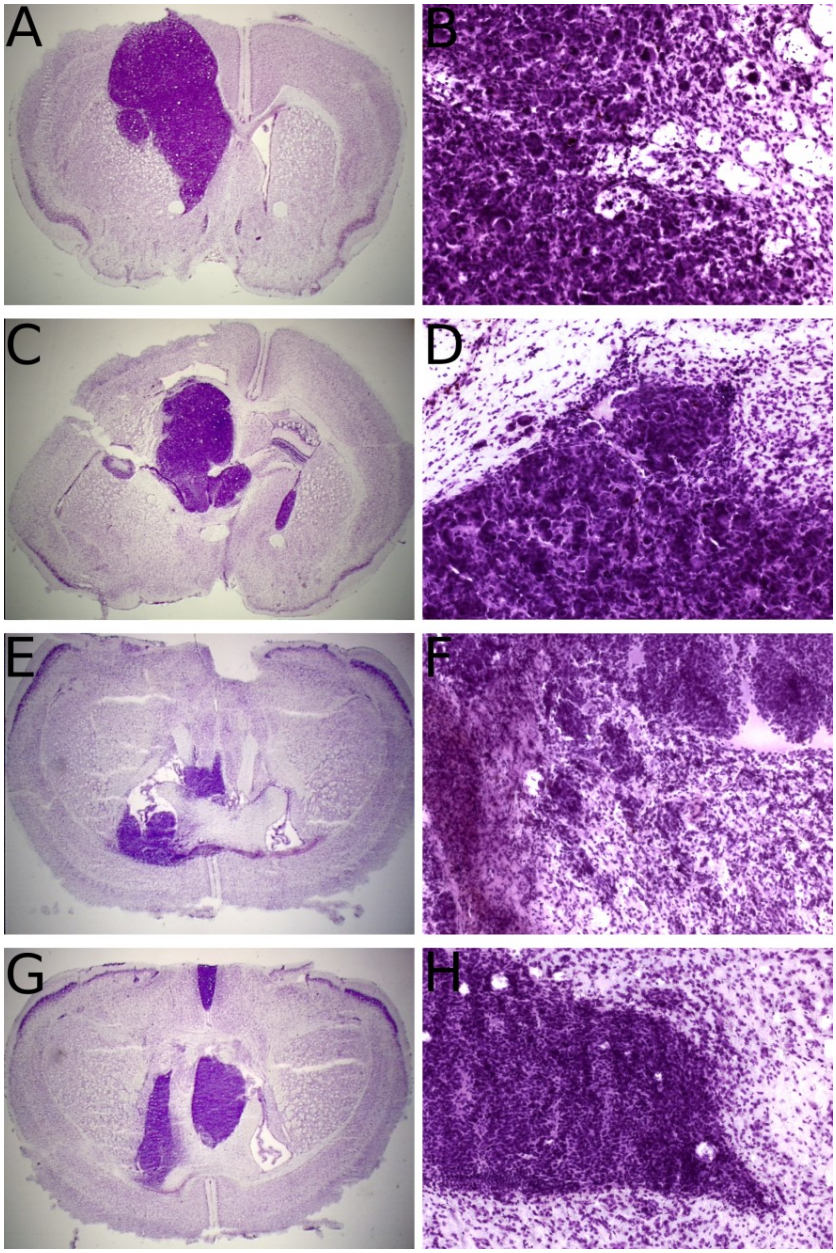

Additional file 5. GFAP Immunohistochemistry staining of paraffin embedded GBM and PDX tissue sections. A) HROG33 primary GBM, stained with new fuchsine B) HROG33 PDX after first in vivo transfer, C) HROG33 PDX after second in vivo transfer, D) HROG59 primary GBM, E) HROG59 PDX after first in vivo transfer, F) HROG59 PDX after second in vivo transfer. 200-fold magnification B-F were stained with 3,3′-Diaminobenzidine.

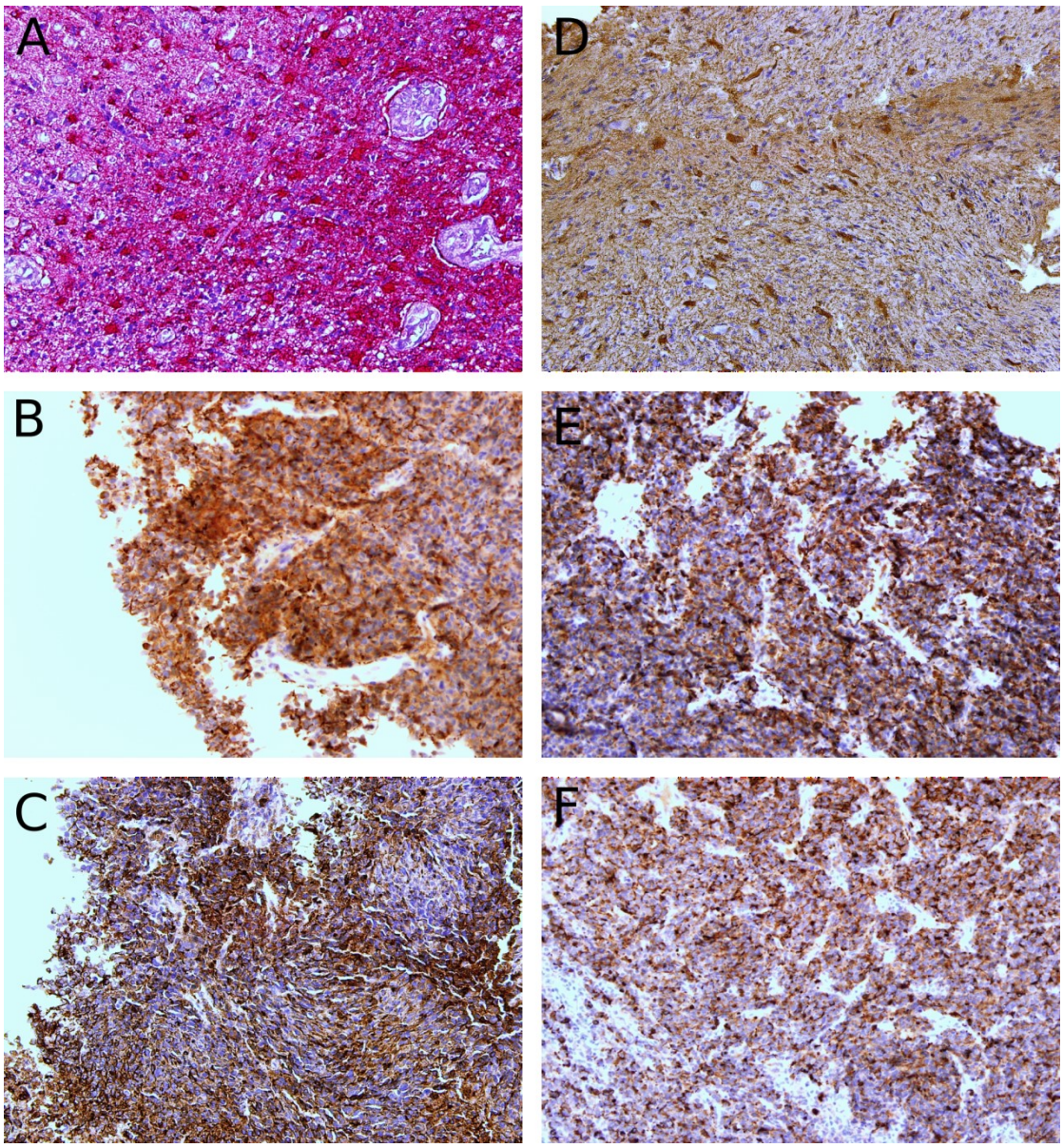

Additional file 6. Results of genetic fingerprint analysis. Identity verification of all PDX cases over several in vivo passages by genetic fingerprint analysis.

Additional File 6: Results of genetic fingerprint analysis									
Sample ID	**D5S818**	**D7S820**	**D16S539**	**D13S317**	**Amelogenin**	**vWA**	**TPOX**	**TH01**	**CSF1**
HROG05									
Tumor	10, 11	7, 11	10, 11	11, 12	f	17, 18	8, 11	11, 12	12, 13
PDX P2	10, 11	7, 11	10, 11	11, 12	f	n.a.	n.a.	n.a.	n.a.
HROG06									
Tumor	10, 11	8	11	11, 12	m	15, 18	8, 10	12	12, 13
PDX P0	10, 11	8	11, 12	11, 12	m	15, 18	8, 10	12	12, 13
PDX P1	10, 11	8	11, 12	11, 12	m	15, 18	8, 10	12	12, 13
PDX P2	10, 11	8	11, 12	11, 12	m	15, 18	8, 10	12	12, 13
PDX P3	10, 11	8	11, 12	11, 12	m	15, 18	8, 10	12	12, 13
PDX P4	10, 11	8	11, 12	11, 12	m	15, 18	8, 10	12	12, 13
PDX P5	10, 11	8	11, 12	11, 12	m	15, 18	8, 10	12	12, 13
HROG07									
Tumor	12, 13	8, 11	8, 10	8, 11	m	13, 16	8	12, 13	11
PDX P2	12, 13	8, 11	8, 10	8, 11	m	13, 16	8	12, 13	11
PDX P4	12, 13	8, 11	8, 10	8, 11	m	13, 16	8	12, 13	11
HROG12									
Tumor	10, 11	10	n.a.	8	m	16, 18	8, 10	7, 9	10, 13
PDX P0	10, 11	10	11, 12	8	m	16, 18	8, 10	7, 9	10, 13
HROG13									
Tumor	11	n.a.	n.a.	11, 12	f	16, 17	8	11	n.a.
PDX P1	11	9, 12	12	11, 12	f	16, 17	8	11	12, 13
PDX P2	11	9, 12	12	11, 12	f	17	8	11	12, 13
PDX P3	11	9, 12	10, 12	11, 12	f	16, 17	8	11	12, 13
HROG17									
Tumor	n.a.	n.a.	n.a.	n.a.	n.a.	15, 17	8, 12	9, 10	11
PDX P2	11, 12	9, 10	9, 10	9, 11	f	15, 17	8, 12	10	10, 11
HROG22									
Tumor	10, 12	8, 9	11	12, 14	m	14, 15	8	11, 14	13
PDX P0	10, 12	8, 9	11	12, 14	m	14, 15	8	11, 14	13
PDX P1	10, 12	8, 9	11	12, 14	m	14, 15	8	11, 14	13
PDX P3	10, 12	8, 9	11	12, 14	m	14, 15	8	11, 14	13
PDX P5	10, 12	8, 9	11	12, 14	m	14, 15	8	11, 14	13
HROG33									
Tumor	10, 11	7, 13	8	10	f	16, 18	8, 11	6, 9	10, 11
PDX P1	10, 11	7, 13	8	10	f	16, 18	8, 11	6, 9	10
HROG59									
Tumor	10, 12	9, 11	8, 10	8	m	16, 18	11	12, 15	11
PDX P2	10, 12	9, 11	8, 10	8	m	16, 18	11	12, 15	11
PDX P3	10, 12	9, 11	8, 10	8	m	16, 18	11	12, 15	11
PDX P4	10, 12	9, 11	8, 10	8	m	16, 18	11	12, 15	11
PDX P5	10, 12	9, 11	8, 10	8	m	16, 18	11	12, 15	11

5. Anhang

5.1. Publikationen

William D, Mokri P, Lamp N, Linnebacher M, Classen CF, Erbersdobler A, et al. Amplification of the EGFR gene can be maintained and modulated by variation of EGF concentrations. PLoS ONE 2017;12(9): e0185208.

William D, Mullins CS, Schneider B, Orthmann A, Lamp N, Krohn M, et al. Optimized creation of glioblastoma patient derived xenografts for use in preclinical studies. J Transl Med. 2017;15(1):27. doi: 10.1186/s12967-017-1128-5.

William D, Walther M, Schneider B, Linnebacher M, Classen CF. Temozolomide-induced increase of tumorigenicity can be diminished by targeting of mitochondria in in vitro models of patient individual glioblastoma. PLoS ONE 2017;13(1):e0191511. https://doi.org/10.1371/ journal.pone.0191511

Fiedler T, Strauss M, Hering S, Redanz U, **William D**, Rosche Y, et al. Arginine deprivation by arginine deiminase of Streptococcus pyogenes controls primary glioblastoma growth in vitro and in vivo. Cancer Biol Ther. 2015;16(7):1047-55. doi: 10.1080/15384047.2015.1026478.

Maletzki C, Rosche Y, Matzack C, Scholz A, **William D**, Classen CF, et al. Deciphering molecular mechanisms of Arginine Deiminase-based therapy – comparative response analysis in paired human primary and recurrent glioblastomas. Chem Biol Interact. 2017; doi: 10.1016/j.cbi.2017.10.007

5.2. Tagungsbeiträge

5.2.1. Vorträge

William D, Walther M, Schneider B, Classen CF. “Characterization of Glioblastoma multiforme in vitro models and the role of cancer stem cells” 11th Rostock Symposion for Tumor Immunology and Brain Tumor Research in Pediatrics (2017), Rostock, Deutschland

William D, Walther M, Schneider B, Classen CF. “In vitro models of Glioblastoma multiforme – characteristics of cancer stem cells” 10th Rostock Symposion for Tumor Immunology and Brain Tumor Research in Pediatrics (2016), Rostock, Deutschland

William D, Walther M, Schneider B, Classen CF. “Characteristics of Glioblastoma multiforme cancer stem-like cells” 25. GPOH-Arbeitstagung Experimentelle Neuroonkologie (2016), Minden, Deutschland

William D, Mokri P, Schneider B, Classen CF. “Optimization of Glioblastoma multiforme in vitro culture conditions for preservation of EGFR gene amplification” 24. GPOH-Arbeitstagung Experimentelle Neuroonkologie (2015), Minden, Deutschland

William D, Schneider B, Classen CF, Linnebacher M. “Subcutaneous mouse models of Glioblastoma – what do we learn?” 12th HGG-IMMUNO Meeting (2014), Würzburg, Deutschland

William D, Schneider B, Classen CF. “Analysis and applicability of different in vitro models of Glioblastoma multiforme” 8th Rostock Symposion for Tumor Immunology and Brain Tumor Research in Pediatrics (2014), Rostock, Deutschland

William D, Schneider B, Classen CF, Linnebacher M. “Subcutaneous mouse models of Glioblastoma – what do we learn?” 23. GPOH-Arbeitstagung Experimentelle Neuroonkologie (2014), Minden, Deutschland

William D, Schneider B, Classen CF. “Analysis and applicability of different in vitro models of Glioblastoma multiforme” 11th HGG-IMMUNO Meeting (2013), Leuven, Belgien

5.2.2. Poster

William D, Schneider B, Classen CF. “In vitro models of glioblastoma multiforme - characteristics of cancer stem cells” ISPNO 2016, Liverpool, UK

Walther M, **William D**, Schneider B, Classen CF. “GBM tumor cells achieve tumor stem-like properties after Temozolomide treatment” The International Symposium on Pediatric Neuro-Oncology (ISPNO) 2016, Liverpool, UK

William D, Mokri P, Schneider B, Classen CF. “Optimization of Glioblastoma multiforme in vitro culture conditions for preservation of EGFR gene amplification” CIMT 2015, Mainz, Deutschland

Schneider B, **William D**, Classen CF, Erbersdobler A. “The miR-183 cluster is activated is glioblastoma carrying EGFR amplification.” 100. Jahrestagung der DGP, Berlin, Deutschland

5.3. Lebenslauf

Persönliche Informationen

Name:	Doreen William
Geburtsdatum:	12.02.1989
Geburtsort:	Dresden
Familienstand:	ledig

Ausbildung

01/2013-12/2017	Promotionsstudentin an der Kinder- und Jugendklinik der Universitätsmedizin Rostock Thema: Etablierung und Analyse patientenindividueller Glioblastoma multiforme Modelle *in vitro* und *in vivo*
08/2011 – 09/2012	Masterarbeit („Characterization of the c-terminal domain of Mycobacterium tuberculosis porin A") am Department für Mikrobiologie der University of Alabama at Birmingham, AL, USA
10/2010 – 10/2012	Studium der Zell- und Molekularbiologie an der Friedrich Alexander Universität Erlangen/Nürnberg. Abschluss: Master of Science
06/2010 – 08/2010	Bachelorarbeit („Generation and analysis of fluorescent HERV-K particles") am Zentrum für biologische Sicherheit 4 des Robert Koch Instituts in Berlin.
04/2007 – 09/2010	Studium der Biologie an der Friedrich-Alexander Universität Erlangen/Nürnberg. Abschluß: Bachelor of Science

09/1999 – 07/2007 Vitzthum-Gymnasium Dresden

Abschluss: Abitur

Weiterbildungen

Seit 09/2013 Tierversuchskunde; FELASA-B Zertifikat

Seit 11/2015 Weiterbildung nach §15(4) der Gentechnik-Sicherheitsverordnung

5.4. Danksagung

Zunächst gilt mein besonderer Dank Herrn Prof. Dr. Carl Friedrich Classen. Nicht nur für die Überlassung des Promotionsthemas, sondern insbesondere auch für den wissenschaftlichen Freiraum, den er mir gewährt und das Vertrauen das er dabei in mich gesetzt hat. Das ist keine Selbstverständlichkeit und dafür möchte ich mich ausdrücklich bei ihm bedanken.

Ich danke Herrn Prof. Dr. Reinhard Schröder für seine Bereitschaft bei der Übernahme des Zweitgutachtens. Ich danke ihm auch für die Möglichkeit meine Arbeit im Forschungskolloquium am Institut für Biowissenschaften vorzustellen und zu diskutieren.

Weiterhin möchte ich der AG MOI um Herrn PD Dr. Michael Linnebacher danken. Viele hilfreiche Diskussionen und die Nutzung der MOI-Labore haben viel zu dieser Arbeit beigetragen.
Mein besonderer Dank gilt Frau Dr. Claudia Maletzki, die immer ein offenes Ohr und eine gute Idee für mich hatte. Über einer Tasse Kaffee konnten so manche Experimente geplant und Durchführungen ausgetüftelt werden.

Ein riesengroßes Dankeschön geht auch an das Institut für Pathologie, besonders an Herrn Dr. Björn Schneider und Frau Dr. Maja Hühns. Danke für alles, für die wunderbare Zusammenarbeit, für die vielen hilfreichen Diskussionen, für eure jederzeit guten Ratschläge und für bestimmt 200 Liter Kaffee.

Meinen Dank verdienen auch meine drei Medizinerinnen, Poroshista Mokri, Madlin Walther und Luise Fersterra, die unter meiner Anleitung ihre Doktorarbeiten machen mussten. Ihr wart großartig und es hat so viel Spaß gemacht mit euch zusammen arbeiten zu dürfen.

Weiterhin gilt mein Dank auch Frau PD Dr. Dagmar-Christiane Fischer für die Gastfreundschaft in ihrem Labor.
Besonderer Dank gilt auch meinen beiden Lieblings-TAs in der Kinderklinik, Anja Rahn und Birgit Salewski für ihre Unterstützung und Hilfe.

Schließlich möchte ich mich herzlich bei meiner Familie und meinem Partner bedanken. Ich danke euch für eure bedingungslose Unterstützung, nicht nur während meiner Promotion sondern in allen Lebenslagen. Vielen Dank fürs Mutmachen, fürs Zuhören, fürs Aufbauen, fürs Mitlachen, fürs Mitfreuen und für bestimmt weitere 200 Liter Kaffee. Ohne euch wäre nichts von alledem so möglich gewesen.

Vielen Dank.

5.5. Eidesstattliche Erklärung

Ich versichere an Eides statt, dass ich die vorliegende Arbeit selbstständig angefertigt und keine außer die von mir angegebenen Hilfsmittel und Quellen dazu verwendet habe. Die den benutzten Werken inhaltlich und wörtlich entnommenen Stellen habe ich als solche kenntlich gemacht.

Dresden, den _____ _____

Doreen William